ISSN 0035-0419

Revista Portuguesa de Química

Computer-aided molecular design:
Techniques and capabilities

Raman spectroscopy:
a survey on selected topics

Kinetics of intramolecular
electron exchange:
Application of Marcus theory

New reactions involving
addition to and substitution at
carbon-carbon π bonds

The planets and Thermodynamics

SOCIEDADE PORTUGUESA DE QUÍMICA

THE JOURNAL OF
THE PORTUGUESE CHEMICAL SOCIETY

1994

Revista Portuguesa de Química
Journal of the Portuguese Chemical Society
(Rev. Port. Quím.)

Série II – Vol. 1 – Anual

ISSN 0035-0419

DEPÓSITO LEGAL: 79910/94

SGMJ: 101240

Propriedade da Sociedade Portuguesa de Química
Property of the Portuguese Chemical Society
Av. da República, 37, 4º
1000 Lisboa, PORTUGAL
Tel.: (351-1) 793 46 37
Fax: (351-1) 755 23 49

DESIGN GRÁFICO DESIGN
Luís Moreira

FOTOCOMPOSIÇÃO TYPING
Cristina Cardoso

Impresso na JM3

TIRAGEM CIRCULATION
2500 exemplares

PREÇO DE VENDA PRICE
1 000$00 individual personal
2 000$00 bibliotecas libraries

Revista Portuguesa de Química

Instruções para os Autores
Instructions for Authors

Tendo em vista um aumento significativo do alcance e impacto da *Rev. Port. Quím.*, os artigos serão obrigatoriamente escritos e publicados em inglês, não excedendo as 20-30 páginas dactilografadas (formato A4 a dois espaços, margens de 2,5 cm), incluindo todas as tabelas, esquemas e figuras. As referências e notas *mencionadas no texto do manuscrito* serão ordenadas e numeradas entre parêntesis rectos. No final do manuscrito, antes das tabelas e figuras, essas referências e notas aparecerão numeradas sem parêntesis.

Exemplos:

1. P.R. Kemper, J. Bushnell, von G. Helden, M.T. Bowers, *J. Phys. Chem.* **97** (1993) 52.

2. J.P. Colloman, L.S. Hegedus, J.R. Norton, R.G. Finke, *Principles and Applications of Organotransition Metal Chemistry;* University Science Books: Mill Valey, 1987; pp. 279-354.

3. P.B. Armentrout, in *Gas Phase Inorganic Chemistry*; D.H. Russel, Ed.; Plenum Press: New Tork, 1989; pp 1-42.

As figuras e tabelas aparecerão numeradas em árabe e agrupadas no fim do manuscrito, após as referências e em folhas separadas. As tabelas só deverão ser utilizadas quando representarem uma vantagem para a exposição do texto ou quando não possam ser substituídas por gráficos ou figuras. As figuras devem ser enviadas com grande qualidade gráfica.

No caso de existir mais do que um Autor, deverá ser assinalado com um asterisco (*) o nome daquela a quem toda a correspondência ou comentários deverão ser enviados. Os manuscritos devem ser enviados em **triplicado** ao *Editor da Revista Portuguesa de Química, Sociedade Portuguesa de Química, Av. da República, 37, 4º, 1000 Lisboa, Portugal.*

Do Projecto de Estatuto Editorial da *Revista Portuguesa de Química*

Pretende a Revista Portuguesa de Química (Rev. Port. Quím.) publicar os resultados originais da investigação em Química na forma de revisões críticas concisas e que reflictam a actividade científica levada a cabo por investigadores ou pelas suas equipas.

Os artigos serão predominantemente solicitados através de um **convite** da responsabilidde do *Editor da Rev. Port. Quím.*, e poderão incidir sobre qualquer das áreas e disciplinas da Química, perspectivando a contribuição dos autores no quadro mais geral do seu desenvolvimento internacional e interdisciplinar e referenciando as opiniões e os autores mais relevantes, constantes na literatura.

Pretende-se que pelo seu conteúdo e formato se possa estabelecer um compromisso entre o interesse de uma audiência geral, mas atenta, e uma audiência especialmente ligada ao campo de investigação do(s) Autor(es). A concisão dos artigos submetidos, bem como o esforço de uma boa definição dos conceitos, referência e enquadramento crítico da investigação levada a cabo em torno dos temas propostos da Comissão Editorial ou de avaliadores por ela seleccionados. A inclusão de resultados não publicados deverá ser feita de uma forma moderada e quando significativamente necessária. Pelo contrário, as conclusões finais devem reforçar e perspectivar o significado dos resultados obtidos mais importantes. A submissão de artigos à *Rev. Port. Quím.* implica que o mesmo trabalho não seja ou tenha sido submetido noutro Jornal ou Revista.

A Comissão Editorial é nomeada, por um período de três anos, pela Direcção da Sociedade Portuguesa de Química e tem a responsabilidade por todas as decisões editoriais. **A Sociedade Portuguesa de Química e a Comissão Editorial da Rev. Port. Quím.** não assumem, no entanto, qualquer responsabilidade pelas afirmações e opiniões expressas pelos autores dos artigos publicados. Os comentários ou outros textos da responsabilidade dos membros da Comissão Editorial não envolvem a Sociedade ou a própria *Rev. Port. Quím.*

Com este número inicia-se uma nova série da *Revista Portuguesa de Química*, a publicação científica da Sociedade Portuguesa de Química, continuadora da *Revista de Química Pura e Aplicada,* que nasceu em 1905 pela mão de Ferreira da Silva, A. Aguiar e J.P. Salgado. Justificam-se algumas palavras para explicar sucintamente as razões que motivaram a actual (e profunda) mudança na *Revista.*

A abundância de revistas de química, publicadas por grandes editoras ou por sociedades científicas de grande dimensão, conduziu a uma queda acentuada da qualidade média dos artigos submetidos a revistas publicadas por sociedades de menor dimensão, no contexto internacional. A *Revista Portuguesa de Química* não conseguiu enfrentar essa competição desigual, apesar dos esforços dos seus sucessivos editores. A hipótese de adiar *sine die* a publicação da *Revista* foi assim devidamente ponderada pela Sociedade Portuguesa de Química. Considerou-se injustificado continuar a alimentar um projecto de qualidade insatisfatória, para o qual, a prosseguir nos mesmos moldes, não se anteviam melhorias. Por outro lado, uma eventual participação activa da Sociedade Portuguesa de Química numa futura publicação de química a nível europeu, pareceu uma melhor alternativa para canalizar os esforços editoriais. Por muito que pesassem estes dois (e outros) argumentos, houve sempre a sensação de que terminar um titulo que é mais antigo do que a própria Sociedade, era uma decisão polémica. Surgiu então a ideia, aprovada pela Direcção da Sociedade, de transformar a *Revista Portuguesa de Química* numa publicação cujos artigos fossem exclusivamente revisões breves do trabalho de investigação mais recente de químicos portugueses ou estrangeiros, submetidos por convite do Editor (ver o Estatuto Editorial). Acredita-se que este modelo não só garantirá um aumento substancial da qualidade da *Revista*, e logo da sua divulgação nacional e internacional, como a tornará numa «memória» da melhor química que se faz em Portugal.

A new series of *Revista Portuguesa de Química (Journal of the Portuguese Chemical Society)* begins with the present issue and a few words to justify the major changes that have been adopted are appropriate. This journal was first published in 1905 under the name of *Revista de Química Pura e Aplicada (Journal of Pure and Applied Chemistry)*, led by Ferreira da Silva, A. Aguiar, and J.P. Salgado.

The abundance of chemistry journals owned by big publishers or by big national scientific societies led to a noticeable decrease in the average quality of papers submitted to journals published by smaller national scientific societies. The *Revista Portuguesa de Química* was not able to face that unequal competition, despite the efforts of its several editors. The decision to suspend publication of the journal was thus debated by the Portuguese Chemical Society. There seemed to be no justification to insist on a project of unsatisfactory quality, for which, if pursued along the same lines, no improvement could be anticipated. On the other hand, a possible involvement of the Portuguese Chemical Society in a future European Chemistry journal seemed a better alternative at which to aims our efforts. Despite the weight of the two previous arguments, it was considered that discontinuing a journal that is older than the Society itself, would be controversial. An alternative approach, approved by the Society's Directive Council, was then adopted: from now on the papers published by the Journal will be brief accounts of recent work done by Portuguese or foreign chemists, submitted by invitation from the Editor (see Editorial Guidelines). It is believed that the quality of the Journal will be substantially improved by this model, leading to a considerable increase of its visibility here and abroad. It is also our conviction that with the present editorial policy the *Revista Portuguesa de Química* will mirror the best chemistry done in Portugal.

J. A. Martinho Simões
Secretário-Geral
Secretary-General

O ressurgimento da Revista Portuguesa de Química *(Rev. Port. Quím.)*, numa base regular e com uma orientação editorial distinta das anteriores, ocorre com a publicação deste primeiro número da II Série. Pretende-se, assim, corresponder à necessidade, várias vezes expressa pela comunidade dos químicos do nosso País, em voltar a ter um jornal de qualidade onde possam ver reflectida a melhor perspectiva do seu trabalho de investigação.

Este primeiro número, como todos os que se lhe seguirão, é parcelar na escolha dos temas e na variedade das direcções em que as Ciências da Química evoluem. Mas será através das sucessivas contribuições dos próximos números que pretendemos formar um conjunto bem representativo da qualidade e do lugar da Química que se faz em Portugal num contexto internacional.

A ideia base, para a "nova" *Rev. Port. Quím.*, corresponde a transformá-la numa publicação (de periodicidade anual e em inglês) que seja **de facto** útil para a comunidade científica, reflectindo a melhor Química que se faz em Portugal. Um número da Revista terá um conjunto de pequenos artigos de revisão convidados (6-10 páginas impressas, incluindo figuras e tabelas), com incidência particular no trabalho dos autores. Cada artigo apresentará um tipo de linguagem e um texto científico que se aproxime do leitor não especializado na área, pela pertinência e boa apresentação dos conceitos, ideias e resultados fundamentais (recentes), sem cair nos pormenores de uma informação de pequeno alcance, por limitada a um público demasiado restrito. Com estes objectivos tentaremos, a par de uma garantida periodicidade e na qualidade dos artigos, romper com o isolamento da nossa Revista e projectá-la, também internacionalmente, como um instrumento de trabalho útil para quem a lê e prestigiante para quem aí publica.

Por circunstâncias várias, entre as quais se encontra o meu acordo em dar corpo a um novo editorial e em recuperar a periodicidade perdida da sua publicação, aceitei o convite e o desafio que me foram endereçados pela presente Direcção da SPQ e assumi a coordenação do projecto da *Rev. Port. Quím.*.

Espero que este projecto e este número despertem o interesse dos Químicos. Agradeço aos Autores dos textos apresentados a sua colaboração no arranque da nova série. Ao Secretário-Geral e à actual Direcção da nossa Sociedade, aos colegas pertencentes à nova Comissão Editorial da *Rev. Port. Quím.*, a força e o estímulo para que o projecto se iniciasse e para que se venha a concretizar. E ainda aos Doutores Jill Dias e Mário Nuno Berberan e Santos a colaboração prestada durante a sua preparação.

The reappearance of *Revista Portuguesa de Química (Rev. Port. Quím.)*, the Journal of the Portuguese Chemical Society, after a long absence is most welcome. It is hoped that the first issue of the Second Series will go some way towards meeting the often stated need of the Portuguese community of Chemists for a good quality Journal in which they can publish the best of their research work. This first issue covers a number of topics which represent some of the various directions in which the Chemical Sciences will evolve. We intend that contributions to future issues will cover other areas that are representative of the quality of chemical research done in Portugal today.

The idea behind the "new" *Rev. Port. Quím.*, is to produce annually an English language Journal that not only serves the Internal scientific community, but also showcases of the best Portuguese chemistry. Each issue will contain a collection of short *invited* reviews (6-10 printed pages, including tables and figures), which reflect the author's scientific interest and recent research. It is hoped that these reviews will be accessible to all research chemists whatever their specialist interest. Most importantly, the authors should communicate the concepts that lie behind their most significant results. This should enable us to project our Journal to the international scientific community, as a useful working tool for those who read it and prestigious for those who publish there.

The decision to produce *Rev. Port. Quím.* currently together with a shift in editorial policy persuaded me to accept the kind invitation of the Committee of the Portuguese Chemical Society (SPQ) to edit the Journal. I hope that this issue will be of interest not only to Portuguese chemists, but also to those engaged in chemical research elsewhere.

I am extremely grateful to the Authors who submitted such diverse and interesting contributions to the first issue. I would also like to thank my colleagues on the Editorial Board for their support which provides a firm foundation for the continued publication of *Rev. Port. Quím.* Finally preparation of this issue would not have been possible without the assistance of Doctors Jill Dias and Mário N. Berberan e Santos whose contribution is recognized.

BELARMINO A. SALVADO BARATA
Director
Editor

Computer-aided molecular design: techniques and capabilities

Desenho molecular assistido por computador: técnicas e possibilidades

M. J. RAMOS

DEPARTAMENTO DE QUÍMICA, FACULDADE DE CIÊNCIAS, UNIVERSIDADE DO PORTO, 4000 PORTO, PORTUGAL

Computer-aided molecular design is a recent area of research which can have a major contribution to decide which molecules are expected to be important for a given purpose. Computer-aided molecular design involves both molecular graphics and theoretical calculations and, in this article, the reader is given a brief idea of its present development, as well as being introduced to some of the research that our group is carrying out in this field.

O desenho molecular assistido por computador faz parte de uma área de investigação recente capaz de contribuir decisivamente na escolha de quais as moléculas que são importantes para atingir um determinado objectivo. O desenho molecular assistido por computador envolve não só grafismo molecular mas também cálculos teóricos e, neste artigo, é dado ao leitor um resumo do seu desenvolvimento actual. É, ainda, feita uma exposição breve de alguns dos projectos de investigação que o nosso grupo desenvolve presentemente nesta área.

Introduction

Computer-aided molecular design is an exciting new field, and a rapidly developing area to which both chemists and biologists contribute to the investigation of molecular structure, function and interaction. Attempts are being made everyday at studying more and more complex systems, which is reflected by the number of publications in the area of macromolecular simulations. These studies are contributing to the interpretation of experiments and to further our understanding of living systems. Computer-aided molecular design involves both molecular graphics and theoretical calculations and this combination can play a major part in deciding which molecules are important for the experimentalist to synthesize.

In this article, I should like to give the general reader a brief idea of the present development of this fascinating area of research which has stimulated my interest over the last two years. I shall begin with an introduction to databases of molecular structure and to molecular graphics followed by a general view of some of the methods used in the theoretical calculations which should accompany the graphics research, namely molecular mechanics, quantum mechanics and free energy perturbation methods. The bibliography given does not intend to be exhaustive but rather to give an ample documentation on the subject. Subsequently, I shall introduce the reader to some of the research that our group is carrying out in this field .

Databases of molecular structure

Experimental three-dimensional molecular structures have been crucial for the development of computer-aided molecular design in general. However, the growing number of well characterized structures started making it very difficult for the user to keep track of all the significant information. To make this task easier, databases of molecular structure were developed,where the concepts to use are clearly defined and consistent with the various possible entries. One of the main databases is Cambridge Structural Database (CSBD), compiled at Cambridge Crystallographic Data Centre, which contains information relating to small molecule and polymer X-ray and neutron diffraction data for more than 70,000 compounds [1]. Another data compilation is Protein Data Bank (PDB), from Brookhaven National Laboratory, containing information relating to macromolecular structures [2]. Some of the data contained in the latter comprise the name of the macromolecule, references and authors, sequence, secondary structure, residues involved in the active centre and cartesian coordinates of atoms' positions

The above databases were primarily designed as archives and a source of coordinates. However, in the last few years, software for three-dimensional substructu-

ral searching has been developed [1,3-8] based mainly on molecular graphics concepts [9], the availability of the program CONCORD [10], and work already done on two-dimensional substructural searching [11-14]. This development has turned the role of databases even more essential.

Molecular graphics

Molecular graphics provides an extremely useful tool for the chemist and the biologist as a means of visualizing and manipulating the three-dimensional structure of a molecule. Clearly, the bigger the system we want to study the more difficult it is to be able to visualize it and, therefore, the development of molecular graphics has been particularly important in the study of proteins and macromolecular systems.

Molecular graphics requires a computer and, therefore, available software is a must. Nowadays, there are several software packages commercially available; there are, also, innumerable other programs developed in academic and industrial laboratories all around the world. Some of the most widely used commercial molecular graphics packages are Insight II from Biosym [15], Quanta from Molecular Simulations Inc. [16] and Sybyl from Tripos [17]. With them, essentially you can build molecules on the screen by reading in a molecule from some other source, by sketching chemical structures in 2D, by construction from a library of 3D chemical fragments, by working out a polymer from templates, by accessing external data bases and by editing an existing model; you can move the molecules, label and superimpose them, use colouring facilities to study 3D structures, make predictions about a protein, build protein fragments and mutate a protein or a fragment.

Most of the packages commercially available, including those mentioned above, will have facilities, other than molecular graphics, accessible by means of an interface with the graphics. These facilities range from quantum mechanics calculations to molecular dynamics, enabling the user to perform a much wider study of the particular system in question. Some of them will be mentioned in the following sections.

Molecular mechanics

Molecular mechanics provides a computational method designed to yield reliable energies and structures of molecules. This method is currently the only viable computational approach available for large systems of biological interest. Nowadays, the expression "molecular mechanics" is often used in a wide sense, i.e., meaning both the determination of static properties of a system and/or molecular dynamics calculations on single or multiple interacting molecules.

Molecular mechanics views molecules as models in which the atoms are charged soft spheres linked by bonds which act as springs. This collection of masses interact with each other via quasi harmonic forces which are described by potential energy functions.

Considerable effort has been put into developing simple but accurate enough analytical functions to both simulate the properties of complex systems and yield meaningful estimates of structures and energies [18-29]. These force fields, i.e., the equations and parameters that define the energy surface of a molecule, have thus steadily evolved over the years. However, one of the fundamental ideas is that the total energy, E_{total}, of a molecule can be divided into several parts,

$$E_{total} = E_{bonds} + E_{angles} + E_{dihedrals} + E_{nonbonded} \qquad (1)$$

due to bond stretching, angle bending, torsional and dihedral angles and nonbonded interactions (van der Waals and Coulomb), respectively. More refined force fields exist, which consider cross-terms between those interactions and also other terms due e.g. to hydrogen bonding. As an example, the AMBER force field for proteins and nucleic acids [24] is presented in equation (2)

$$\begin{aligned} E_{total} = & \sum_{bonds} K_r (r-r_e)^2 + \sum_{angles} K_\theta (\theta-\theta_e)^2 + \\ & \sum_{dihedrals} V_n/2 \, [1 + \cos (n\varphi - \gamma)] + \\ & \sum_{i<j} [A_{ij} / R_{ij}^{12} - B_{ij} / R_{ij}^{6} + q_i q_j / \varepsilon R_{ij}] + \\ & \sum_{H\text{-}bonds} [C_{ij} / R_{ij}^{12} - D_{ij} / R_{ij}^{10}] \end{aligned} \qquad (2)$$

where both terms for bond stretching and angle bending are quadratic, the torsional energy is approached by a Fourier series, the van der Waals term is given by a Lennard-Jones interaction (i.e. a 6-12 function), and the electrostatic term is described by a Coulomb interaction; this force field also contains a 10-12 function to account for hydrogen-bonding.

Understandably, the force field plays a major role in the reliability of the results obtained with molecular mechanics calculations; however, these are also heavily dependent on the parameterization, i.e., the numerical values of the parameters that are incorporated in the potential energy functions. As these have different forms, in general, parameters are not transferable from one force field to another. Care needs to be taken when a decision has to be made regarding the inclusion, into the calculation, of missing parameters. Furthermore, the quality and nature of the experimental or theoretical data available determines the quality of the parameters.

The potential energy function provides the basis for energy minimization and for molecular dynamics. The energy of the system is minimized as a function of the atomic coordinates. For complex biological systems, this method is not effective because there is a large number of low energy structures to explore. This means that energy minimization is generally not effective as far as reaching the global minimum energy conformation of enzymes and proteins, for instance. However, it is still widely used to refine structures and

particularly useful before initiating a molecular dynamics study or, indeed, other simulation studies.

Molecular dynamics calculations are used to study the dynamic behaviour of molecules as a function of time [30]. A molecular dynamics simulation is performed by integrating Newton's equations of motion over time, for the system. Therefore, for a molecular system of N atoms,

$$\mathbf{F}_j(t) = m_j \mathbf{a}_j(t) = m_j \partial^2 \mathbf{r}_j(t) / \partial t^2 \quad j = 1, ..., N \qquad (3)$$

where $\mathbf{F}_j(t)$, $\mathbf{a}_j(t)$ and $\mathbf{r}_j(t)$ are, respectively, the force, acceleration and position of atom j at time t. The force parameter is calculated as the negative gradient of the potential energy function V,

$$\mathbf{F}_j = - \partial V (\mathbf{r}_1, \mathbf{r}_2, ..., \mathbf{r}_N) / \partial \mathbf{r}_j \qquad (4)$$

Although there is a fair number of algorithms that have been applied to integrate the equations of motion, the Verlet algorithm [31] is the most common. It uses the forces and the previous positions of the atoms to compute their new position vectors.

The choice of a particular force field depends on the type of system under study. Accordingly, there are several examples of force fields which are widely used, such as MM2 [19] (based on gas phase structures of small organic compounds), AMBER [24] and CHARMM [21] (both aimed at descriptions of proteins and nucleic acids), GROMOS [23] (set up for the simulation of biomolecules in aqueous environment), OPLS [27] (aimed at a proper description of solvation properties), etc.

Both the length and size of the molecular system play major roles in the convergence of computed properties. Molecular dynamics has been used in a wide variety of simulations such as analysis of molecular processes at the atomic level [32-35], determination of spatial molecular structure based on X-ray, neutron diffraction or 2D-NMR data [36], prediction of structural changes [37] and free energy calculations [34,38]. There are, however, quite a few number of complicated problems which are still unsolvable by molecular dynamics: Protein folding and crystallization, for example, present obstacles due to the time scale in which they occur, the size of the configurational spaces involved and also the small free energy differences between folded and unfolded states, for protein folding, or between crystalline and liquid states, for the crystallization process. Molecular dynamics is, however, continuously benefiting from the continuous growth of computing power.

Quantum mechanics

In this section, I shall try to explain why one should want to use quantum mechanics in computer-aided molecular design, rather than try to treat the theory itself [39-43]. In fact, most of the systems of interest here are effectively biological and, more often than not, very complex ones. Why, then, this section in quantum mechanics? Very simply, because there are innumerous cases in which the solution of the problem can be subdivided in such a way that a part of it can and should be treated quantum mechanically. Before going into this, however, a few comments on quantum mechanics itself might be of use to the reader.

It is known that to solve the Schrödinger equation for most molecules, one must resort to several approximations which, within the molecular orbital theory, are time independence assumption, neglect of relativistic effects, Born-Oppenheimer approximation, orbital approximation and linear combination of atomic orbitals approximation. With these approximations one does, in fact, solve the Hartree-Fock self-consistent field equation which resembles the Schrödinger equation. The obtained solutions are named *ab initio* and have certainly made their place in molecular design. GAUSSIAN [44] is a series of programs widely used for this type of calculations. If electron correlation needs to be accounted for, two approaches [41,42] are generally used: Møller-Plesset many-body perturbation theory and configuration interaction. To conclude these brief comments on *ab initio* calculations, one should not underestimate the very important role played by the chosen basis set. There are several excellent reviews and textbooks on the matter [41,42].

Perhaps even more widely used than ab *initio* calculations are the methods termed semi-empirical which deal with very difficult integrals by parameterizing them using empirical data. Several of these methods exist, depending on which kind of parameterization is used. The computer series of programs AMPAC and MOPAC [45] deal with the more used semi-empirical methods to date.

When, then, is quantum mechanics of use in this field of research? Below are some cases where it comes in handy.

If one concentrates on the design of molecules of biological interest, the exercise is quite often that of designing a small molecule that binds to the active centre of a macromolecule. The study of the binding in a case like this can often be treated quantum mechanically with good results [46,47].

One other important use for quantum chemistry, in this field, is the calculation of free energy differences of reactions occurring in the gas state; these values can often be very important to close a thermochemical cycle [48].

Molecules which resemble transition states should be able to act as enzyme inhibitors due to the fact that the major role of catalysts is to reduce the reaction activation energy barrier and, therefore, recognition of transition state structures by enzymes should happen [49]. Pennicillin, for example, is thought to act in this manner. The transition state structures are unstable intermediates with bond lengths and angles unlikely to

be identical to stable compounds; it is thus imperative to use quantum mechanics to define the geometry. There are several algorithms which try to solve this problem [50-52].

Very important too, is the quantum mechanical calculation of parameters of small model species for potential functions that constitute an empirical force field. Subsequently, with those same parameters, large molecules which are impossible to study with quantum mechanics can be treated by molecular mechanics methods [53,54].

Are quantum mechanics and molecular mechanics competitive techniques? The answer is no, as might be deduced from what has been written previously. In fact, in some instances, the two approaches can be regarded as complementary. As far as rigor, capability of determination of electronic properties, generality of parameterization and applicability to short-lived species, quantum mechanics is by far superior to molecular mechanics. However, this latter approach is invaluable in the treatment of large molecules and solvation. One additional advantage of molecular mechanics is that it benefits more from the fast development of computing power than quantum mechanics does. The time needed for a molecular dynamics calculation is linearly dependent on the period of simulation and the number of particles involved, whereas in quantum mechanical calculations the computing time needed is approximately proportional to N (electronic degrees of freedom) to the power of n which ranges from 3 to 5 when considering semi-empirical, Hartree-Fock or configuration interaction, respectively.

Free energy perturbation methods

Statistical mechanics provides a way of calculating the change in the Gibbs or Helmholtz energies for two states, 0 and 1, of a molecular system [55]. Thus, this difference is given as a function of the ratio of the partition functions for the two states, Z_0 and Z_1; for the Helmholtz energy, ΔA

$$\Delta A = A_1 - A_0 = - kT \ln Z_1/Z_0 \qquad (5)$$

with the expression of the partition function, Z_N given by

$$Z_N = \int....\int \exp [- \beta V (\mathbf{r}_1, \mathbf{r}_2,..., \mathbf{r}_N)] \, d\mathbf{r}_1, ..., d\mathbf{r}_N \qquad (6)$$

and

$$\beta = 1 /kT \qquad (7)$$

The perturbational approach defines a parameter λ which links state 0 to state 1. The potential energy V is written as a function of λ, $V(\mathbf{r}, \lambda)$, and the change of λ from 0 to 1 converts the potential for state 0, V(0), into the potential for state 1, V(1).

The Helmholtz energy can, thus, be written as a function of λ

$$A(\lambda) = A_1 - A_0 = kT \ln Z(\lambda) \qquad (8)$$

and be calculated through perturbation methods [37,38]. These convert the value of A in an expression of the kind

$$\Delta A = - kT \ln \langle \exp [- \beta \Delta V(\mathbf{r}_N)] \rangle_0 \qquad (9)$$

where $\langle \rangle_0$ is an ensemble average, of potential $V = V_1 - V_0$, relative to state 0, i.e., the ensemble configurations are all representative of state 0. Equation (9) is applicable only to small perturbations. In general, the method is limited to states which differ by no more than ~2kT (~6.3 kJ/mol at 298 K). In practice, and for processes which involve values of $\Delta A > 2kT$, the perturbation can be considered as a sum of discrete steps along the coordinate and, for each step, $\Delta A < 2kT$. The perturbational approach can, subsequently, be applied to each step i and ΔA, for the total perturbation, is given by the sum over all the steps

$$\Delta A = \sum_{j=0}^{n-1} \Delta A_j \, (\lambda_j -> \lambda_{j+1}) \qquad (10)$$

Free energy perturbation methods (together with other free energy methods) have now been implemented in each of the major distributed simulation programs such as AMBER [24], CHARMM [21] and GROMOS [23].

Design of Enzyme Inhibitors

My interest in computer-aided molecular design started, just over two years ago, with the design of enzyme inhibitors, expressly β-factor Xlla inhibitors. This particular enzyme belongs to the group of blood coagulation proteins which are part of a large group of proteolytic enzymes whose function is to decompose other proteins by reducing them into fragments. There is a great deal of interest in these blood coagulation proteins but, despite the sequence information available, no X-ray studies have been successfully performed on them due to the lack of crystallization forms or quantities needed for such purposes. Human Hageman factor, or factor Xll, is the first component of the complex cascade reactions which form the human blood coagulation system. When in the presence of kallikrein and an anionic surface, factor Xll is activated and converted into β-factor Xlla; subsequent proteolysis yields β-factor Xlla. The structure of β-factor Xlla consists of two polypeptide chains of molecular weights 28,000 and 2,000, respectively, held together by a disulphide bond. Although this is the only external disulphide bond, β-factor Xlla has six other internal disulphide bonds, all part of the heavy chain or H-chain. This one is composed by 243 amino acid residues with the light chain, or L-chain, being constituted by only 9 amino acid residues [56]. Within

the large group of proteins of which the blood coagulation proteins belong, there are others such as the serine proteases. Although the physiological functions of the members of the family are diverse, they all seem to follow the same catalytic mechanism to promote the cleavage of a specific type of chemical bond. Namely, the H-chain of β-factor XIIa has a high degree of homology with trypsin. This latter protein is a pancreatic enzyme which participates in the transformation of the ingested proteins in the constituent amino acids which are subsequently absorbed in the bloodstream.

The design of effective inhibitors of β-factor XIIa is very interesting due to their importance in the medical world; however, the quest for a good inhibitor of the human blood coagulation agent β-factor XIIa requires a structure of the protein. As mentioned before, little is known about the terciary structure of β-factor XIIa [57]. Therefore, the first thing to be done was to build a computer model of the enzyme which remains its only means of visualization. The three-dimensional model for β-factor XIIa [58] was built based on sequence homology with the well known pancreatic serine proteases, bovine trypsin [59], chymotrypsin [60] and elastase [61]. This means that we have made an alignment of regions of all enzymes with identical amino acid sequences. Priority was given to all the cysteines which give rise to homologous disulphide bonds and the catalytic triad in the pancreatic enzymes (His 57, Asp 102 and Ser 195 to use the numbering system of chymotrypsinogen [62]) has been kept in the model of β-factor XIIa; the active site of all enzymes appear highly conserved. The resulting three-dimensional model was subsequently energy minimized with AMBER; it was very interesting to see that minimization of the β-factor XIIa model led to the pairing of all the cysteines, as we know is the case, which in the starting model were not bound together (see Figures 1 and 2).

Bovine pancreatic trypsin inhibitor, BPTI, is a natural inhibitor of trypsin; however, it does not inhibit β-factor XIIa. We thought that it was worth finding out why this does not happen and also modify BPTI to actually inhibit β-factor XIIa, if possible. The terciary structure of the complex formed by BPTI and trypsin has been determined by X-ray crystallography [59] and forms a tetrahedral adduct with a small proportion of both molecules in contact (see Figures 3 and 4). By "contact", it is meant a complicated network of hydrogen bonds and van der Waals and electrostatic interactions. Some external sidechains of the inhibitor (I) which participate in the contact with the enzyme are Lys 15 (I) and Arg 17 (I); the former fills the trypsin binding pocket and interacts, amongst others, with Asp 189 from trypsin which is at the bottom of the pocket, and the latter interacts with Tyr 151, forming a hydrogen bond with the oxygen of His 40. After close inspection of the complex β-factor XIIa:BPTI built with the computer, three changes have been proposed to be made in BPTI, to increase its chance to actually binding β-factor XIIa:

- change Thr 11 (I) to Arg, to allow the formation of hydrogen bonds between residue 11 in modified BPTI and Glu 149 in β-factor XIIa.

- change Lys 15 (I) to Arg. In β-factor XIIa, there is an alanine instead of a serine at position 190. The small size of the alanine as compared to the serine should allow the pocket to accommodate a larger residue, i.e., an arginine would have a more effective binding to Asp 189.

- change Arg 17 (I) to Gly, as there seems to be a bad contact between Arg 17 (I) in BPTI and Ser 40A in β-factor XIIa.

Minimization of the complex β-factor XIIa:BPTI was attempted without any success; however, it was gratifying to see that the complex formed by β-factor XIIa and modified BPTI rapidly converged during the minimization procedure. [63].

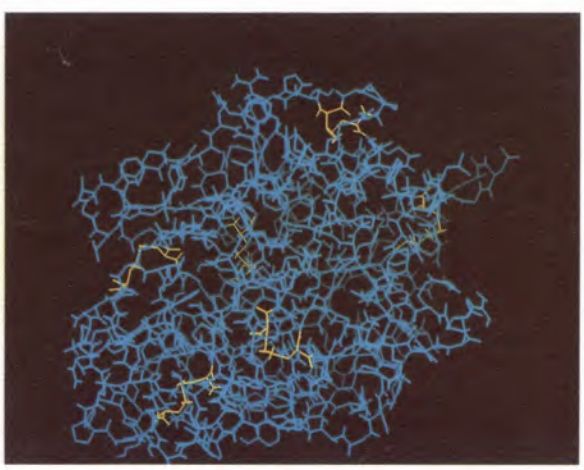

Figure 1. Three-dimensional computer model of human β-factor XIIa complete with sidechains and the six internal disulphide bridges coloured in yellow.

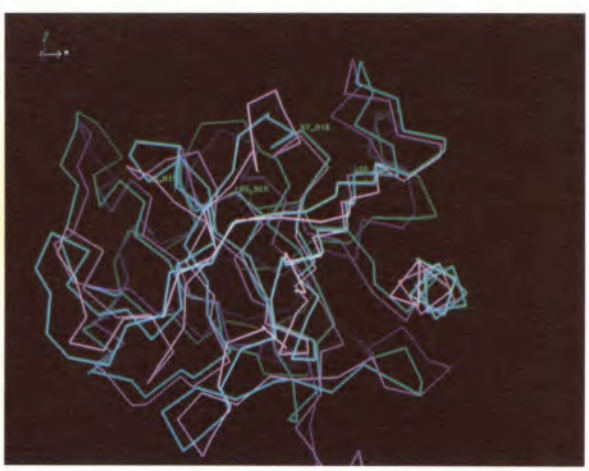

Figure 2. Residues His 40, His 57, Asp 102 and Ser 195 of human, β-factor XIIa (in purple) superimposed on bovine pancreatic trypsin (in green). Only the α-carbons of both enzymes are shown for simplicity.

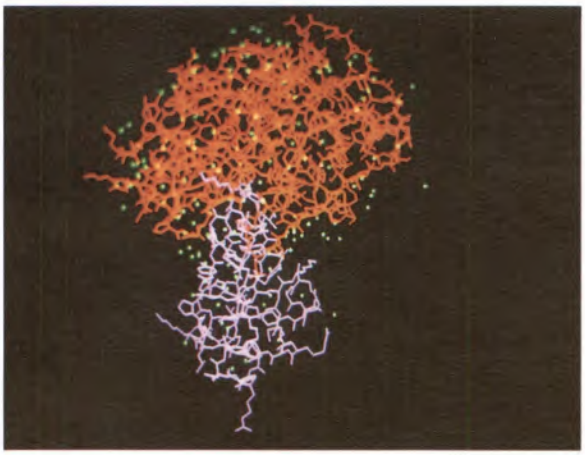

Figure 3. View of the three-dimensional complex formed by BPTI (in purple) and bovine pancreatic trypsin (in red). Crystallization water molecules are shown in green.

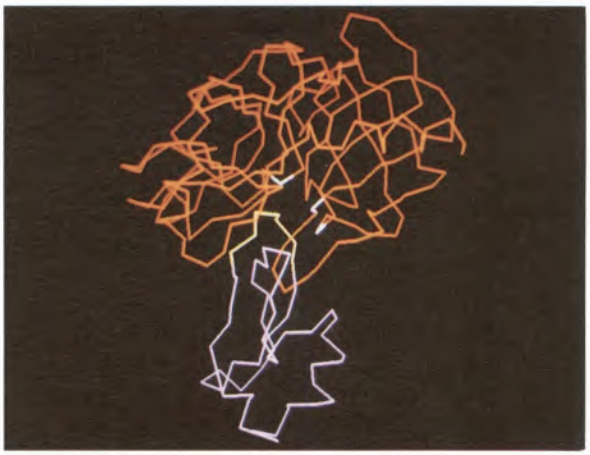

Figure 4. A simplified view (only the α-carbons are shown) of the three-dimensional complex formed by BPTI (in purple) and bovine pancreatic trypsin (in red). The catalytic triad, i.e. residues His 57, Asp 102 and Ser 195, are coloured white and, in yellow, is the contact region of BPTI with trypsin.

Enzyme: inhibitor binding interaction

Despite the study described above, there might be an additional problem caused by the non-existence of a hydrogen bond between Ile 19 (I) and Gly 39 (in β-factor XIIa). In the model of β-factor XIIa, Gly 39 cannot lead to the formation of a hydrogen with Ile 19 (I) or any other residue in BPTI, and this could be the reason why BPTI does not bind to β-factor XIIa, since the corresponding Ile 19 (I) - Tyr 39 (in trypsin) interaction is an important one for the binding of trypsin by BPTI [64]. We are studying this very interaction quantitatively, using free energy perturbation methods to calculate the change in the Gibbs energy ΔΔG

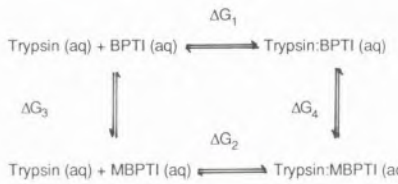

(10)

where MBPTI stands for mutated BPTI, i.e., BPTI with a mutated amino acid and $\Delta\Delta G = \Delta G_2 - \Delta G_1 = \Delta G_4 - \Delta G_3$. In fact, $(\Delta G_2 - \Delta G_1)$ cannot be calculated directly, through free energy perturbation methods, given the enormity of the configurational space which would be necessary to sample and also because the reaction involves desolvation steps which are very slow; therefore, it is $(\Delta G_4 - \Delta G_3)$ the determined quantity.

In the case of the Ile 19 (I) - Tyr 39 interaction, the mutation of one of these amino acids to another, incapable of forming a hydrogen bond, will give rise to a ΔΔG which will be a measure of the strength of that same interaction. Preliminary results suggest that this interaction is not imperative for the binding of BPTI to trypsin and, therefore, to β-factor XIIa [65]. The same sort of study is being carried out for some other important interactions in the complex trypsin:BPTI, namely the P1 binding site, in an attempt to better understand them. This will certainly be of use in the design of new inhibitors for β-factor XIIa, given the fact that the active sites of both proteases present a great degree of homology. Yet, the functional differences of both sets of enzymes must be translated somehow into differences in the respective active sites or putative extended substrate binding sites that surround the active site [56,66,67] and, therefore, a good understanding of one might help to develop inhibitors for the other.

We have also carried out some other studies of the enzyme:inhibitor binding interactions. In the β-factor XIIa:modified BPTI complex Arg 15 (I) fills the β-factor XIIa binding pocket and interacts, amongst others, with Asp 189 from β-factor XIIa. This type of interaction, arginine-aspartate, is very important in proteins and, in fact, accounts for more than 40% of the ionic pairs interactions found in proteins [68,69]. A conformational analysis has been performed, using the semi-empirical method AM1, for the interactions of guanidinium and methylguanidinium with formate and acetate (see Figure 5), in vacuo, to simulate arginine-carboxylate interactions in proteins. Its interpretation has also been done with the total energy partitioned in different components and by centres [70]. The importance of the guanidinium--carboxylate interactions has arisen from the observed salt bridges often present in biological systems involving the arginine, glutamate and aspartate sidechains. The strength of these interactions has been suggested as fundamental for the stability of such systems [68]. Usually, this is explained on the basis of a great coulombic energy gain, due to the closeness of two charges of opposite sign and the occurrence of H-bond interacti-

ons. However, the relaxation of the complex geometries, for each conformation, allow the hydrogen atoms to move in the hypersurface potential and choose the most suitable position between the ions. We have found an increase in the absolute value of the interaction energy in regions where proton transfer occurs, with the consequent annihilation of charge. The importance of these results arises from the fact that normal X-ray crystallography experiments cannot provide information on the positions of hydrogen atoms, so that a complete description of these interactions may fail if we restrict these atoms to the amino acid sidechains to which they normally belong. The process of proton transfer is being confirmed by more sophisticated *ab initio* calculations carried out at the minimum energy conformations obtained by the above mentioned work [71].

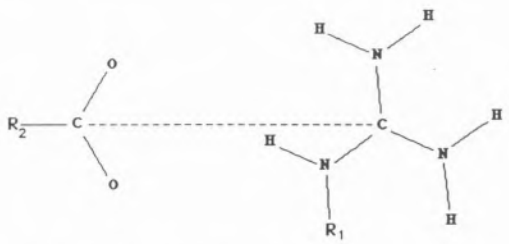

Figure 5. Schematic representation of guanidinium (R1 = H) or methylguanidinium (R1 = CH3) and formate (R2= H) or acetate (R2 = CH3).

The same sort of study is being done for the interaction lysine-aspartate which also occurs often in proteins, e.g. in the pocket of the trypsin:BPTI complex, as stated previously. This latter work has been preceded by a small semi-empirical study of the behaviour of the lysine and glutamine sidechains on their own and as part of a minipeptide (see Figures 6 and 7), both *in vacuo* and solvated [72] using the supermolecule approach [73]. We have found that although glutamine does not seem to be particularly affected by either its inclusion in a peptide or the solvation effect, lysine seems to

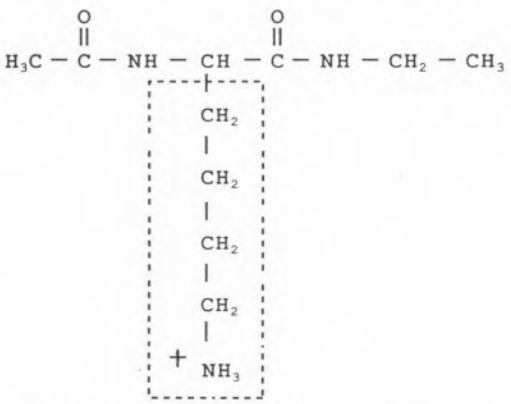

Figure 6. Schematic representation of lysine as part of a minipeptide. The sidechain of lysine is enclosed in a broken line rectangle

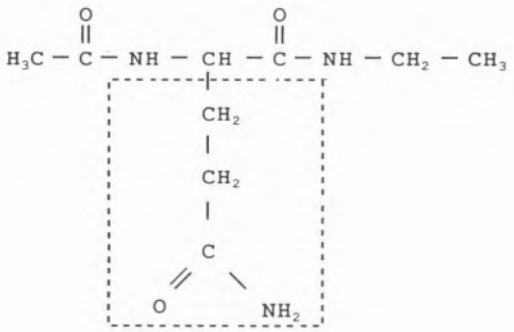

Figure 7. Schematic representation of glutamine as part of a minipeptide. The sidechain of glutamine is enclosed in a broken line rectangle.

adopt a *gauche* conformation when under the influence of the mainchain of a peptide; this tendency for a *gauche* conformation is somewhat attenuated by the solvation effect, thus increasing the possibility of appearance of a *trans* conformation.

Simulations of biomolecular systems

One of the systems that I am interested in is the complex formed between copper, diazepam (DZP) and GABA, $[Cu\ (DZP)\ (GABA)]^{2+}$ (aq). The diazepam is a drug with a hipnotic action, commonly referred to as Valium. On the other hand, it is well known that there is copper in the human brain, playing an important role in its development, maintenance and function. Thus, a study of the interactions between copper and psycho-therapeutic drugs, such as Valium, are bound to be important in the study of psychic phenomena. Finally, GABA is a neurotransmittor which is able to interact with the complex between Cu and diazepam; it is precisely the effect of the metallic ion in the pharmaco-transmittor interaction that is interesting.

The constant of formation of this complex via the reaction

$$Cu^{2+}(aq) + DZP(aq) + GABA(aq) \longleftrightarrow [Cu\ (DZP)\ (GABA)]^{2+}(aq) \qquad (11)$$

is unknown; it is, however, being determined experimentally [74] and our group is presently engaged in obtaining it by theoretical means. We are doing it using some of the techniques previously mentioned, namely molecular mechanics, quantum mechanics and free energy perturbation methods. More precisely, we are calculating the constant of formation of that complex through the determination of the change in the Gibbs energy for reaction (11) using the following thermochemical cycle:

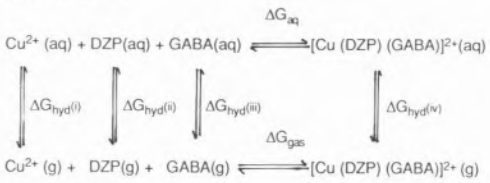

(10)

ΔG_{aq} and K_{form} are related by:

$$\Delta G_{aq} = 2.303\ R\ T\ pK_{form} \quad (13)$$

$$= \Delta G_{gas} - \Delta G_{hyd(i)} - \Delta G_{hyd(ii)} - \Delta G_{hyd(iii)} + \Delta G_{hyd(iv)} \quad (14)$$

One of the reasons why we cannot calculate ΔG_{aq} directly, via free energy perturbation methods, having to use this thermochemical cycle, is because for aqueous systems (such as biomolecules in water) there is a huge number of accessible states in the configurational space for us to be able to sample successfully this same space through a molecular dynamics simulation.

We are calculating ΔG_{gas} using quantum mechanical methods, i.e., determining the *ab initio* energies which lead us to the enthalpies at 0 K without the zero-point corrections. However, second derivatives calculations allow us to find out the harmonic frequencies through the hessian matrix and, thus, obtain the zero-point energies with which we can derive ΔH and ΔS at 298 K. These zero-point corrections are small and easily obtained using semi-empirical methods, such as AM1 [75]. Figures 8 and 9 show the structures of DZP and GABA, respectively, which are being used in these calculations.

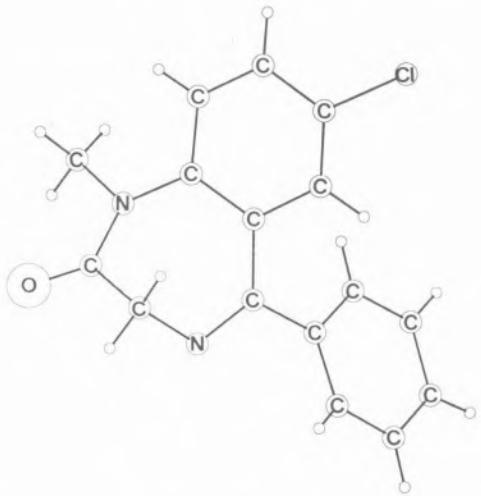

Figure 8. Schematic representation of diazepam. All the unnamed atoms are hydrogen atoms.

On the other hand, $\Delta G_{hyd}(i)$, $\Delta G_{hyd}(ii)$, $\Delta G_{hyd}(iii)$ and $\Delta G_{hyd}(iv)$ are being determined using free energy perturbation methods and, therefore, molecular dynamics. We are obtaining some of the force field parameters also using *ab initio* methods. Others can be found in the literature. One must be specially careful with the atomic charges, for the involved species, to use in the force field. The Mulliken charges are not reliable and, therefore, we are deriving net atomic charges from *ab initio* calculations using a least squares fit of the quantum mechanically calculated electrostatic potential to that of the partial charge model.

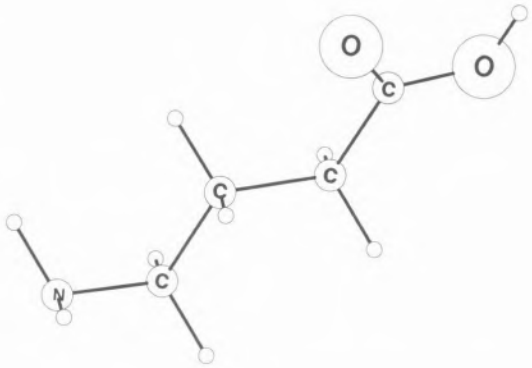

Figure 9. Schematic representation of GABA. All the unnamed atoms are hydrogen atoms.

Conclusion

This short article tried to give the reader a general idea of computer-aided molecular design and examples of the type of work that our group is doing in this field of research. Although the area is very recent, it has already been covered by a few books [26,32,76-79] and over a couple of thousand articles are being published annually on predicted molecular properties in satisfactory agreement with experiment. These properties range from geometric data to transport properties focussing also on electronic properties, molecular interactions, energies and thermodynamics, and spectroscopic properties. Computational chemistry techniques are also being used to predict longer life herbicides and more potent drugs. The literature refers to cases in which computing has been of invaluable assistance in the design of products already commercially available [78]. These are actually difficult to account for due to the degree of secrecy in the industry. However, what has been published already is more than enough to demonstrate that computer-aided molecular design can have a major contribution to decide which molecules are expected to be important for a given purpose.

Hardware and software capable of high resolution graphics display, molecular mechanics, quantum mechanics and statistical mechanics computer programs are essential for this field of research as well as access to the appropriate databases. And, above all, one should wish for close collaboration between theoreticians and experimentalists!

Acknowledgements

Financial support from JNICT (Stride/Bio/364/92) is gratefully acknowledged .

References

1. F. H. Allen, S. Bellard, M.D. Brice, B.A. Cartwright, A. Doubleday, H. Higgs, T. Hummelink, B.G. Hummekink-Peters, O. Kennard, W.D.S. Motherwell, J.R. Rodgers, D.G. Watson, *Acta Cryst.* **835** (1979) 2331.

2. E.E. Abola, F.C. Bernstein, S.H. Bryant, T.F. Koetzle, J. Weng, in *Crystallographic Databases: Information Content, Software Systems, Scientific Applications,* F.H. Allen, G. Bergerhoff, R. Sievess, eds. Data Commission of the International Union of Crystallography, Cambridge, England, 1987.

3. J.H. Van Drie, D. Weininger, Y.C. Martin, *J. Comput.-Aided Mol.Design* **3** (1989) 225.

4. P.A. Bartlett, G.T. Shea, S.J. Telfer, S. Waterman, *Chemical and Biological Problems on Molecular Recognition,* S.M. Roberts, S.V. Ley, M.M. Campbell, eds. Royal Society of Chemistry, 1990.

5. Anon. MedChem Software Manual, Release 3.54, Daylight Chemical Information Systems, Inc. Claremont, CA, USA, 1989.

6. A. Rusinko III, R.P. Sheridan, K.S. Nilakantan, N. Haraki, Bauman, Venkataraghavan, *J. Chem. Inf. Comput. Sci.* **29** (1989) 251.

7. MACCS-II, MACCS-3D, Molecular Design Limited, San Leandro, California, 94577, USA.

8. S.E. Jakes, N. Watts, P. Willett, D. Bawden, J.D. Fischer, *J. Mol. Graphics* **5** (1987) 41.

9. R. Langridge, T.E. Ferrin, I.D. Kuntz, M.L. Connolly, *Science* **211** (1981) 661.

10. A. Rusinko III, J.M. Skell, R. Balducci, R.S. McGarity, Pearlman, The University of Texas at Austin and Tripos Associates, St. Louis, Missouri, USA, 1988.

11. N.A. Dittmar, W. Farmer, R.C. Fisanick, J. J. Haines, Mockus, *Chem. Inf. Comput. Sci.* **23** (1983) 93.

12. D.E. Knuth, The Art of Computer Programming, 3: Sorting and Searching, Addison-Wesley, Reading, MA,1973.

13. D. Harel, *Algorithmics: The Spirit of Computing,* Addison-Wesley, Reading, MA, 1987.

14. W.T. Wipke, T.M. Dyott, *J. Am. Chem. Soc.* **96** (1974) 4834.

15. INSIGHT II, Biosym Technologies, 10 quai Léon Blum, 92150 Suresnes, France.

16. QUANTA, Molecular Simulations Inc. 200 Fifth Avenue, Waltham, MA 02154, USA.

17. SYBYL, Tripos Associates, St. Louis, Missouri, USA.

18. A. Paskin, A. Rahman, *Phys. Rev. Lett.* **16** (1966) 300.

19. N.L. Allinger, *J. Am. Chem Soc.* , **99**, (1977) 8127; U. Burkert, N.L. Allinger, *Molecular Mechanics,* American Chemical Society, Washington D.C.

20. L.G. Dunfield, A.W. Burgess, H.A. J. Scheraga, *Phys. Chem.* **82** (1978) 2609.

21. B.R. Brooks, R.E. Bruccoleri, B.D. Olafson, D.J. States, S. Swaminathan, M. J. Karplus, *Comput. Chem.* **4** (1983) 187.

22. G. Nemethy, M.S. Pottle, H.A. Scheraga, *J. Phys. Chem.* **87** (1983) 1883.

23. J. Hermans, H.J.C. Berendsen, van W.F. Gunsteren, J.P.M. Postma, *Biopolymers* **23** (1986) 1513.

24. S.J. Weiner, P.A. Kollman, D.T. Nguyen, D.A. Case, (1986) *J. Comput. Chem.* **7** (1984) 230.

25. van W.F. Gunsteren, H.J.C. Berendsen, *Groningen Molecular Simulation (GROMOS) Library Manual,* Biomos, Groningen, 1987.

26. M.P. Allen, D.J. Tildesley, *Computer Simulations of Liquids,* Clarendon, Oxford, 1987.

27. W.L. Jorgensen, J. Tirado-Rives, *J. Am. Chem Soc.***110** (1988) 1657.

28. S.N. Ha, A. Giammona, M. Field, J.W. Brady, *Carbohydr. Res.* **180** (1988) 207.

29. Heinzinger in C.R.A. Catlow, S.C. Parker, M.P. Allen, eds. *Computer Modelling of Fluid Polymers and Solids* (NATO ASI Ser. C 293, (1990) **357**.

30. van W.F. Gunsteren, H.J.C. Berendsen, *Angew. Chem. Int. Ed. Engl.* **29** (1990) 992.

31. L. Verlet, *Phys. Rev.* **159** (1967) 98.

32. J.A. McCammon, S.C. Harvey, *Dynamics of Proteins and Nucleic Acids,* Cambridge University Press, London, 1987.

33. E. Egberts, H.J.C. Berendsen, *J. Chem. Phys.* **89** (1988) 3718.

34. van Gunsteren, P.K. Weiner, eds. *Computer Simulations of Biomolecular Systems,* Escom, Leiden, 1989.

35. de J. Vlieg, H.J.C. Berendsen, van W.F. Gunsteren, *Proteins* **6** (1989) 104.

36. R. Kaptein, R. Boelens, R.M.Scheek, van W.F.Gunsteren, *Biochemistry* **27** (1988) 5389.

37. P. Gros, M. Fujinaga, A. Mattevi, F.M.D. Vellieux, van W.F. Gunsteren, W.G.J. Hol, in *Molecular Simulation and Protein Crystallography* (Proc. Joint CCP4/CCP5 Study Weekend) SERC, J. Goodfellow, K. Henrick, R. Hubbard, eds. Daresbury, 1989.

38. D.L. Beveridge, F.M. DiCapua, *Ann Rev. Biophys. Chem.* **18** (1989) 431.

39. J.P. Lowe, *Quantum Chemistry,* Academic Press Inc. Orlando, 1978.

40. J.A. Pople, *Ab Initio Molecular Orbital Theory,* Wiley-Interscience, New York, 1986.

41. A. Szabo, N. Ostlund, *Modern Quantum Chemistry: Introduction to Advanced Electronic Structure Theory,* McGraw-Hill, New York, 1989.

42. T. Clark, *A Handbook of Computational Chemistry: A practical Guide to Chemical Structure and Energy Calculations,* Wiley-Interscience, New York,1985.

43. M.J.S. Dewar, *The Molecular Orbital Theory of Organic Chemistry,* McGraw-Hill, New York,1969.

44. GAUSSIAN, Carnegie Office Park, Building 6, Pittsburgh, PA 15106 U.S.A.

45. AMPAC and MOPAC, QCPE, Creative Arts Bldg. 181, Indiana University, 840 State Highway 46 Bypass, Bloomington, IN 47405, U.S.A.

46. C.A. Reynolds, W.G. Richards, P.J. Goodford, *Anti-Cancer Drug Design* **1** (1987) 291.

47. C.A. Reynolds, P.M. King, W.G. Richards, *Nature* **334** (1988) 80.

48. C.A. Reynolds, P.M. King, W.G. Richards, *J. Chem. Soc. Chem. Commun.* (1988) 1434.

49. L. Pauling, *Am. Scient.* **36** (1948) 51.

50. K. Jug, *Theoret. Chim. Acta* **54** (1980) 263.

51. J.D. Head, B. Weiner, M.C. Zerner, *Int. J. Quantum Chem.* **23** (1988) 177.

52. R. Fletcher, in *Numerical Methods for Unconstrained Optimization,* W. Murray ed. Wiley, London,1981.

53. D.B. Boyd, *Drug Inf. J.* **17**(1983) 121.

54. J.R. Maple, U. Dinur, A.T. Hagler, *Proc. Natl. Acad. Sci. U.S.A.* **85** (1988) 5350.

55. D.A. McQuarrie, *Statistical Mechanics,* Harper & Row, rew York, 1976.

56. K. Fujikawa, B.A. McMullen, *J. Biol. Chem.* **258** (1983)10924.

57. M. Baron, D. Norman, A. Willis, I.D. Campbell, *Nature* **345** (1990) 642.

58. M.J. Ramos, *J. Mol. Graphics* **9** (1991) 91.

59. M. Marquart, J. Walter, J. Deisenhofer, W. Bode, R. Hüber, *Acta Crystallogr. Sect. B* **39** (1983) 480.

60. G.H. Cohen, E.W. Silverton, D.R. Davies, *J. Mol. Biol.* **449** (1981) 148.

61. L. Sawyer, D.M. Shotton, J.W. Campbell, P.L.Wendell, H. Muirhead, H.C. Watson, R. Diamond, R.C. Ladner, *J. Mol. Biol.* **118** (1978)137.

62. B.S. Hartley, D.L. Kauffman, *Biochem. J.* **101** (1966) 229.
63. M.J. Ramos, W.G. Richards, *Drug News & Perspectives* **5** (1992) 325.
64. J. Janin, C. Chothia, J. *Mol. Biol.* **100** (1976) 197.
65. M.J. I Ramos, to be published.
66. B. I Furie, B.C. Furie, *Cell,* **53** (1988) 505.
67. B. Furie, D.H. Bing, R.J. Feldmann, D.J. Robison, J.P. Burnier, B.C. Furie, *J. Biol. Chem.* **257** (1982) 3875.
68. D.J. Barlow, J.M. Thornton, J. *Mol. Biol.* **168** (1983) 867.
69. J.B.D. Mitchell, J.M. Thornton, J. Singh, S.L. Price, *J. Mol. Biol.* **226** (1992) 251.
70. A. Melo, J.F.R. Leão, A.L. Magalhães, M.J. Ramos, *J. Chem Soc. Faraday Transactions,* submitted.
71. A. Melo, M.J. Ramos, to be submitted.
72. A. Melo, M.J.S. Ferreira, A.M. Ferreira, M.J. Ramos, *J. Mol. Structure (THEOCHEM),* submitted.
73. A. Pullman, B. Pullman, *Q. Rev. Biophys.* **7** (1975) 505.
74. B. Castro, private communication.
75. M.J.S. Dewar, E.G. Zoebisch, F. Heale, J.J.P. Stewart, *J. Am. Chem. Soc.* **107** (1985) 3902.
76. C.L. Brooks, M. Karplus, B.M. Pettitt, *Proteins: a theoretical perspective of dynamics, structure and thermodynamics,* l. Prigogine, S. Rice, eds. John Wiley, New York, *Adv. Chem. Phys.* (1988) **71**.
77. W.G. Richards, ed. *Computer-Aided Molecular Design,* IBC Technical Services Ltd. London, 1989.
78. K.B. Lipkowitz, D.B. Boyd, eds. *Reviews in Computational Chemistry,* VCH Publishers, Inc. New York,1990.
79. K.B. Lipkowitz, D.B. Boyd, eds. *Reviews in Computational Chemistry,* vol. **2**, VCH Publishers, Inc., New York, 1991.

Raman spectroscopy: a survey on selected topics

Espectroscopia de Raman: alguns tópicos

J. J. C. TEIXEIRA-DIAS

DEPARTAMENTO DE QUÍMICA, UNIVERSIDADE DE COIMBRA, P-3049 COIMBRA, PORTUGAL

Raman spectroscopy is a widely used and powerful analytical tool, being regularly used to provide information on the structure and dynamics of molecular systems and their interactions. In this article, the time-independent second order perturbation expression for the intensity of a Raman transition is examined and discussed in connection with i) the selectivity of a Resonance Raman process, ii) the lifetime of the intermediate state, iii) the distinction between a scattering and an absorption + emission (fluorescence) process, and iv) the saturation effect in a Raman transition. The setup of a Raman experiment is briefly considered. Conformational studies of a number of organic compounds (amines, α-substituted toluene molecules, α,β-unsaturated carbonyl compounds) are presented to illustrate the potentialities of Raman spectroscopy in providing structural information on molecular systems.

Para além de ser uma técnica espectroscópica muito utilizada e de ter enormes potencialidades analíticas, a Espectroscopia de Raman fornece informações sobre a estrutura e a dinâmica de sistemas moleculares e suas interacções. Neste artigo, estuda-se a expressão da intensidade de uma transição de Raman obtida pela teoria das perturbações dependentes do tempo, considerando-se, em especial, a selectividade do processo de Raman de Ressonância, o tempo de vida do estado intermédio, e a distinção entre o processo de difusão da radiação e o conjunto dos processos de absorção seguida de emissão (fluorescência). Considera-se também o efeito de saturação numa transição de Raman. As potencialidades da Espectroscopia de Raman como fonte de informação estrutural são ilustradas através da apresentação dos resultados de estudos conformacionais em vários compostos orgânicos (aminas, moléculas de tolueno α-substituídas, compostos de carbonilo α,β-insaturados).

1. Introduction

In the issue of *Nature*, March 31, 1928, page 501, a scientific note signed by C.V.Raman and his student K.S.Krishnan was published, entitled "A new type of secondary radiation" [1]. Using an analogy with X-ray scattering, it was claimed that two types of scattering, one determined "by the normal optical properties of the atoms or molecules, and another representing the effect of their fluctuations from their normal state", should be expected also in the case of ordinary light [1]. A simple experiment with a beam of sun light and a liquid sample in between two light filters — a blue-violet filter and a green-yellow one — supported these conclusions. In a subsequent issue of *Nature* (April 21), another paper, this time signed only by Raman and entitled "A change of wave-length in light scattering", was published in page 619 [2]. It is interesting to note the worries of Raman at the time, and his reasoning to convince himself that the observed secondary radiation was not a fluorescence. The "excessive feebleness" of this "modified scattering" and its "polarization characteristics" were also pointed out [2]. A month later, in another issue of *Nature* (this time May 5), Raman and Krishnan published an explanatory note of the observed effect, entitled "The optical analogue of the Compton effect" [3].

When monochromatic light of frequenc ν_o is incident on a transparent sample and the scattered light is analysed in frequency and measured in intensity, the spectrum of inelastically scattered radiation, the Raman spectrum of the sample, is obtained. Nowadays, Raman spectroscopy is a widely used and powerful analytical tool, which provides information on the structure and dynamics of molecular systems and their interactions. This article surveys on a few selected topics to show some of the capabilities of Raman spectroscopy. On the whole, they all emerge from the time-independent second order perturbation expression for the intensity of a Raman transition, as it will be shown herein. The setup of an up to date Raman experiment will be briefly

considered. Conformational studies of a number of organic compounds (amines, α-substituted toluene molecules, α,β-unsaturated carbonyl compounds) will be presented to illustrate the possibilities of Raman spectroscopy in providing structural information on molecular systems.

2. Intensity of a Raman transition

Raman cross section

The intensity of a Raman transition from the initial vibronic state, $/n> = /gi>$, to the final vibronic state, $/m> = /gi>$, is given by

$$I_{nm} \approx \sigma_{nm} I_o \qquad (1)$$

where uninteresting constants have been omitted (≈ should be read "is proportional to"), I_0 represents the intensity of the monochromatic source of radiation (a laser), and σ_{nm} is the angular differential cross section for the inelastic scattering of radiation. In turn, this quantity is given by

$$\sigma_{nm} \approx \nu_o \nu_S^3 \rho_n \Sigma / (\alpha_{\rho\sigma}) / ^2 \qquad (2)$$

where ν_o and ν_S represent the excitation and scattered frequencies, ρ_n is the population of the inital state, $/n>$, $\alpha_{\rho\sigma}$ represents the polarizability transition moment, with the incident and scattered polarizations of the radiation represented by σ and ρ, respectively, the summation being over these subscripts. Time-independent second order perturbation theory shows that $\alpha_{\rho\sigma}$ is given by

$$\alpha_{\rho\sigma} \approx \Sigma < n / \rho / e > < e \nu / \sigma / m > (\nu_{e\nu} - \nu_o + i\Gamma_{e\nu})^{-1} + \text{non-resonance term} \qquad (3)$$

where Γ stands for the bandwidth of the intermediate state $/e\nu >$ and the summation is over the intermediate states. In this summation, the term associated with the downard transition, from $< e\nu /$ to $/ m >$, has been neglected, since its denominator, $\nu'_e + \nu_o + i\Gamma \nu_e$, is comparatively large. This term excludes the possibility of resonance, due to the addition of frequencies in the denominator. For that reason it is often referred to as the *nonresonance term*.

Resonance Raman

Expression (3) enables one to consider the intensity variation as a function of excitation frequency (excitation profile of a band). In particular, when the laser frequency approaches a resonance with a discrete transition, the excited state corresponding to that resonance is singled out as the denominator in (3) decreases drastically and the Raman cross section increases abruptly, sometimes by a factor of 10^6. This *selective enhancement* has pratical consequences of great relevance as it enables to single out, even in a macromolecule, a particular chromophore by its Resonance Raman (**RR**) spectrum obtained in very diluted solutions. For example, considering myoglobin, excitation at ≈ 210 nm allows to single out the Raman spectrum of the **-(H)NC(=O)-** group, whereas excitation at 225 nm enables to select the aromatic aminoacids tyrosine and tryptophane. In addition, if the laser frequency is close to 400 nm, then the heme is singled out, and at ≈ 500 nm the vibrational bands characteristic of the iron-ligands bonds are observed [4].

Lifetime of the intermediate state

The lifetime of the intermediate state, τ, is related with the bandwidth of that state, Γ, through the well known relationship,

$$\Gamma \tau > 1/2 \pi \qquad (4)$$

For example, for $\Gamma = 3\ cm^{-1}$, $\tau > 2$ ps. The experimental determination of τ requires a pulsed laser. In particular, when a rectangular pulse of 100 ns duration is applied to gaseous diatomic iodine, one or two time-dependent phenomena may be observed, depending on whether the excitation frequency is in exact resonance with a discrete rovibronic transition—time constant of the order of 5×10^2 ns, RR effect—, or slightly out-of-resonance (for instance, 1.2 GHz away from that transition) [5]. In this case two different time constants are observed, one extraordinarily short, tipical of an almost instantaneous process (normal Raman effect), the other being equal to the RR time constant mentioned before [5].

The nature of the process for the interaction of radiation with matter—radiation scattering or absorption followed by emission (fluorescence)—results from the lifetime of the intermediate state. For a sufficiently short lifetime, the up and down transitions are part of the same process (radiation scattering). On the other hand, if the residence time of the molecule in the intermediate state is sufficiently long to enable the occurrence of *molecular collisions* (these lead to non-radiative vibrational relaxation), then one cannot speak of a single process, but rather of an absorption followed by emission (fluorescence). In gaseous phase, the increase of pressure will undoubtly decrease the time between collisions, thus giving rise to a gradual transition between a single RR process and two distinct processes, one of absorption, the other of fluorescence.

In the inelastic scattering of radiation, the up and down transitions are physically undistinguishable processes. By a well known principle of quantum mechanics, in order to obtain the total intensity of the process, one has to add the individual amplitudes—*interference is* then taken into consideration—and take the square of the total amplitude to obtain the intensity. On the other hand, if two physically distinguishable

processes are occurting (absorption + fluorescence), then one simply adds the individual intensities. This happens when an intertuption of phase occurs in the intermediate state, as caused, for example, by molecular collisions.

Interference between intermediate states in RR

As it was mentioned before, the summation in (3) is over the intermediate states in a Raman process. In principle, each term is a complex quantity, with real and imaginary parts. Hence, the square of this summation is not simply the sum of the squares of the terms, as crossed terms should be considered. The contribution of these corresponds to *interference between different intermediate states* and has been experimentally confirmed. For instance, in the case of the totally symmetric breathing mode of benzene, the excitation profile obtained with excitation around the $6^1_0 1^5_0$, ($^1B_{2u} < — \ ^1A_{1g}$) transition could only be theoretically reproduced when interference between different excited states of benzene was explicitly considered [6].

Saturation in a Raman transition

Substitution of (2) in (1) seems to suggest that the Raman intensity increases linearly with the intensity of the radiation source, I_o, or, in the case of a pulsed laser, with the energy flux (units: number of photons.area^{-1}) of each laser pulse. This is not always the case. For instance, the intensity of the 1578 cm^{-1} band of tryptophanamide decreases as the energy flux increases, for sufficiently high values of this [4]. This saturation effect can be understood looking again at the expression which results from substitution of (2) in (1). In fact, for sufficiently large energy fluxes, the population of the initial state, ρ_n, depends on time, as the rate of repopulating the initial state may be smaller than its depletion rate. In other words, ρ_n depends indirectly on I_o. Apparently, this is not a desirable situation, as a decrease of a band intensity reflects unfavourably on its signal/noise ratio. However, the saturation effect may be used in the future to the experimentalist advantage, in a technique similar to the NMR multiple irradiation decoupling technique [4]. In fact, if two distinct Raman bands display quite different saturation effects, it is possible, in principle, to subtract out one of the bands by spectra difference (the band which displays a stronger saturation effect will show out in the difference of spectra). This technique, named *Raman decoupling spectroscopy* [7], has been successfully applied to the pyrene molecule in two distinct chemical environments [7].

3. Experimental setup

A dispersive instrument for Raman spectroscopy includes a source of monochromatic radiation, a sample device, a dispersing system and a detection/ /recording system. An adequate choice of the frequency of the laser is required to fulfil the objectives of the experiment. In particular, fluorescence may be avoided if a sufficiently long wavelength is selected [8,9]. Modern Raman spectrometers are usually equipped with both a macro sample compartment and a microscope. In fact, so important is the possibility of studying microscopic samples that *Raman Micro-spectroscopy* is a new experimental field on its own [10]. The dispersing system consists of a monochromator to disperse the ligth scattered by the sample. Through scattering at optical surfaces, particularly the gratings, a small fraction of light with the laser frequency will appear in the output focal plane at positions corresponding to other frequencies in the neighbourhood of the excitation frequency. In order to improve *stray light rejection,* double, or triple dispersion preferably, should be used [11]. At the detection stage, monochannel and multichannel detectors can be employed. In particular, comparison of the quantum efficiency curves of a PMT (PhotoMultiplier Tube) with a CCD (ChargeCoupled Device) [12] in the studied wavelength region should be done before one of these detectors is selected.

4. Conformational studies

Conformers

Rotation about a single bond, like the rotation around a single CC bond, may occur in a molecule without alteration of its covalent structure, resulting in different spatial arrangements or *conformations.* Each conformation may have a distinct energy, and lower energy conformations will be populated in preference to those of higher energy. The conformations which correspond to energy minima are called *conformational isomers* or *conformers.*

The concept of conformation lies on that of potential energy surface. In turn, the potential energy surface of a molecule emerges as a function of nuclear motion, when the electronic and nuclear Schrodinger equation is solved in the fixed nuclei approximation (Born--Oppenheimer approximation).

The basic idea underlying *Conformational Analysis* is that the chemical and physical properties of compounds are closely related to preferred conformations. To emphasize this point, the concept of "molecule" is sometimes generalized to include that of conformer. This should not be of a surprise, as a conformer corresponds to a minimum of potential energy. In fact, in this broad sense, a conformational change involves a "reactive" motion, though a relatively simple one, as it does not alter the covalent structure of the molecule. To distinguish between the motion inside a potential well and the motion associated with a conformational change, we refer to the first as a "nonreactive" motion.

Vibrational band intensities vs. ΔH° between conformers.

In principle, a particular vibrational mode of a molecule in two different stable conformations (A and B) corresponds to different frequencies and distinct band intensities (I_A and I_B) If the energy barrier for the interconversion of these conformations is not sufficiently high in comparison with kT (at T=298K, kT≈ 207 cm^{-1}), an equilibrium is established whose constant satisfies the equality

$$\ln K = \ln(c_B/c_A) = (-\Delta H^\circ/R)\ (1/T) + \Delta S^\circ/R. \qquad (5)$$

As the concentrations are related with band intensities of the corresponding forms, $c_A = IA/\alpha_A$, $c_B = I_B/\alpha_B$, (α_A and α_B represent molar intensities), one concludes that

$$\ln(I_B/I_A) = (-\Delta H^\circ/R)\ (1/T) + \Delta S^\circ/R + \ln(\alpha_B/\alpha_A) \qquad (6)$$

Hence, the logarithmic ratio of band intensities plotted against inverse temperature should give a straight line whose slope is $-\Delta H^\circ/R$.

Ethylmethylamine-N,d

This molecule *(EMA-d)* has one conformational degree of freedom, namely, the rotation about **CN—CC**. Besides the *trans (T)* conformer, two additional stable conformations are expected, both *gauche (G, G'):* one has the nitrogen lone pair of electrons *trans* with respect to the CC bond, the other has instead the HN bond *trans* to the same bond (note that the N atom is asymmetric, *i.e.,* four distinct electron pairs come out from it: three distinct bonds and one lone pair of electrons).

The Raman spectra of EMA-d in the liquid phase presents three bands at 1017, 996 and 975 cm^{-1} which are assigned to νCC+νNC in the T, G e G' conformers, respectively [13]. These bands display tempera-ture-dependent intensities: with decreasing temperature, the bands at 996 and 975 cm^{-1} decrease in their intensities relative to the 1017 cm^{-1} band. In the solid phase, a single band at 1019 cm^{-1} remains. Temperature dependent band intensities in the liquid phase yield the following experimental ΔH° values between conformers [13]

G-T: 303 cm^{-1} (≈ 3.6 kJ mol^{-1})
G'-G: 76 cm^{-1} (≈ 0.9 kJ mol^{-1})

Interestingly, *ab initio* calculations with the 3-21G(N*) basis set yield approximately the same energy difference between conformers G' e T. However, the G form becomes less stable than G', according to these calculations [13]. Inasmuch as these results yield similar energy differences between T and G' conformers which have the nitrogen lone pair with the same orientation relative to the CC bond *(gauche,* for both conformers), they seem to point out to the importance of the nitrogen lone pair in establishing intramolecular interactions. In fact, having the same relative orientation of the lone pair of electrons. conformers T and G' are both likely to establish weak intramolecular hydrogen bond interactions between the nitrogen atom through its lone pair of electrons and one of the methyl hydrogen atoms bonded to the carbon atom which is non-adjacent to N [13]. Hence, these conformers are likely to be equally less affected by intermolecular interactions, as their nitrogen atoms are engaged in intramolecular interactions.

Benzyl and Benzal Chlorides

Overall molecular rotation in the liquid phase

The reorientational correlation functions, G_{2R}, of $C_6H_5CH_3$, $C_6H_5CH_2Cl$, $C_6H_5CCl_3$ and $C_6H_5CCCH_3$ have been obtained within the standard Raman VV-VH procedure applied to the totally symmetric ring mode, near 1000 cm^{-1} [14]. From these results, it was concluded that the molecular motion anisotropy increases in the above mentioned order, as the overall rotation about the major axis becomes increasingly preferred. Additional information in full agreement with the Raman bandshape analysis can also be obtained from ^{13}C T_1 relaxation times [15].

Internal rotation in $C_6H_5CHCl_2$

^{13}C T_1 relaxation times of $C_6H_5CHCl_2$ in deuterochloroform solutions were measured at several temperatures in the range from 233 to 323 K [15]. Among several relaxation mechanisms, the **C-H** dipolar coupling and the spin-rotation interaction stand out as the most important for the aromatic and the alkyl carbon nuclei. As they exhibit different temperature dependences, it was possible to separate their contributions and conclude that the $CHCl_2$ group is the rotating group, since the alkyl carbon atom has the lowest correlation time [15].

In addition, the internal rotation diffusion could be interpreted using a jump model valid in the above mentioned temperature range, and the internal rotation was found to be two times faster than the overall rotation. While this rate is high enough in the NMR time scale to average molecular conformations, it is sufficiently low in the Raman time scale to enable the detection of rotational isomers by Raman spectroscopy, as it will be shown below.

Rotational isomers of $C_6H_5CHCl_2$

Comparison of Raman bands observed in the region of the **CH** stretching vibrations for the hydrogenated compound with its deuterated derivatives enabled the assignment of two Raman bands to the **C-H** vibrator of the **$CHCl_2$** group [16]. This assignment was further confirmed by an independent study of high

overtone infrared spectra of $C_6H_5CHCl_2$ [17]. The dependence of the profiles of the fundamental Raman bands on temperature and dilution in a series of solvents suggested the occurrence of a conformational equilibrium. These results led to the evidence for two probable rotational isomers, designated $CH_{\perp}$ and $CH_{\parallel}$, which were found to be responsible for the two observed Raman bands [16].

Internal rotation of —CH_2Cl in $C_6H_5CH_2Cl$

In the high-resolution gas-phase 269 nm absorption spectrum of benzyl chloride in the *0-0* region, a long sequence on the high wavenumber side of the *0-0* band, assigned to the torsional mode, points to an internal rotation barrier larger in the excited state than in the ground state [18]. To explain this result, *ab initio* calculations at the 6-31G level were performed. In particular, two orientations of the **CH_2Cl** group were considered: one with the **CCl** bond in a plane perpendicular to the benzene ring plane (CCl_ conformation); the other with the **CCl** bond in the benzene ring plane ($CCl_{\parallel}$ conformation). The computations (6-31G//3-21G) indicate a minimum in the torsional potential function for the CCl⊥ conformation. This can be explained by an interaction between the π-electron system and the chlorine atom (the **CH_2Cl** group is known to have a relatively strong π-acceptor character). This interaction is stronger for the CCl⊥ conformation, as it is suggested by the alterations of the geometric parameters with conformation. In particular, there is a large decrease in the **CCCl** angle (3.6°) and in the C_1-C_7 bond length (≈2.0 pm) with a simultaneous increase of the **C-Cl** bond length (≈2.7 pm), for the CCl⊥ conformation, with respect to the $CCl_{\parallel}$ form [18]. The *ab initio* calculations yield an S_0CH_2Cl torsional barrier of 927.9 cm^{-1} (11.1 kJ mol^{-1}) [18]. A barrier of 1889.2 cm^{-1} (22.6 kJ mol^{-1}) is estimated in S_1 from the gas-phase absorption spectrum [18].

α,β–unsaturated carbonyl compounds

The understanding of the conformational and vibrational properties of α,β-unsaturated carbonyl compounds have been of interest for many years, as these compounds have important chemical and biochemical applications [19,20]. In particular, they have been used as model compounds for enzyme-substrate complexes formed within the enzyme's active site during some catalytic reactions involving serine proteases [20].

Despite the sophisticated level already attained by the experimental work on the active site data, the most recent studies on these systems have stressed the importance of precise and structural information. In particular, the study of the internal rotation about the **C_α-C** and **C-O** bonds in α,β-unsaturated carbonyl compounds is fundamental for the understanding of catalytic reactions involving serine proteases [20].

Unfortunately, little attention has been directed in the past towards elucidating the details of the structure and vibrational properties of these compounds, methyl acrylate being the single one which has already been studied in some detail. In particular, it has been shown that this molecule exists in two conformations in the liquid phase: the *s-cis* and the *s-trans* forms (**C=C-C=O** dihedral angles of 0 and 180°, respectively), with $\Delta H_{(s\text{-}trans)\text{-}(s\text{-}cis)} = 1.90 \pm 0.20$ kJ mol^{-1} [21]. The main factors which were found to determine the relative stability of these conformers are (i) mesomerism within the carboxylate group, (ii) mesomerism involving both **C=C** and **C=O** double bonds and (iii) steric repulsions between **CH_2=CH** and the oxygen atoms. The first factor is the most important one and, together with the third, favours the *s-cis* conformer, while the second factor favours the *s-trans* form. In the solid state, only the *s-cis* form is present [21].

In the following, the conformational freedom about the **C_α-C** bond in some α,β-unsaturated carboxylic esters—methyl acrylate (**MA**), methyl trans-crotonate (**MC**) and methyl trans-cinnamate (**MC_i**)—is considered [21-23] and discussed in relation with the extent of hydrogen bonding between the carbonyl group of the ester compounds and phenol derivatives in carbon tetrachloride solutions [24]. A linear relationship between $\Delta\upsilon_{C=O}$ due to the hydrogen bond and the enthalpy of complex formation was found, enabling the indirect evaluation of the strength of the hydrogen bond from the observed shift in the carbonyl stretching frequency associated with the complex formation.

Internal rotation about the C_α-C bond

Vibrational evidence for the occurrence of different conformers in the pure liquid comes from the analysis of several Raman and ir spectral regions for MA [21], MC [22], and MCi [23]. In particular, for MC, in the 1750-1600 cm^{-1} region (the spectral region where the bands ascribed to the carbonyl and ethylenic vibrations occur), Raman spectra are considerably more simple than the corresponding ir spectra, mainly because overtones - eventually involved in Fermi resonance with the **C=O** stretching mode - are, as usually, much less intense in Raman than in ir. In the liquid phase, it is clear that the higher and lower components of the bands ascribed to the **C=O** and **C=C** normal modes (respectively, 1730 and 1651 cm^{-1} for the light molecule, and 1725 and 1649 cm^{-1} for the deuterated compound), reduce their intensities on lowering the temperature. In the solid state spectra, these components cannot be observed (in the ir spectra of the crystals, the bands at 1726 (MC) and 1734 cm^{-1} (Md_3C) can be ascribed to the first overtone of the **CC** stretching mode). Thus, the liquid phase spectra of both the non-deuterated and deuterated molecules in this region can be schematized as follows:

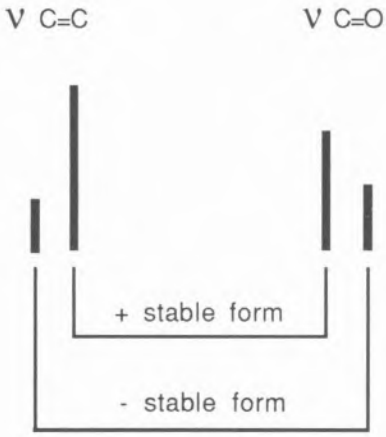

This is a general trend for the carboxylic esters herein studied. Considering both the results of the normal modes calculation and of the charge density analysis [22], it is then possible to establish the following correspondence

more stable conformer —> *s-cis*
less stable conformer —> *s-trans*

in agreement with the predicted relative stabilities of the two forms *(ab initio* MO calculations, and with the results obtained for MA [21].

Consideration of bond dipolar interactions is also in agreement with the above assignment. In particular, the **C=O** bond is found to be more polarized in the *s-cis* conformer thus corresponding to a smaller $\nu_{C=O}$, and the **C=C** bond is more polarized in the *s-trans* conformer, thus leading to a smaller $\nu_{C=C}$ [21, 22].

Temperature-dependent Raman intensities were found for several pairs of bands in these compounds suggesting the occurrence of conformational equilibria. These studies enabled to obtain differences in enthalpy between conformers. In particular, for MC, by plotting the logarithmic ratio of intensities of pairs of bands assigned to **C-C=O** (496 and 453 cm^{-1}) and **O=C-O** (707 and 724 cm^{-1}) deformations, as functions of inverse temperature, one obtains $\Delta H_{(s\text{-}trans)\text{-}(s\text{-}cis)}$=2.65±0.27 kJ mol^{-1} [22].

The internal rotation about the **C-O** bond in MA was found to correspond to an energy difference larger than 40 kJ mol^{-1}, as determined by *ab initio* **SCF-MO** calculations [26]. Due to this large energy difference as compared with the value of kT at room temperature ($(kT)_{298\ K}$ =207.12 cm^{-1}), the stable conformation about the **C-O** bond is definitely *s-cis* [26].

The following table summarizes the differences in energy or in enthalpy between the *s-trans* and *s-cis* conformations, obtained for these carboxylic ester molecules ([21-23]; energies are in kJ mol^{-1} (1kJ mol^{-1} = 83.59 cm^{-1})):

	exp.	*calc*
MA	1.90	2.40
MC	2.65	2.99
MCi	3.43	-

Hydrogen bond formation

The resonance Raman spectra of the covalently-bonded-to-the-enzyme reaction intermediates, during the catalytic action of seline proteases (e.g. chymotrypsin), in the carbonyl stretching region, show a peculiar pattern, with at least two bands which can be ascribed to different species associated with distinct carbonyl environments [20]. A relatively shalp band, associated with a carbonyl group in a pratically hydrofobic environment, occurs near 1727 cm^{-1} — a typical carbonyl stretching frequency of an ester in a solution of non-polar solvents —, while a broad band at lower frequencies results from a different carbonyl population which is hydrogen bonded in the active site and corresponds to the active form of the intermediate [20]. In addition, it has been shown that the deacylation rate constants of several acyl-enzymes correlates well with the proportion of their hydrogen bonded population with respect to other non-reactive species, together with the degree of polarization of the carbonyl bond, as monitored by the carbonyl stretching frequency [20]. In fact, it seems that the strength of the hydrogen bond (which reflects in both the carbonyl stretching frequency and the **C-O** bond lengths) is a decisive factor in the catalytic deacylation process. The hydrogen bond possibly acts as a factor which stabilizes the **C-O**$^-$ bond of the tetrahedral intermediate of deacylation [20].

Along this line of reasoning, one should get information on the enthalpy associated with the hydrogen bond, directly from the enzyme active site spectroscopical data, once ΔH can be correlated with the shift produced in the carbonyl stretching frequency upon complexation. However, such correlation needs confirmation for simpler systems, where the relevant variables can be well controlled.

With this in view, the hydrogen bond between simple α,β-unsaturated carboxylic esters (MA, MC and MCi) and substituted phenols (phenol, 4-methylphenol and 3,5-dichlorophenol) were studied by means of ir spectroscopy [24]. Ortho-substituted phenols were excluded to eliminate the possibility of intramolecular hydrogen bond or any other undesirable interaction within the hydrogen donor system. Formation constants, and enthalpies and entropies of hydrogen bond formation were evaluated from ir spectroscopic data [24]. It was found that both the formation constants and enthalpies depend on the electronic properties of the substituents within the hydrogen donor and acceptor molecules, increasing with the electron attracting ability of the substituent. A single linear relationship was found

between $\Delta\upsilon_{C=O}/cm^{-1}$ due to the hydrogen bond formation and $\Delta H/kJ\ mol^{-1}$ of complex formation ($\Delta\upsilon_{C=O}$ = -9.947 + 2.191 (-ΔH)), for all the studied systems. Thus, at least for similar molecules, the strength of a hydrogen bond can be obtained indirectly from the observed shift in the carbonyl stretching frequency associated with the complex formation. These findings support the interpretation of spectroscopic data for enzyme-substrate intermediates [20] and open new perspectives in this field of study. In consonance with theoretical predictions, a stronger hydrogen-bonded complex corresponds to a larger shift in the carbonyl stretching frequency, *i.e.*, to a more important perturbation within the **C=O** moiety.

References

1. C.V. Raman, and K.S. Krishnan, *Nature* **121** (1928) 501.
2. C.V. Raman, *Nature,* **121** (1928) 619 .
3. C.V. Raman, and Krishnan, K.S. *Nature,* **121** (1928) 711.
4. S.A. Asher, *Anal. Chem.* **65** (1993) 59*A*.
5. D.L. Rousseau, P.F, Williams, *J. Chem. Phys.* **64** (1976) 3519.
6. P.A. Harmon, and *S.A. Asher, J.Chem. Phys.* **88** (1988) 2925.
7. J.M. Dudik, C.R. Johnson, S.A. Asher, *J. Phys.Chem.* **89** (1985) 3805
8. Shimidzu, R. private communication ("Merits of excitation at 7525 A in Raman spectroscopy").
9. D.R. Porterfield, and A. Campion, *J. Am.Chem.Soc.* **110** (1988) 408.
10. G.F. Puppels, F.F.M. de, Mul, C. Otto, J. Greve, M. Robert-Nicoud, D.J. Amdt-Jovin, and T.M. Jovin, *Nature,* **347** (1990) 301.
11. Long. *D.A."Raman spectroscopy",* McGraw-Hill International Book Company. London; 1977 pages **139-40**.
12. J.E. Pemberton, R.L. Sobocinski. M.A. Bryant, and D.A. Carter, *Spectrosc. Intern. 26* (1990) *(also* appeared in *Spectrosc.* **5** (1990) 26*)*.
13. L.A.E. Batista de Carvalho. *"Estudos conformacionais em monoaminas acíclicas"*, dissertação de doutoramento, 1990, Coimbra.
14. P.J.A. Ribeiro-Claro, A.M. Amorim da Costa, and J.J.C. Teixeira-Dias, J. *Raman Spectrosc.* **18** (1987) 497.
15. P.J.A. Ribeiro-Claro, C.F.G.C. Geraldes and J.J.C. Teixeira-Dias, 1. *Magn. Reson.* **71** (1987) 132.
16. P.J.A. Ribeiro-Claro and J.J.C. Teixeira-Dias,1. *Raman Spectrosc.* **15** (1984) 224.
17. M.K. Ahmed, D.J. Swanton, B.R. Henry, *J. Phys. Chem.* **91** (1987) 293.
18. J.M. Hollas, J.J.C. Teixeira-Dias, and P.J.A. Ribeiro-Claro, *Chem. Phys. Lett.* **157** (1989) 31.
19. P.R.Carey, *Biochemical Applications of Raman and Resonance Raman Spectroscopies.* Academic Press, London; 1982.
20. P.R.Carey and P.J. Tonge, *Chem. Soc. Rev.* L 293 (1990*)*, and references herein . 21. M.Dulce G. Faria, J.J.C.Teixeira-Dias and R.Fausto, *Vibrational Spectrosc.* **7** (1991) 43.
22. M.Dulce G.Faria. J.J.C.Teixeira-Dias and R.Fausto, *Vibrational Spectrosc.* **2** (1991) 107.
23. M.Dulce G.Faria, J.J.C.Teixeira-Dias and R.Fausto, J. *Raman Spectrosc.* **22** (1991) 519.
24. M. Dulce G. Faria, J.J.C. Teixeira-Dias and R.Fausto, J. *Molec.Struct.*, **263** (1991) 87.

Kinetics of intramolecular electron exchange in radical-anions of isodisubstituted aromatic compounds: Application of Marcus theory

Cinética da permuta intramolecular de electrão em radicais aniões de compostos aromáticos isodisubstituídos. Aplicação da teoria de Marcus

M. CÂNDIDA B. L. SHOHOJI, JOÃO P. TELO

INSTITUTO SUPERIOR TÉCNICO, QUÍMICA ORGÂNICA - AV. ROVISCO PAIS, 1096 LISBOA CODEX, PORTUGAL

Rate constants of intramolecular electron exchange in isodisubstituted aromatic radical anions were estimated through the analysis of temperature dependent line broadening of their EPR spectra in protic and aprotic solvents.
Application of the Marcus theory and the Rips and Jortner approach for the uniform adiabatic limit of electron transfer led to estimated values of the amount of transferred charge. The external reorganisation energies, λ_o, were calculated by applying an ellipsoidal cavity model. Values of λ_i were estimated from the measured activation energies and the calculated values for the resonance energy splitting.

Mediram-se constantes de velocidade para a reacção de permuta intramolecular de electrão, induzida pelo solvente, através da análise dos efeitos de alargamento alternante de risca nos espectros RPE de radicais aniões de compostos aromáticos isodissubstituídos.
Por aplicação da teoria de Marcus e do modelo de Rips e Jorner para o limite uniforme e adibático, calcularam-se os valores da quantidade de carga transferida. A energia de reorganização externa, λ_o, foi calculada usando o modelo da cavidade elipsoidal. Os valores da energia de reorganização externa λ_i, foram estimados a partir dos valores experimentais da energia de activação e dos valores calculados da energia de acoplamento electrónico, H_{12}.

1. Introduction

Single electron transfer (ET) is one of the most fundamental chemical reactions and plays an important role in many synthetic and biological processes. Recent experimental work on both thermal and photoinduced ET has focused attention on the predictions of standard ET theories[1-6] and, in particular, on the influence of the temperature, geometry, medium, distance and exoergicity on the rates. Most of the experiments deal with ET between two metallic centers and within this area intermolecular ET has caught more attention than intramolecular ET reactions, although the latter offer distinct advantages for testing ET theories, because diffusion processes obviously do not take place in this type of unimolecular reactions.

There are several reports[7-13] on the kinetic investigations on thermal intramolecular ET in systems containing one electron donor and one electron acceptor separated by a spacer of variable length, with relevance to the important investigations on Marcus "inverted region" performed by Miller and co-workers for radical anions of compounds of type **1**, by means of pulse radiolysis[8,9]. For paramagnetic species, Electron Paramagnetic Resonance (EPR) can also be an important tool, mainly to study ET processes in which products are chemically indistinguishable from the reactants (electron exchange reactions). The analysis of line broadening effects[14] of the spectra can allow the measurement of rates, because the frequency of the ET processes often lies within the hyperfine time scale (10^6-10^{10} s^{-1}). Several works of this type are particularly pertinent to this review. Harriman and Maki[15] studied radical anions of bis(p-nitrophenyl) compounds **2** and found solvent dependent rate constants of ca. 10^6 s^{-1} for X= S, O and CH_2CH_2. Later, some experiments have

shown that high rates ($>10^6$ s^{-1}) of intramolecular electron exchange (IEE) can occur even over distances of 1000 pm. In one study performed on radical anion of **3**, rate constants are of the order of 10^8 s^{-1} for distances of 700 pm[16]. This fast long-range IEE has been attributed to a mechanism of coupling which mixes the orbitals of the donor and the acceptor. More systematic EPR and ENDOR analysis on the distance dependence of IEE was carried out on radical anions of compounds **4**, where two naphthalene moieties are attached to a spacer of variable length[17]. Whereas the process is slow for n=3 and n=5, the radical anion with n=1 showed two conformations, *syn* and *anti*, exhibiting respectively fast and slow exchange. Rate constants in radical anions of **5** can exceed 10^7 s^{-1} even when a rigid spacer separates the two π moieties by as many as 6 C-C bonds[18]. Rate constants in the range of 10^8 s^{-1} were measured for radical anions of linear poliacene diquinones **6** [19].

1

A = 2-naphthyl, 9-phenanthryl, 1-pyrenyl and various aromatic 2-quinonyl B = 4-biphenylyl

2

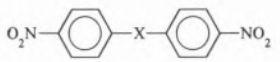

X : CH_2, S, O, CH_2CH_2 and absent

3

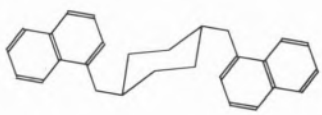

4

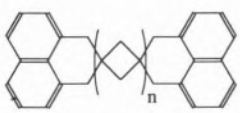

n = 1,3,5

5

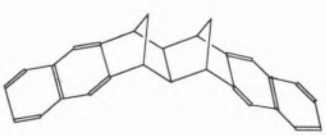

6

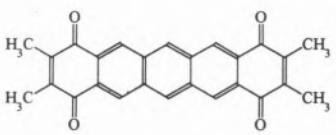

Most of the experiments described above were carried out for compounds with spacers formed by a saturated carbon skeleton. However, there are few works dealing with radical anions with aromatic spacers, in which the overlap between the orbitals of the donor and the acceptor should be more extensive. The pioneering investigations of this type were carried out by Rieger, Freed and Fraenkel for dinitrobenzenes. These authors interpreted the line broadening effects in EPR spectra of 1,3-dinitrobenzene radical anion as a result of the modulation of nitrogen hyperfine coupling constants caused by a reaction of IEE induced by an asymmetric solvation mechanism such that only one group at a time interacts strongly with the solvent (scheme 1)

Scheme 1

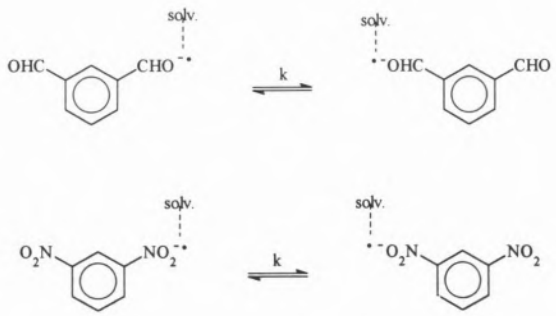

Following the line initiated by Rieger, Freed and Fraenkel[20,21] but neglected in the past few years, we have chosen to study IEE in simple radical anions which have an aromatic spacer[22-25] as those derived from compounds **7**, **8** and **9*** . The kinetics of the reaction was investigated by the EPR line broadening method and the data were treated in terms of the Marcus theory[1,5].

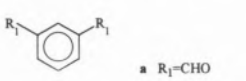

7

a R_1=CHO
b R_1=NO_2
c R_1=$COCH_3$
d R_1=CN
e R_1=$COOCH_3$

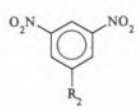

9

a R_2=CN
b R_2=CF_3
c R_2=$OOCCH_3$
d R_2=$COOCH_3$
e R_2=Cl
f R_2=I
g R_2=F
h R_2=$CONH_2$
i R_2=OCH_3
j R_2=CH_2OH
k R_2=$NHCOC_6H_5$
l R_2=CH_3
m R_2=COO^-
n R_2=$C(CH_3)_3$
o R_2=NH_2
p R_2=O^-

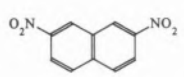

8

* In this paper, 7^-, 8^- and 9^- will stand for radical anions of 7, 8 and 9, respectively.

2. Theory

According to Marcus theory[1] the rate constant of an outer sphere electron transfer assumes, in the high

temperature limit, the well-known equation 1, taking into account contributions of both the intramolecular vibrations and the solvent, considered as an infinite dielectric continuum, to the reaction barrier.

$$k = A \cdot \exp(-\Delta G^{*}/RT) \quad (1)$$

When $\Delta G^{0}=0$, ΔG^{*} is given by

$$\Delta G^{*} = (\lambda_i + \lambda_o)/4 - H_{12} \quad (2)$$

where λ_i is the internal reorganisation energy, which depends on the changes in bond lengths of the reactants along the reaction coordinates and λ_o the external reorganisation energy that depends on the reorientation of the solvent molecules. H_{12} is the resonance energy splitting (fig. 1).

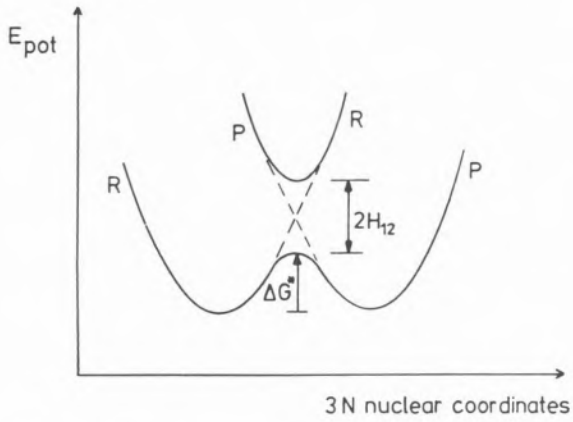

Figure 1 - Profile of potencial energy surfaces of reactants (R) and products (P), plotted versus nuclear configuration of all the atoms in the system. The dashed line describes the surface for zero electronic interaction at the crossing point. The full line describes the adiabatic surface with electronic interaction and a resonance splitting energy of H_{12}>RT.

2.1. The inner sphere reorganisation energy λ_i

In the high temperature limit λ_i can be calculated from changes in bond lengths Δq_j between forms α (reactant) and β (product) together with the corresponding force constants $f_j^{\alpha,\beta}$, according to the following equation[1]

$$\lambda_i = \sum_j \frac{f_j^{\alpha} f_j^{\beta}}{f_j^{\alpha} + f_j^{\beta}} (\Delta q_j)^2 \quad (3)$$

Since no crystallographic data are available for the investigated radical anions, the changes in bond lengths might be estimated from Hückel-MO calculations through the bond-order/bond-length relations published by Gordy[26].

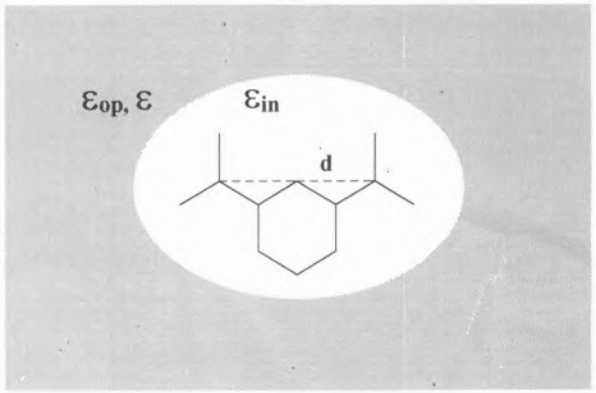

Figure 2 - Ellipsoidal cavity model for calculation of the outer sphere reorganization energy λ_o.

2.2. The outer sphere reorganisation energy λ_o

For spherical molecules λ_o can be calculated through the classical Marcus equation[1]. As the shape of our molecules deviates significantly from spherical, this model is not satisfactory. Therefore the ellipsoidal cavity model[27-30] seems to be a better approach for calculating λ_o. In this model (fig. 2) the reacting molecule is situated in a cavity of relative permittivity ε_{in} (for organic compounds $\varepsilon_{in} \cong 2$), surrounded by the solvent that is supposed to behave as a continuum characterised by the static and optical relative permittivities, ε and ε_{op} (ε_{op} is usually taken as the square of the refractive index, $\varepsilon_{op} \cong n^2$).

In this model λ_o is not an explicit function of the solvent polarity parameter γ, expressed by

$$\gamma = 1/\varepsilon_{op} - 1/\varepsilon \quad (4)$$

as in the classical Marcus equation. However we looked for a simple relation by calculating λ_o for several values of ε_{op} and ε, assuming an ellipsoidal cavity with semiaxes estimated from molecular models. Within the range of solvents used, a linear relation between λ_o and γ was found[23,25].

$$\lambda_o = pz^2\gamma \quad (5)$$

with z being the fraction of transferred charge and p a proportionality constant characteristic of the ellipsoidal cavity shape. p = 223 kJmol^{-1} for **7**$^{\bullet}$ and p = 424 kJmol^{-1} for **8**$^{\bullet}$

2.3. The resonance energy splitting H_{12}

A useful source of information about the magnitude of the resonance energy splitting H_{12} is provided by intervalence transfer absorption spectra[31,32]. We hope in the near future to be able to carry out such measurements.

An estimated value of H_{12} can be obtained from Hückel-MO calculations by using the equation proposed by Hale and Ratner[33]

$$H_{12} = \sum_{J=1}^{n} \frac{c_{J\mu} \cdot c_{J\nu}}{E_I - E_J} \beta_{N\mu} \beta_{N\nu} \quad (6)$$

herein $c_{J\mu,\nu}$ are the LCAO-coefficients of the atoms μ and ν in the molecular orbital J and $\beta_{N\mu,\nu}$ the resonance integrals of the nitrogens (or carbonyl carbons) with the bonded C atoms. Resonance integrals were obtained from Ref. [34] and [35]. E_I refers to the electronic energy with the electron fully localised on one redox site and E_J the energy of the orbital J.

2.4. The Pre-exponential factor

The original theory of Marcus[1] rested on the assumption that the electron transfer process is adiabatic and therefore the pre-exponential factor is given by:

$$A = \kappa \cdot \nu \quad (7)$$

κ being the electronic transmission coefficient and ν the effective nuclear frequency of the reactants. For a unimolecular adiabatic reaction κ≅1. Levich and Dogonadze[36] treated the nonadiabatic process and derived for the pre-exponential factor the following equation:

$$\kappa.\nu = (2\pi/\hbar)(H_{12})^2(4\pi\lambda RT)^{-1/2} \quad (8)$$

The transition probability $P = 1-\exp(-2\pi\gamma_{LZ})$ for the system to jump from the lower to the upper potential surface determines whether the reaction is adiabatic or nonadiabatic. In this equation γ_{LZ} represents the Landau-Zener[37,38] factor defined by:

$$\gamma_{LZ} = (H_{12})^2/h\nu\ |F_2-F_1| \quad (9)$$

where v denotes the velocity of the system in the vicinity of the crossing point and F_2 and F_1 are the slopes of the potential curves. For $\gamma_{LZ}<<1$ the reaction is nonadiabatic, while the adiabatic behaviour occurs for $\gamma_{LZ}>>1$. Using the Landau-Zener length l_{LZ} defined by:

$$l_{LZ} = H_{12}/\ |F_2-F_1| \quad (10)$$

Equation (9) can be rewritten as.

$$\lambda_{LZ} = l_{LZ}\,(H_{12}/\ h\nu) \quad (11)$$

Within this length the energy splitting is smaller than $4H_{12}$.

For an intramolecular process an extensive constant overlap of the reacting orbitals results in $H_{12}>RT$.

The influence of solvent dynamics on adiabatic electron transfer should be found in all cases where the mean free path length l_F of the system across the top of the barrier is smaller than l_{LZ} ($l_F/l_{LZ}<<1$). Papers published earlier[39-43] predicted that under these circumstances an inverse proportionality between the frequency factor and the longitudinal relaxation time of the solvent τ_L should be verified,

$$A \sim \tau_L^{-1} \quad (12)$$

where $\tau_L = (\varepsilon_{op}/\varepsilon)\ \tau_D$ (τ_D denotes the Debye relaxation time of the solvent)[44]. This corresponds to diffusive dynamics along the reaction coordinate.

If, however $l_F/l_{LZ}>>1$, the reaction dynamics might obey the classical transition state theory . Recently Rips and Jortner[45] pointed out that, in such case that they defined as the uniform adiabatic one, rotation of the solvent molecules cannot be neglected, since there is a rotational frequency dependence of the dielectric constant, at least for water and lower alcohols. The moment of inertia I of the solvent molecule has thus to be considered, since the imaginary part of the dielectric constant is a function of I

$$\varepsilon''(\omega) \sim \omega^2 \exp(-I\omega^2/2k_BT) \quad (13)$$

Therefore the pre-exponential factor for uniform adiabatic electron transfer can be written as[45]

$$A = 1/2\pi\ \{[(2\varepsilon + \varepsilon_{op})/6\varepsilon]\ (k_BT/I)\}^{1/2} \quad (14)$$

2.5. The rate constant

A distinction between diffusive and uniform reaction behaviour of the adiabatic reaction is possible by measuring the solvent dependence of the rate constant k. For a diffusive (solvent controlled) behaviour the rate constant is given by[39-43]

$$k_{SC} = 1/\tau_L(\lambda_o/16RT)^{1/2}\ \exp\ [-(\lambda_i+\lambda_o(\gamma))/4RT+H_{12}/RT] \quad (15)$$

Since in equation (5) λ_o is a linear function of γ, a plot of $\ln(k_{SC}\tau_L\gamma^{-1/2})$ vs. γ should yield a straight line at constant temperature.

In contrast to this, the uniform reaction behaviour leads to[45]

$$k_{TST} = 1/2\pi\{[(2\varepsilon + \varepsilon_{op})/6\varepsilon]\ (k_BT/I)\}^{1/2}\ \exp\ [-(\lambda_i+\lambda_o(\gamma))/4RT+H_{12}/RT] \quad (16)$$

which should result in a linear plot for $\ln(k_{TST}\ I^{1/2})$ vs. γ.

3. Solvent induced intramolecular electron exchange (IEE) in isodisubstituted radical anions

3.1 . Estimation of rate constants through linewidth analysis of EPR spectra

EPR spectra of radical anions **7a-c**$^{\bullet}$,**8**$^{\bullet}$ and **9**$^{\bullet}$ show temperature dependent line broadening effects similar to those earlier detected for 1,3-dinitrobenzene radical anion, as shown in figure 3 for **9n**$^{\bullet}$. These effects were interpreted as suggested by Rieger, Freed

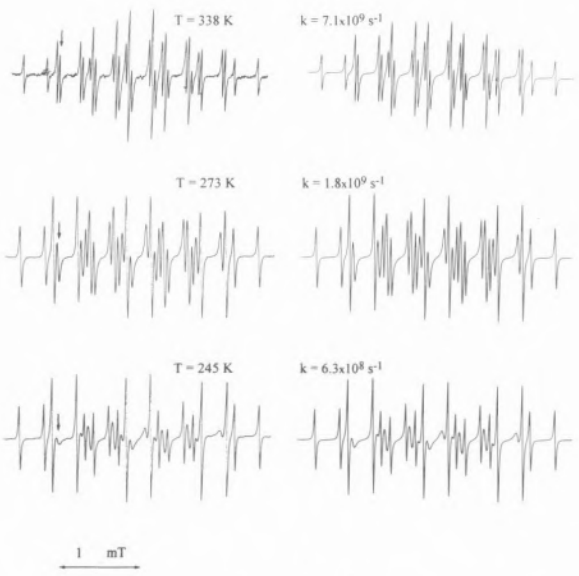

Figure 3 - Experimental spectra of $9n^{-\bullet}$ in acetonitrile at various temperatures (left hand side) and their computer simulations (right hand side). Arrows indicate the line of the nitrogen quintet corresponding to M_N=1, which clearly shows the temperature dependent line broadening effect.

and Fraenkel[20,21] on the basis of an asymmetric solvation mechanism of the type shown in scheme 1 for **7a**$^{-\bullet}$ and **7b**$^{-\bullet}$

EPR spectra of **7a**$^{-\bullet}$ and **7c**$^{-\bullet}$ have additional complexity due to the existence of rotational isomers

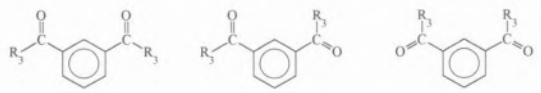

(Z,Z) (Z,E) (E,E)

7a R_3=H
7c R_3=CH_3

For radical anion **7a**$^{-\bullet}$ the relative abundances of the three isomers $(Z,E)^{-\bullet}$, $(E,E)^{-\bullet}$ and $(Z,Z)^{-\bullet}$ in ethanol are 60:26:14, respectively. There is no evidence of interconversion between the rotamers on the EPR time scale. The line broadening effects were interpreted exclusively as a result of IEE. Rate constants and activation parameters were estimated only for the most abundant isomer, $(Z,E)^{-\bullet}$.

Rate constants of IEE reactions in **7a**$^{-\bullet}$, **7b**$^{-\bullet}$ and **8**$^{-\bullet}$ (table 1) were estimated by fitting the experimental spectra with the theoretical curve calculated by solving the modified Bloch equations[14] for a two jump model.

Radical anion **7c**$^{-\bullet}$ showed EPR spectra which could not be interpreted only on the basis of intramolecular electron exchange. Interconversion between the two most abundant rotamers, $(Z,E)^{-\bullet}$ and $(E,E)^{-\bullet}$, had to be included[46]. A "four jump" model[47] as shown in scheme 2 led to satisfactory simulations of experimental spectra. Table 2 shows the mean lifetimes τ_1 and τ_2 of each isomer and the equilibrium constant K in a propan-2-ol/water mixture, at 293 K.

Scheme 2

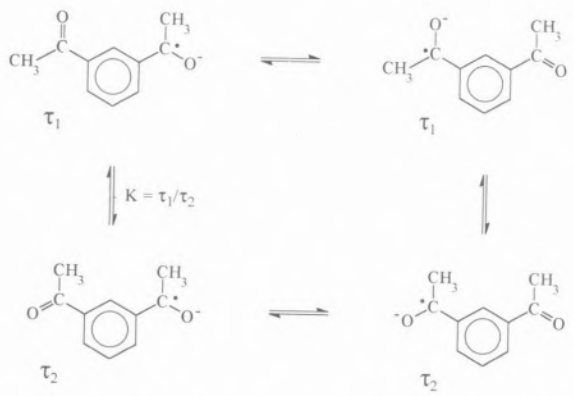

7d$^{-\bullet}$ and **7e**$^{-\bullet}$ do not show temperature dependent line broadening effects on their EPR spectra, which could be simulated by assuming electron delocalization, although our data do not allow a distinction between total delocalization and very fast exchange. Radicals **7d**$^{-\bullet}$ and **7e**$^{-\bullet}$ have small hyperfine coupling constants for nitrogen and methyl protons (a_N=1.05 x10^{-4} T and a_{CH3}=0.25 x 10^{-4} T), therefore even if these constants were modulated by IEE, their fluctuation would be too small to cause line broadening effects.

Table 1 Rate constants k for intramolecular electron exchange reaction **7a**$^{-\bullet}$ **7b**$^{-\bullet}$ and **8**$^{-\bullet}$ and solvent parameter γ, at 293 K.

Solvent	γ[a]	k^b / s^{-1}		
		7a$^{-\bullet}$	**7b**$^{-\bullet}$	**8**$^{-\bullet}$
HMPA	0.437	[c]	3.8 x 10^9	1.0 x 10^9
DMF	0.463	[c]	6.5 x 10^9	1.8 x 10^9
ACN	0.527	[c]	4.0 x 10^9	9.0 x 10^8
2-PrOH	0.474	0.6 x 10^9	5.0 x 10^6	3.9 x 10^6
EtOH	0.500	1.3 x 10^9	2.9 x 10^6	2.1 x 10^6
MeOH	0.537	1.7 x 10^9	2.7 x 10^6	5.9 x 10^5

[a] For values of n and ε see ref [24]. [b] Errors within ± 10 %. [c] We have failed to generate the radical in aprotic solvents. HMPA: Hexamethylphosphoric triamide. DMF: Dimethylformamide. ACN: Acetonitrile. 2-PrOH: Propan-2-ol. EtOH: Ethanol. MeOH: Methanol

Table 2 Mean lifetimes of the two most abundant isomers of **7c**$^{-\bullet}$ and their equilibrium constant at 293K.

τ / 10^{-8} s		K
$(Z,E)^{-\bullet}$	$(E,E)^{-\bullet}$	
1.7	1.1	1.55

3.2. Application of Marcus Theory

3.2.1. Transferred charge ze_0 and outer-sphere reorganisation energy λ_o

As pointed out in chapter 2.5, a distinction between diffusive (controlled by solvent dynamics) and uniform behaviour of an adiabatic reaction is possible through the study of the solvent dependence of the rate constant. If the reaction is uniform, a plot of $\ln(kI^{1/2})$ vs. γ must be linear, according to equation (16), since the term $(2\varepsilon + \varepsilon_{op})/6\varepsilon$ is nearly constant (e.g. at 293 K, it changes from 0.537 in methanol to 0.437 in hexamethylphosphorotriamide (HMPA)). Figure 4 shows such plots for $\mathbf{8}^{-\bullet}$ in protic and aprotic solvents. Plots of the same type were obtained for $\mathbf{7a}^{-\bullet}$ and $\mathbf{7b}^{-\bullet}$ as well. A corresponding plot of $\ln(\kappa\tau_L\gamma^{1/2})$ vs. γ by using equation (15) scattered badly.

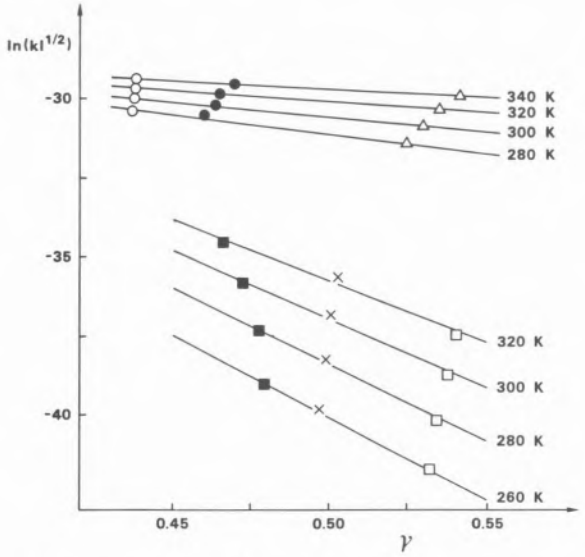

Figure 4 - Dependence of $8^{-\bullet}$ intramolecular electron exchange rates on the solvent parameter γ (according to equation (16) at diferent temperatures. , DMF (filled circles); ACN (open circles); HMPA (triangles); 2-PrOH (filled squares); MeOH (open squares); EtOH (crosses).

These results indicate a uniform adiabatic behaviour for the IEE reaction in isodisubstituted aromatic radical anions of type $\mathbf{7}^{-\bullet}$ and $\mathbf{8}^{-\bullet}$.

Taking into account equation (16) a plot of $\ln(kI^{1/2})$ vs. γ has the slope

$$m = -z^2p / 4RT \qquad (17)$$

and the intercept

$$t = 1/2 \ln [k_BT (2\varepsilon + \varepsilon_{op})/6\varepsilon] - \ln 2\pi - \lambda_i/4RT + H_{12}/RT \qquad (18)$$

In equation (17), p is a constant, since the molecular parameters (which determine the shape of the ellipsoidal cavity) and the distance between the two redox centers are the same for any the solvent at any temperature. Therefore the fraction of transferred charge, z, could be obtained from the slopes of the lines shown in fig. 4 and by using equation (17). Table 3 shows the values of z_{exp} at 293 K together with the calculated z values by using the spin densities from HMO calculations. The agreement is satisfactory. The amount of transferred charge is lower for $\mathbf{7a}^{-\bullet}$ than for $\mathbf{7b}^{-\bullet}$ because the formyl group is a poorer electron atractor than the nitro group and therefore in $\mathbf{7a}^{-\bullet}$ the odd electron tends to spend more time on the aromatic ring. Fig. 5 shows the temperature dependence of z for $\mathbf{7a}^{-\bullet}$, $\mathbf{7b}^{-\bullet}$ and $\mathbf{8}^{-\bullet}$ in protic and aprotic solvents. For all compounds studied, z decreases with increasing temperature. This fact can be explained if we take into account that the electron exchange is induced by asymmetric solvation of the radical anions[20,21] and that at higher temperatures there is lower specific solvation. Therefore the two substituents become more equally solvated with increasing temperature. The range of z is narrower if the interaction between the solvent and radical anions is strong, due to a levelling effect, which is the case in alcohols as compared with aprotic solvents.

Table 3 Experimental and calculated charge transfer numbers z, at 293 K.

Radical Anion	z_{exp} [a]		z_{calc} [b]	
	Protic	Aprotic	Protic	Aprotic
$\mathbf{7a}^{-\bullet}$	0.34	-	0.35	-
$\mathbf{7b}^{-\bullet}$	0.93	0.50	0.73	0.59
$\mathbf{8}^{-\bullet}$	0.98	0.50	0.70	0.57

[a] From equation (17). [b] Calculated from the differences in McLachlan spin densities at both substituents, using the parameters of ref. [23].

From the values of z and γ, values of λ_o were calculated through equation (5). Table 4 includes λ_o at 293 K. The outer sphere reorganisation energies are strongly dependent on the solvent. It can be seen that λ_o is much larger for protic than for aprotic solvents and that it decreases from ethanol to propan-2-ol and from acetonitrile to HMPA according to the decrease of the solvent parameter γ.

In order to discuss the effect of solvent and temperature on λ_o, one has to keep in mind that, in the initial and final states (α and β in scheme 1), the negative charge is largely concentrated on one of the substituents (nitro or formyl group), whereas in the transition state the charge is more spread out over the two substituents and the aromatic ring. This explains the increase of λ_o with solvating power of the solvent

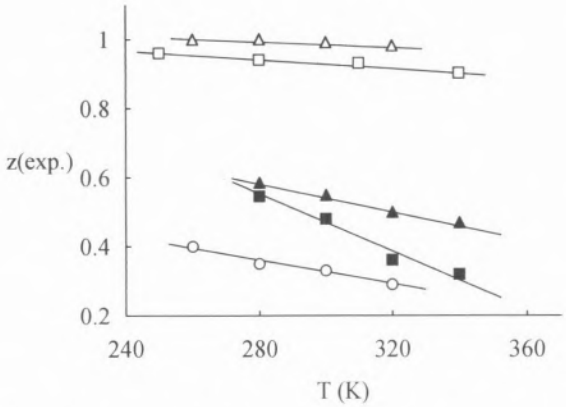

Figure 5 - Temperature dependence of the charge transfer number z for $7a^{-\bullet}$ (circles), $7b^{-\bullet}$ (squares) and $8^{-\bullet}$ (triangles) in protic (open symbols) and aprotic solvents (filled symbols).

the increase of λ_o with solvating power of the solvent and the decrease with increasing temperature. The differences in λ_o between protic and aprotic solvents are clearly ascribed to the presence or absence of hydrogen bonds.

λ_o is larger for $\mathbf{8}^{-\bullet}$, as expected from the more elongated shape[25] of the ellipsoidal cavity as compared with $\mathbf{7b}^{-\bullet}$ .The differences in λ_o between $\mathbf{7a}^{-\bullet}$ and $\mathbf{7b}^{-\bullet}$ are mainly caused by the different amount of transferred charge which is much smaller for the former. As a consequence, rate constants in alcohols are in the fast exchange range for $\mathbf{7a}^{-\bullet}$ and in the slow exchange range for $\mathbf{7b}^{-\bullet}$.

3.2.2. Activation parameters

Equation (16) can be written in the form

$$k = A' T^{1/2} \exp(-\Delta G^*/RT) \qquad (19)$$

with

$$A' = 1/2\pi\{[(2\varepsilon + \varepsilon_{op})/6\varepsilon](k_B/I)\}^{1/2} \qquad (20)$$

In equation (19) , A' can be taken as a constant, because the moment of inertia I is independent of temperature and the term $(2\varepsilon + \varepsilon_{op})/6\varepsilon$ changes very slightly within the temperature range used (from 0.341 at 250 K to 0.345 at 340 K for methanol, for example). Therefore, the activation energies ΔG^* can be derived from the slopes of the lines in plots of $\ln(kT^{-1/2})$ vs. 1/T, for each solvent. Table 4 shows their values together with the values of pre-exponential factors, ln A'.

3.2.3. Internal reorganisation energy λ_i

From the measured activation energies together with measured λ_o (table 4) it is possible to estimate the inner sphere reorganisation energies λ_i from equation (2), provided that the resonance energy splittings H_{12} are known. Table 4 includes the values obtained for λ_i at 293 K.

An approximation of H_{12} can be obtained from equation (6). H_{12} was found to be 14.1 kJmol^{-1} for $\mathbf{7a}^{-\bullet}$, 9.8 kJmol^{-1} for $\mathbf{7b}^{-\bullet}$ and 39.4 kJmol^{-1} for $\mathbf{8}^{-\bullet}$. These values should be taken only as an indication of the order of magnitude of H_{12}, since more accurate values can be obtained from the intervalence band of the radical anions optical spectra. The order of magnitude of H_{12} (>RT) confirms the adiabaticity of the reaction. The variation of λ_i with the solvent is within the experimental error, indicating that in all solvents used the changes in bond lengths necessary to reach the transition state structure are approximately the same. Such behaviour is in agreement with the theoretical prediction[1].

Table 4 Activation parameters, external and internal reorganization energies for intramolecular electron exchange reaction in isodisubstituted aromatic radical anions.

Solvent	ΔG^* / kJmol^{-1}			ln (A' /s^{-1}K$^{-1/2}$)			$\lambda_{o\,(293\,K)}$/kJmol^{-1}			$\lambda_{i\,(293\,K)}$/kJmol^{-1}		
	$\mathbf{7a}^{-\bullet}$	$\mathbf{7b}^{-\bullet}$	$\mathbf{8}^{-\bullet}$	$\mathbf{7a}^{-\bullet}$	$\mathbf{7b}^{-\bullet}$	$\mathbf{8}^{-\bullet}$	$\mathbf{7a}^{-\bullet}$	$\mathbf{7b}^{-\bullet}$	$\mathbf{8}^{-\bullet}$	$\mathbf{7a}^{-\bullet}$	$\mathbf{7b}^{-\bullet}$	$\mathbf{8}^{-\bullet}$
HMPA	-	13.4	12.9	-	25.6	23.2	-	29.2	55.7	-	82.4	153.5
DMF	-	22.1	11.7	-	28.8	23.3	-	24.9	61.1	-	106.0	143.3
ACN	-	22.4	18.6	-	28.5	25.4	-	35.0	69.6	-	108.8	162.4
2-PrOH	11.6	42.6	50.8	22.1	30.1	33.2	12.1	95.8	208.2	90.7	116.0	152.6
EtOH	10.3	42.4	46.9	22.3	29.4	31.0	13.2	100.2	219.4	86.1	110.4	125.8
MeOH	12.4	43.1	49.1	23.5	29.7	30.6	13.6	107.5	235.8	92.4	105.2	118.2

3.3 Effect of the substituent on the intramolecular electron exchange reaction

In order to investigate the effect of the substituent on the IEE reaction, EPR spectra of radical anions $\mathbf{9}^{\bullet}$ derived from 1,3-dinitrobenzenes with various substituents on position 5, were analysed[48].

Rate constants were found to decrease on going from electron atractor to electron donor substituents, as a result of the increase of ΔG^{*}, since the pre-exponential factor in equation (16), at a given temperature, only depends on the solvent. Table 5 shows k, ΔG^{*} and lnA' values for all the sixteen radical anions examined. Rate constants change by a factor of ten on going from electron atractor to electron donor substituents and correlate well with the Hammett substituent parameter σ_m[49,50]. The Hammett parameter ρ was found to decrease with increasing temperature, changing from 0.95 at 240 K to 0.74 at 320 K.

The variations of ΔG^{*} with the substituent can be explained by taking into account the changes in the external reorganisation energy λ_o as the most important contribution, although it is possible that λ_i and H_{12} change with the substituent as well. The reaction of IEE in the type of compound under study is induced by the asymmetric solvation of the two nitro groups such that instantaneously the nitro group which has the highest spin density (and, as a consequence, the highest charge density) is more strongly solvated. This spin density increases with the electron releasing power of the substituent and consequently the interaction of that group with the solvent increases as well. Such interaction is not so important in the transition state which is expected to have more symmetric structure with the spin more delocalised over the two nitro groups and the aromatic ring. Therefore, the difference in the external reorganisation energy λ_o, mainly results from the change in the solvation of the reactants on going from one substituent to another.

The good Hammett correlations with a positive value of ρ (showing that the reaction is accelerated by electron atractor substituents) also point out to an increase of electron density on the aromatic ring in the transition state as compared with the reactant.

Table 5 Substituent parameters σ_m, rate constants at 293 K and activation parameters of the intramolecular electron exchange reaction for compounds $\mathbf{9}^{\bullet}$ in acetonitrile

$\mathbf{9}^{\bullet}$	R_2	σ_m	k / s^{-1}	ΔG^{*} /kJmol^{-1}	ln A'
a	CN	0.61	1.2×10^{10}	13.7	26.0
b	CF_3	0.46	1.0×10^{10}	14.1	26.0
c	$OCOCH_3$	0.39	9.3×10^{9}	15.1	26.3
d	$COOCH_3$	0.38	9.1×10^{9}	14.7	26.1
e	Cl	0.373	8.4×10^{9}	14.1	25.8
f	I	0.35	8.0×10^{9}	14.8	26.0
g	F	0.34	9.5×10^{9}	14.2	26.1
h	$CONH_2$	0.28	5.5×10^{9}	15.7	26.0
i	OCH_3	0.115	*		
j	CH_2OH	0.10	6.9×10^{9}	14.6	25.8
k	$NHCOC_6H_5$	0.02	2.9×10^{9}	17.1	26.0
l	CH_3	-0.069	3.2×10^{9}	16.7	25.9
m	COO^{-}	-0.09	2.7×10^{9}	17.7	26.1
n	$C(CH_3)_3$	-0.10	2.8×10^{9}	16.8	25.8
o	NH_2	-0.21	3.0×10^{9}	17.9	26.3
p	O^{-}	-0.708	1.4×10^{9}	18.4	25.8

* Kinetic data could not be estimated due to lack of accuracy of the simulations caused by coincidence of hyperfine coupling constants of the nitrogens and of the hydrogens on positions 4 and 6

4. Conclusions

Some 1,3-isodisubstituted radical anions of types $\mathbf{7}^{\bullet}$, $\mathbf{8}^{\bullet}$ and $\mathbf{9}^{\bullet}$ show temperature dependent line broadening effects of their EPR spectra as a result of an intramolecular electron exchange reaction induced by asymmetric solvation.

The rate constants of IEE show a strong solvent dependence. The exchange is slower in protic solvents by a factor of the order of 10^3. Linear correlations of $\ln(kI^{1/2})$ vs. the solvent polarity parameter γ were observed for a series of protic and aprotic solvents. According to the Rips and Jortner approach this behaviour is an indication of a uniform adiabatic reaction. The values of the charge transfer number $z_{exp.}$ estimated from the slopes of such plots show a reasonable agreement with the values $z_{cal.}$ obtained from HMO calculations. z is larger for dinitrocompounds than for dialdehyde because the nitro group is a stronger electron atractor than the formyl group. The stabilisation of the negative charge on the oxygen atom by the hydrogen bond with the solvent explains the larger z value in protic than in aprotic solvents. This strong interaction also explains the narrower range of z values at different temperatures in alcohols as compared with aprotic solvents.

For each radical anion the values of λ_o show the expected dependence on the solvent parameter γ and on the charge transfer number z. The higher the values of these parameters the larger the values of λ_o. The shape of the ellipsoidal cavity has a strong influence on the λ_o values as well. Thus, λ_o is larger for $\mathbf{8}^{\bullet}$ than for $\mathbf{7b}^{\bullet}$ due to the more elongated ellipsoidal cavity of the former.

Only approximated values were estimated for λ_i due to the difficulty of obtaining accurate values for H_{12}. However, the results show that the variation of λ_i with the solvent is within experimental error.

A substituent effect was observed on the IEE reaction in 5-substituted 1,3-dinitrobenzene radical anions. Rates increase by a factor of 10 on going from electron donor to electron atractor substituents. Good correlations between the rate constants and the Hammett substi-

tuent parameter σ_m were obtained. Positive values of ρ show that the reaction is accelerated by electron atractor substituents, pointing out to an increase of the electron density on the aromatic ring in the transition state as compared with the reactants. The variation of the ΔG^* with the substituent can be explained by considering the changes in λ_o, as the most important contribution.

Acknowledgements

We thank all co-authors of our previous papers on the subject discussed in this article for provision of active collaboration and helpful insights. The financial support of INIC and JNICT through the "Centro de Processos Químicos da Universidade Técnica de Lisboa" is gratefully acknowledged.

References

1. R. A. Marcus *Annu. Rev. Phys. Chem.* **15** (1964) 155.
2. R. D. Cannon *"Electron Transfer Reactions"* Butterworth, London, 1980..
3. N. Sutin, *Prog. Inorg. Chem.* **30** (1983) 442.
4. M. D. Newton and N. Sutin *Annu. Rev. Phys. Chem.* **35** (1984) 457.
5. R. A. Marcus and N. Sutin *Biochem. Biophys. Acta* **811** (1985) 265.
6. L. Eberson *"Electron Transfer Reactions in Organic Chemistry"*, Springer-Verlag, Berlin; 1987.
7. L. T. Calcaterra G. L. Closs and J. R. Miller *J. Am. Chem. Soc.* **105** (1983) 670.
8. J. R. Miller L. T. Calcaterra and G. L. Closs *J. Am. Chem. Soc.* **106** (1984) 3047.
9. G. L. Closs, L. T. Calcaterra, N. J. Green, K. W. Penfield and J. R. Miller *J. Phys. Chem.* **90** (1986) 3673.
10. K. W. Penfield, J. R. Miller, M. N. Paddon-Row, A. M. Oliver and N. S. Hush, *J. Am. Chem. Soc.* **109** (1987) 5061.
11. S. F. Nelsen, J. A. Thompson-Colon and M. Kaftory *J. Am. Chem. Soc.* **111** (1989) 2809.
12. G. L. Closs, M. D. Johnson, J. R. Miller and P. Piotrowick *J. Am. Chem. Soc.* **111** (1989) 3751.
13. M. D. Johnson, J. R. Miller, N. S. Green and G. L. Closs *J. Phys. Chem.* **93** (1989) 1173.
14. N. M: Atherton *"Electron Spin Ressonance"*, Ellis Horwood, Chichester, 1973.
15. J. E. Harriman and A. H. Maki *J. Phys. Chem.* **39** (1963). 778.
16. K. Shimada and M. Szwarc *Chem. Phys. Lett.* **28** (1974) 540.
17. F. Gerson, W. Huber, W. B. Martin JR., P. Caluwe, T. Pepper and M. Szwarc *Hel. Chim. Acta* **67** (1984) 416.
18. F. Gerson, T. Wellauer, A. M. Oliver and M. N. Paddon-Row *Helv. Chim. Acta* **73** (1990) 1586.
19. S. F. Rak and L. L. Miller *J. Am Chem. Soc.* **114** (1992) 1388.
20. P. H. Rieger and G. K. Fraenkel *J. Chem. Phys.* **39** (1963) 609.
21. J. H. Freed and G. K. Fraenkel *J. Phys. Chem.* **41** (1964) 699.
22. M. C. B. L. Shohoji. B. J. Herold H. M. Novais, and S. Steenken *J. Chem. Soc., Perkin Trans.* **2** (1986) 1465.
23. G. Grampp, M. C. B. L. Shohoji and B. J. Herold *Ber. Bunsenges. Phys. Chem* **93** (1989) 58.
24. G. Grampp, M. C. B. L. Shohoji, B. J. Herold and S. Steenken *Ber. Bunsenges. Phys. Chem.* **94** (1990) 1507.
25. J. P. Telo, M. C. B. L. Shohoji, B. J. Herold and G. Gramp *J. Chem. Soc. , Faraday Trans.* **88** (1992) 47.
26. W. Gordy, *J. Chem Phys.* **15** (1947) 305.
27. J. G. Kirkwood and F. H. Westheimer *J. Chem. Phys.* **6** (1937) 506.
28. F. H. Westheimer and J. G. Kirkwood *J. Chem. Phys.* **6** (1938) 513.
29. B. S. Brunschwig, S. Ehrenson and N. Sutin *J. Phys. Chem.* **90** (1986) 3657.
30. B. S. Brunschwig, S. Ehrenson and N. Sutin *J. Phys. Chem.* **91** (1987) 4714.
31. N. S. Hush, *Prog. Inorg. Chem.* **8** 1967. 391.
32. N. S. Hush, *Coord. Chem. Rev.* 1985. **64** (1967) 135.
33. P. D. Hale and M. A. Ratner, *Int. J. Quantum Chem. Symp.* **18** (1984) 195.
34. V. M. Berdnikov and G. A. Bogdanchikov, *Russ. J. Phys. Chem.* **53** (1979) 155.
35. A. Streitwieser, *"Molecular Orbital Theory for Organic Chemists"*, Wiley, New York; 1961.
36. V. G. Levich and R. R. Dogonadze, *Dokl. Acad. Nauk. USSR* **124** (1959) 123.
37. L. Landau, *Phys. Z. Sowjet* **1** (1932) 89.
38. C. Zener, *Proc. Roy. Soc. A* **137** (1932) 696.
39. L. D. Zusman, *Chem. Phys. Lett.* **49** (1980) 295.
40. I. V. Alexanderov and V. I. Gol'danskii, *Chem. Phys.* **87** (1984) 455.
41. A. B. Helman *Chem. Phys.* **79** (1983) 235.
42. C. F. Calef and P. G. Wolynes *J. Phys. Chem.* **87** (1983) 3387.
43. H. Sumi and R. A. Marcus *J. Chem. Phys.* **84** (1986) 4272; **84** (1986) 4894.
44. H. Fröhlich, *"Theory of Dielectrics"*, 2nd ed. Oxford University Press; 1958.
45. I. Rips and J. Jorner, *J. Chem. Phys.* **87** (1987) 2090.
46. M. C. B. L. Shohoji, unpublished results.
47. A. Carrington, *Mol.Phys.* **5** (1962) 425.
48. J. P. Telo and M. C. B. L. Shohoji, *Ber. Bunsenges. Phys. Chem.*, **98** (1994) 172.
49. C. D. Ritchie, *"Physical Organic Chemistry"* 2nd Ed. Marcel Dekker Inc., New York; 1990, pp 105.
50. C. Hansch and A. J. Leo, *"Substituent Constants for Correlation Analysis in Chemistry and Biology"* Wiley-Interscience, New York; 1979.

New reactions involving addition to and substitution at carbon-carbon π bonds†

Novas reacções envolvendo adição a e substituição em ligações π carbono-carbono

ANA M. LOBO and SUNDARESAN PRABHAKAR

SECÇÃO DE QUÍMICA ORGÂNICA APLICADA, DEPARTAMENTO DE QUIMICA, and SINTOR-UNINOVA, *CAMPUS* FCT-UNL, QUINTA DA TORRE, 2825 MONTE DA CAPARICA
CENTRO DE QUÍMICA ESTRUTURAL, COMPLEXO I, UTL, AV. ROVISCO PAIS, 1096 LISBOA CODEX , PORTUGAL

The work involving addition to and substitution at carbon-carbon π bonds, conducted in the authors' laboratory, during the last five years, is reviewed. The first part refers to the synthesis of various heterocycles, obtained through a reaction which involves a formal [3,3]-sigmatropic rearrangement, in which a nitrogen-oxygen bond is cleaved. The second part describes a new aziridinating agent derived from hydroxamic acids. The third part refers to an aryl arly coupling through the use of radical reactions, which was applied in the synthesis of various *Amaryllidaceae* alkaloids.

Este artigo passa em revista o trabalho realizado no laboratório dos autores nos últimos cinco anos, relacionado com a adição e a substituição em ligações carbono-carbono π. A primeira parte refere a síntese de vários heterociclos, obtidos através de uma reacção envolvendo um rearranjo formal 3,3]-sigmatrópico, em que se quebra uma ligação azoto-oxigénio. A segunda parte trata de um novo agente de aziridinação derivado de ácidos hidroxâmicos. A terceira parte refere a formação através de reacções radicalares de acoplamento aril-aril, aplicado na síntese de vários alcaloides da família das *Amaryllidaceae*.

Carbon-carbon π bonds have always been of paramount importance in organic synthesis for the functionality that can be added to them or for the substitution reactions in which they can intervene.

Of particular interest in the last decade has been the drive to invent new chemical reactions which use very mild conditions, whereby a high regio, stereo and chemoselectivity of bond formation is achieved.

The present article summarizes the work conducted in our laboratory in the past few years in the development of new reactions involving addition to and substitution at carbon - carbon π bonds. These reactions have proved useful in the synthesis of a variety of heterocycles, such as imidazolinones, oxindoles, phenanthridines, benzo(c)phenanthridines, aziridines and imidazoles — substances of actual or potential use in the pharmaceutical, agrochemical and micro-electronics industries.

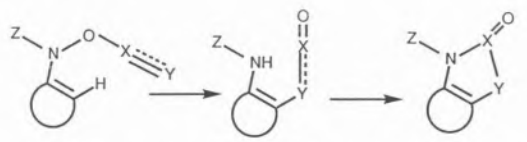

Figure 1. 3,3 - Sigmatropic rearrangement of ene-hydroxylamine derivatives

† This review is dedicated to Professor Sir Derek Barton on the occasion of his 75th birthday

1. Substitutions at Carbon-Carbon π Bonds Triggered by Nitrogen-Oxygen Cleavage. Synthesis of Benzimidazolinones, Oxindoles, Imidazoles, N-Iminocarboxybenzimidazoles and Amidines

Let us consider the general rearrangement depicted in Figure 1, where Z is an acyl or aroyl group, X is a carbon atom and Y a nitrogen atom. This rearrangement which can formally be placed under the more-general heading of 3,3 - sigmatropic rearrangement [1] draws its driving force at least in part from the cleavage of the weak N—O bond (*ca.* 50 Kcal mol $^{-1}$) [2] and in the formation of a strong carbonyl group. Thus, when equimolecular quantities of N - phenyl benzohydroxamic acid (**1a**) (Scheme I) and cyanogen bromide were treated with a base such as triethylamine, under mild conditions (-40°C to room temperature), a fast and clean reaction occurred to give rise to N - benzoyl benzimidazolinone (**2a**) in 65% yield.[3] .Variation in the electronic character of either the hydroxylamine moiety or the acyl portion of the hydroxamic acids **1** (*cf.* Table 1 and Scheme II) did not significantly alter either the yield or the regiospecificity of the reaction. We therefore believe that, in the light of exclusive formation of benzimidazolinones and the

Scheme I

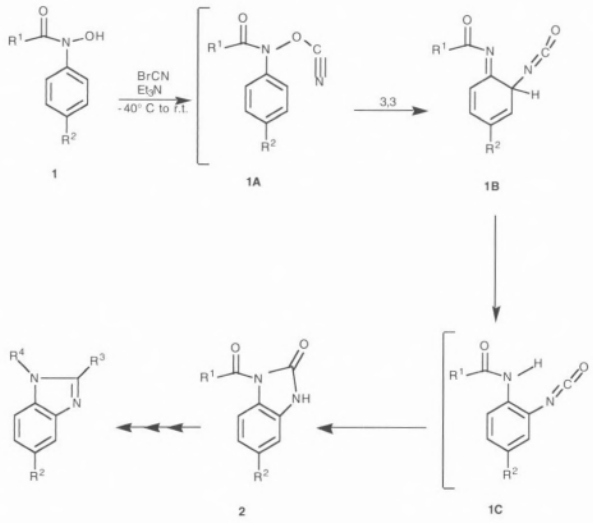

a: $R^1 = C_6H_5$ $R^2 = H$

b: $R^1 = C_2H_5O$ $R^2 = H$

c: $R^1 = C_6H_5$ $R^2 = CH_3$

d: $R^1 = C_2H_5O$ $R^2 = CH_3$

e: $R^1 = C_6H_5$ $R^2 = Br$

f: $R^1 = C_2H_5O$ $R^2 = Br$

g: $R^1 = CF_3$ $R^2 = H$

Table I

Starting material	Product	Yield
1a	**2a**	65%
1b	**2b**	59%
1c	**2c**	52%
1d	**2d**	72%
1e	**2e**	81%
1f	**2f**	77%
1g	**3**[a]	64%
4a	**5a**	69%
4b	**5b**	63%
6	**7**	99%

[a] After hydrolysis of **2g**.

Scheme II

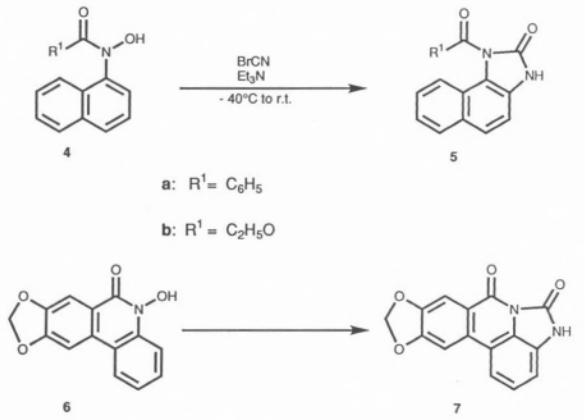

Scheme III

Synthesis of 3 - Substituted N - Benzoyl Oxindoles

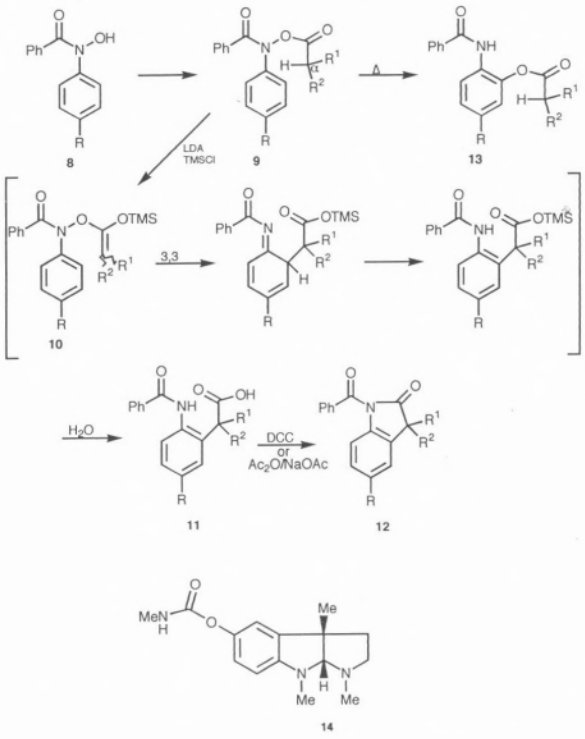

high yields obtained in all cases, the rearrangements are intramolecular and most probably concerted in nature as shown in Scheme I. The 2-substituted benzimidazoles, many of them known to possess useful properties,[4] are, in principle, accessible from these benzimidazolones by standard chemical reactions.

Considering again Figure 1, an analogous reaction can be envisioned if the system X=Y constitutes part of an olefinic system, i.e. X=Y=C. This system can be generated *in situ* [5] if compounds **9**, easily obtained from benzohydroxamic acids **8** (*cf.* Scheme III) by acylation with an acid chloride or with an acid in the presence of dicyclohexylcarbodiimide (DCC), are treated with a strong base such as lithium di-isopropyl amide (LDA)

at low temperature in the presence of trimethylsilyl chloride (TMSCl) . The resulting silyl enol ethers **10** thus formed underwent a spontaneous 3,3-sigmatropic rearrangement to yield, after aqueous work-up, the *o* - aminobenzoyl - phenyl acetic acids **11** (Table II). These substances can be cyclised smoothly (DCC or NaOAc-Ac_2O) to the corresponding oxindoles **12** (Table III) of obvious utility as starting material for the synthesis of a biologically active alkaloid such as physostigmine (**14**) and related molecules.

The results show that the presence of carbanion stabilizing groups (SPh, Ph or olefin) α to the carbonyl function in the acetyl fragment of **9** is necessary to prevent a rapid reversion to the parent hydroxamic acid **8** (*cf.* behaviour of **9**, R=R^1=R^2=H in Table II) and to favour the rearrangement. [6] Functional groups such as *p*-OMe, *p*-Cl and *p*-CO_2Me in the aniline moiety of **9** do not seriously interfere with the reaction. Of particular synthetic interest is the ready access the method provides for phenylthio-oxindoles, with the nitrogen already suitably protected, thus permitting further useful chemical transformations to be performed at C-3 by radical and/or carbanion chemistry.

It is also interesting to note that the esters **9** are thermally unstable and rearrange[6] to the corresponding *o* -acyloxybenzanilides **13**. However, in the presence of base a radically different chemical reactivity is manifested.

We have previously shown that aroyl and acyl cyanides tend predominantly to *O*-acylate N-aryl hydroxylamines.[8] It was thus of interest to study the chemistry of alkoxycarbonyl cyanide **15** in which the electronic character of the carbonyl group has been slightly modified. With this substance as electrophile, the reaction with hydroxylamines took a different course.[9] The products obtained were the addition compounds **16** (Scheme IV) arising from the attack of the nitrogen atom of the hydroxylamines at the *sp* carbon of the cyanide group. The structure of one (**16a**) of these highly functionalised molecules, containing a number of adjacent functional groups, was shown to possess unambiguously the nitrone structure by X-ray crystallography (Figure 2). Further evidence for predominance of the nitrone form for these compounds in solution came from the comparative study of the UV spectra of **17** in Scheme V and **16a-16f**.[9]

Table II

Synthesis of N-Aryl-O-acyl Hydroxamic Acids and Products of Rearrangement

9			9, Yield	11, Yield
R	R^1	R^2		
H	H	H	92%	8%[a]
H	H	Ph	72%	68%[b]
H	Ph	Ph	73%	25%[b,c]
H	H	SPh	76%	50%[b]
Cl	H	SPh	69%	50%[b]
CO_2Me	H	SPh	89%	54%[b]
Me	H	SPh	72%	71%[b]

[a] Recovered starting material 90%.
[b] Characterised as methyl esters.
[c] The corresponding benzanilide isolated in *ca.* 40%.

Table III

3-Substituted N-Benzoyl Oxindoles

12			Yield
R	R^1	R^2	
H	H	Ph	65%
H	Ph	Ph	25%[a]
H	H	SPh	46%
Cl	H	SPh	49%
CO_2Me	H	SPh	51%
Me	H	SPh	53%
OMe	H	SPh	34%

[a] The corresponding benzanilide was isolated in *ca.* 40%.

Scheme IV

Synthesis of α-Aminonitrones

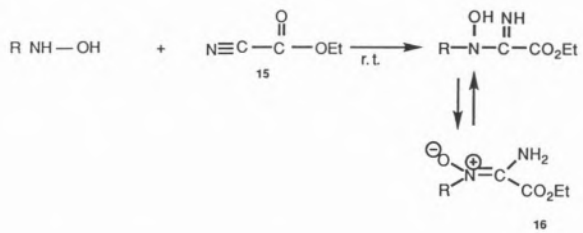

Product	R	Yield
16a	Me	65%
16b	^{i}Pr	73%
16c	Ph	79%
16d	4 - MeC_6H_4	72%
16e	3 - MeC_6H_4	62%
16f	4 - BrC_6H_4	67%

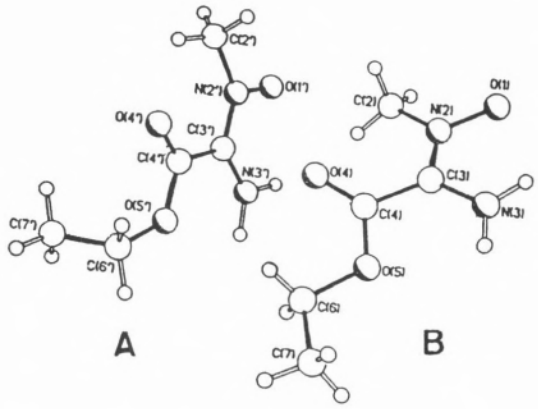

Figure 2. X-Ray structure of compound **16a**, showing the presence of two crystallographically independent molecules **A** and **B**.

Scheme V

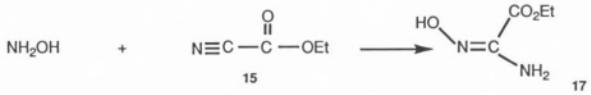

Scheme VI

α-Aminonitrones and Mesylchloride

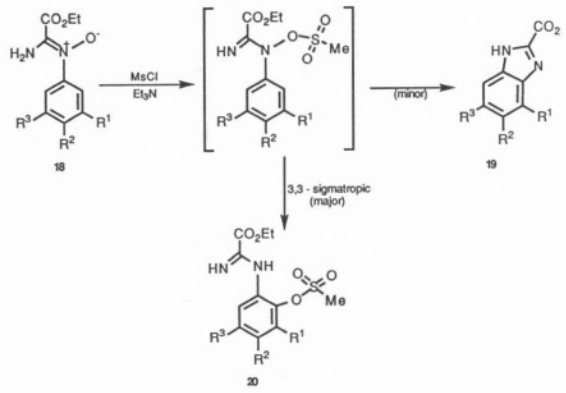

Starting material	Product	R^1	R^2	R^3	Yield
18a	20a	H	H	H	60%
18b	20b	H	Me	H	56%
18c	20c	H	H	Me	50%
	20c'	Me	H	H	15%
18d	20d	H	Br	H	40%

Reaction of **18** with mesyl chloride[9] (Scheme VI) yielded as the major product, the mesyloxy amidine **20** — the hoped for benzimidazole-2-carboxylate **19** being formed only in 7% yield.

Similarly, reaction with bromocyanogen and **18** (Scheme VII) afforded the N - substituted benzimidazolones **23**. The intermediate **21A** formed from **18** undergoes a rapid 3,3-sigmatropic rearrangement to give **22**. Rearomatisation results in the formation of the benzimidazolones **23**. It is interesting to note that in none of the compounds studied the alternative 3,3-hetero-oxy-Cope rearrangement involving the conformer **21B** leading to the triazolone **21'** was observed. A

Scheme VII

α-Aminonitrones and Bromocyanogen

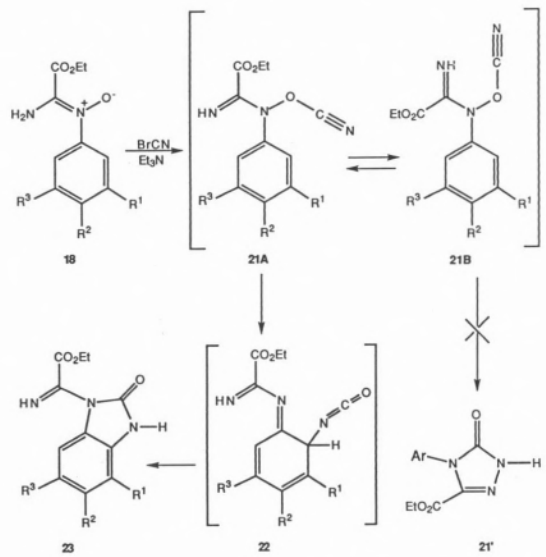

Starting Material	Product	R^1	R^2	R^3	Yield
18a	23a	H	H	H	66%
18b	23b	H	Me	H	82%
18c	23c	Me	H	H	87%
18d	23d	H	Br	H	75%

Scheme VIII

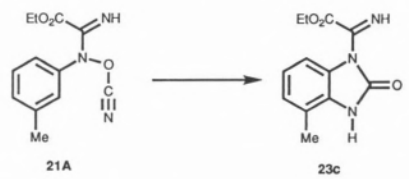

possible reason, other than one conformational in origin, could be due to considerable weakening of the N—O bond with significant positive charge already developed in the aromatic ring in the intermediate **21A**. Also intriguing is the exclusive formation of the benzimidazolone **23c** resulting from attack *ortho* to the methyl group. Obviously the conformation of the intermediate **21A** depicted in Scheme VIII is preferred, the reason for such preference, however, remains obscure.

The N-imidoylbenzimidazolones **23** (Scheme IX) were all sensitive to acid and to heat, the action of both of them leading to the formation of the corresponding benzimidazolones **24** in excellent yields.

The failure of the aminonitrones **16a** and **16b** (Scheme IV) to give any useful products with cyanogen bromide led us to employ the less powerful electrophile, the propiolate esters. Indeed, when **16a** (Scheme X) was treated at room temperature for an hour with methyl propiolate in the presence of triethylamine, and then boiled for 15 min, an excellent yield of an imidazole dicarboxylic ester was obtained. *A priori*, the product formed could be either the 2,4-disubstituted imidazole **26** or its 2,5-regioisomer **27**, depending on the nature of the rearrangement, namely 3,3 or 1,3, suffered by the intermediate **25** (Scheme X). Since the spectral characteristics (^{13}C and ^{1}H NMR) and the m.p. of the known 2,5-dimethyl ester [10] **27** (R=Me) were significantly different from those found for our product it follows that the latter is to be represented by structure **26**.

Scheme IX

Benzimidazolones from N-imidoylbenzimidazolones

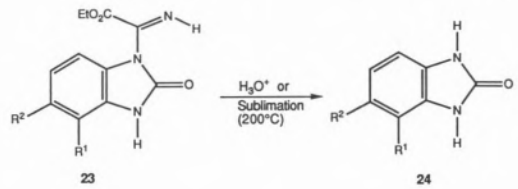

23 **24**

Starting material	Product	R^1	R^2	Yield
23a	**24a**[a]	H	H	95%
23b	**24b**[b]	H	Me	93%
23c	**24c**[c]	Me	H	95%
23d	**24d**[c]	H	Br	92%

[a] Hershenson, F. ; Bauer, L.; King. K. *J. Org. Chem.*, *33* (1968) 2543.
[b] Staab, H. *Ann.*, *609* (1957) 75.
[c] Robert, L. ; Arsenio, A. *J. Am. Chem. Soc.*, *80* (1958) 1657.

Scheme X

Imidazoles from α-Aminonitrones

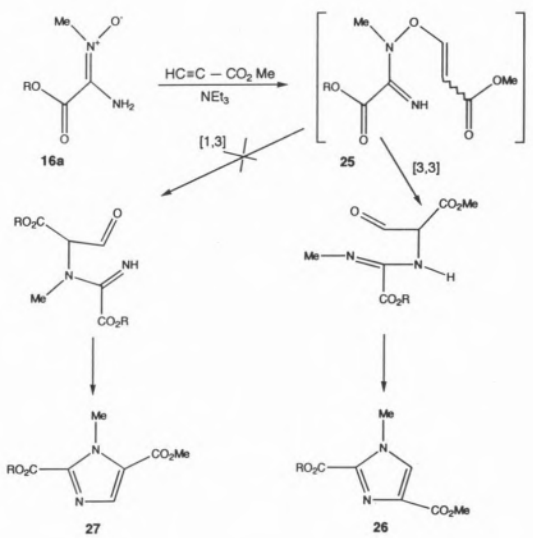

16a **25** **27** **26**

Scheme XI

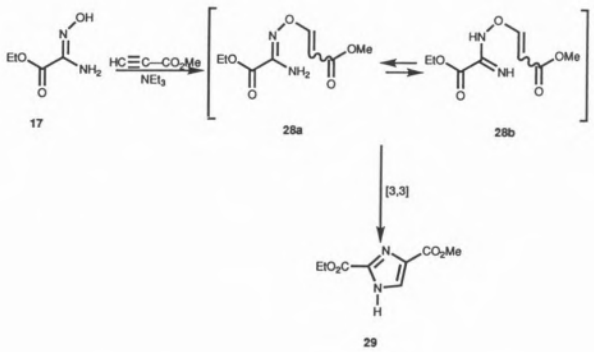

17 **28a** **28b** **29**

In the case of the oxime **17** (Scheme XI) it was possible to isolate the initial Michael adduct **28a** or **28b** consisting of the *trans* isomer (80%) and the *cis* isomer (20%). On thermolysis the mixture was cleanly converted into the imidazole derivative **29** in a sequence of reactions involving a 3,3-sigmatropic rearrangement and a 1,3-prototropic shift followed by dehydration.

2. Addition to Carbon-Carbon π Bonds — A New Aziridination Triggered by Nitrogen-Oxygen Cleavage

The discovery by our group that a variety of acylating agents[11] can specifically O-acylate N-aryl hydroxylamines to yield **30** (R=H, R^1=Ph,Me, *t* -Bu) (Scheme XII) has enabled the examination of reactivity towards carbon—carbon π bonds of these substances hitherto accessible only with difficulty. It was anticipated that the anion **31** (R=H, R^1=Ph), generated from **30** (R=H, R^1=Ph) would react with a carbon—carbon π bond of a Michael acceptor by an AE (addition-elimination) mechanism[12] and provide a new method for 2-substituted aziridines **32**. In the event, **31** (R=H, R^1=Ph) with ethyl acrylate yielded azoxybenzene, azobenzene, the amide **33** (R=H, R^1=Ph), benzoic acid and the aziridine **32** (R=H, R^2=H, EWG=CO_2Et, 27%).[13] The use of *tert* - butyl ester **31** (R=H, R^1= *t* -Bu) with ethyl acrylate or phenyl vinyl sulfoxide did not significantly improve the yield of **32** , the former affording in addition to the aziridine **32** (R=R^2=H, EWG=CO_2Et) the Michael adduct **34** (EWG= CO_2Et, 19%), and the latter affording **32** (R=R^2=H, EWG=SOPh, 32%) as a mixture of two diastereoisomers. However with the sodium hydroxamate **35b** (X=Na, R^1=*t* -Bu) generated *in situ* from the corresponding hydroxamic acid **35a** with sodium hydride in the presence of the same electrophile, phenyl vinyl sulfoxide, yielded the aziridine **32** (R=H, R^2=Ph, EWG=SOPh) in 65% at room temperature in 30 min. The results (Table IV) clearly demonstrate that a variety of hydroxamic acids bearing different ring substituents (except entry 15; *p* - MeO) afford in good to excellent yields the corresponding aziridines,[13] which can be used for further useful chemical transformations.[14] While a single ß - alkyl substituent (*cf.* entries 6 and 7) in the electrophile tends to reduce the yield, the presence of ß,ß - disubstitution (*cf.* entries 16 and 17) inhibits the reaction completely. Also noteworthy is the complete stereospecificity observed for this aziridination. Thus

Scheme XII

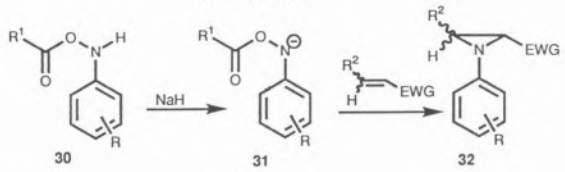

EWG = electron-withdrawing group

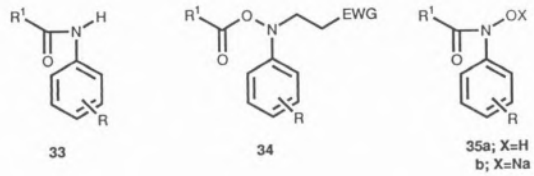

33 34 35a; X=H b; X=Na

Table IV

Aziridines 32 prepared from Hydroxamic Acids 35a

Entry	Starting material R	Olefin R^2	Olefin EWG	Aziridine 32 R^2	Aziridine 32 EWG	Aziridine 32 R	Yield (%)[a]
1	4-Br	H	SOPh	H	SOPh	4-Br	77 (2:1)
2	4-Cl	H	SOPh	H	SOPh	4-Cl	68 (2:1)
3	3-Me	H	SOPh	H	SOPh	3-Me	70 (1:1)
4	4-Me	H	SOPh	H	SOPh	4-Me	77 (1:1)
5	4-NO_2	H	SOPh	H	SOPh	4-NO_2	43 (11:1)
6	H	H	CO_2Me	H	CO_2Me	H	67
7	H	Me *(trans)*	CO_2Me	H	CO_2Me	Me *(trans)*	48
8	4-Br	H	CO_2Me	H	CO_2Me	4-Br	62
9	4-Cl	H	CO_2Me	H	CO_2Me	4-Cl	60
10	4-Cl	H	CO_2Et	H	CO_2Et	4-Cl	95
11	3-Me	H	CO_2Et	H	CO_2Et	3-Me	93
12	4-Me	H	CO_2Et	H	CO_2Et	4-Me	90
13	3-Br	H	CO_2Me	H	CO_2Me	3-Br	62
14	4-NO_2	H	CO_2Me	H	CO_2Me	4-NO_2	67
15	4-OMe	H	CO_2Me	H	CO_2Me	4-OMe	9
16	H	H	COMe	H	COMe	H	80
17	H	Δ^4-Cholestenone		—	—	—	0
18	H	CO_2Me *(trans)*	CO_2Me	CO_2Me *(trans)*	CO_2Me	H	41
19	H	CO_2Me *(cis)*	CO_2Me	CO_2Me *(cis)*	CO_2Me	H	41

[a] Isomeric ratio by ^{1}H NMR in brackets.

Table V

^{1}H NMR Data for C_2-H and C_3-H of Aziridines

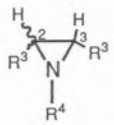

Compound R_3	Compound R_4	δ_{cis}	δ_{trans}
COPh	cyclohexyl	3.38[a]	4.07[a]
COPh	Me	3.25[a]	3.92[a]
COPh	CH_2Ph	3.38[a]	4.10[a]
CO_2Me	4-MeOC_6H_4	2.86[b]	3.31[b]
		3.05[c]	3.44[c]
CO_2Me	Ph	3.31[d]	3.85[d]
CO_2Me	3-MeC_6H_4	3.11[d]	3.47[d]

[a] Turner, A.B.; Heine, H.W.; Irving, J.; Bush, J.B. *J. Am. Chem. Soc.*, *87* (1965) 1050.
[b] Huisgen, R.; Scheer; W.; Huber, H. *J. Am. Chem. Soc.*, *89* (1967) 1753.
[c] Huisgen, R.; Szeimies, G., *Chem. Ber.*, *99* (1966) 491.
[d] Reference 19.

dimethyl maleate afforded exclusively the *cis* aziridine (entry 19) with no traces of the *trans* isomer being formed (within the limits of detection by thin layer chromatography). Likewise the fumarate yielded solely the *trans* compound (entry 18). The stereochemical assignments were based on the chemical shifts of the two equivalent methine protons at C-2 and C-3, of the corresponding *cis* and *trans* aziridines. It is known that in a series of N-substituted aziridines bearing two identical electron withdrawing groups at C-2 and C-3, the methine proton of the *trans* isomer invariably resonates at *lower field* than the corresponding proton of the *cis* isomer (Table V).

The essentially nucleophilic but not the nitrenic nature of the aziridinating agent was demonstrated by its total incapacity to produce the corresponding aziridines (or products resulting therefrom) with cyclohexene, styrene or dihydropyran. In each case the products were azobenzene (*cis* and *trans*, 80%), azoxybenzene and N-pivaloylaniline, the latter two constituting *ca.* 10%, virtually the same percentage distribution observed when the hydroxamate alone was left to decompose in solution.

Germane to the discussion of any possible mechanism are the following observations:

a) the N-pivaloyl hydroxamic acids consistently give better yields of aziridines than the corresponding benzoyl analogs;

b) the Michael adduct **34** (R=H, R^1= *t* -Bu, EWG = CO_2Me) does not yield the aziridine on treatment with a variety of bases, showing that *it is not the precursor of the aziridine* **32**;

c) no aziridination occurs with N-acyloxy hydroxylamine in the absence of base;

d) slow addition of **30** to an excess of methyl acrylate in the presence of base causes a significant increase in the yield of the aziridine (75%);

e) change of solvent from THF to cyclohexane does not significantly decrease the yield of the product, thus precluding the involvement of a solvent stabilized singlet aryl nitrene[15] as the reactive nucleophilic species;

f) the anion of N-pivaloylaniline (**37**) (Scheme XIII) and ethyl glycidate (**38**), which in principle could be formed by the initial Michael adduct **36** suffering a *3-exo-tet* ring closure, do not react by ring opening of the epoxide, followed by N- to O- transacylation and subsequent ring closure to afford the aziridine.

Scheme XIII

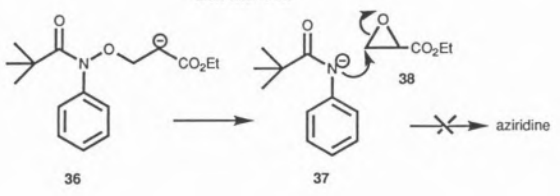

Scheme XIV

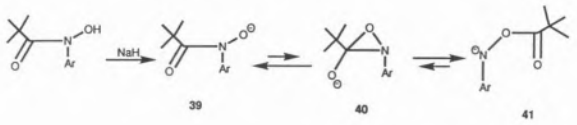

Scheme XV

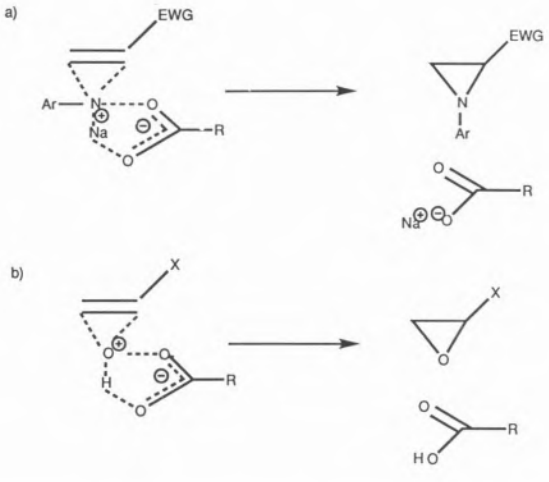

Scheme XVI

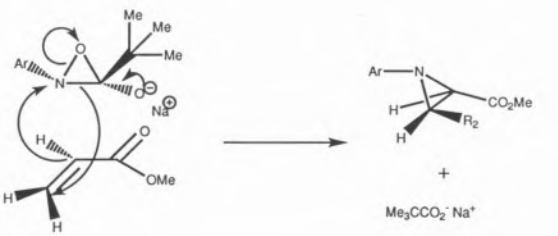

On the basis of this evidence two possible mechanisms could be written for this novel reaction. The formation of the Michael adduct **34** implied a thermodynamically driven isomerisation[16] of the hydroxamate anion **39** (Scheme XIV) to the N-acyloxyaniline anion **41** through the oxaziridine intermediate **40**. Both of these latter two species, **40** and **41**, could, in principle, act as the aziridinating agent (see Schemes XV and XVI), provided it is assumed that an equilibrium exists between them with the former having a sufficient half-life to permit its reaction with external electrophiles. In Scheme XV-a) is depicted a concerted aziridination

mechanism which draws its analogy from the epoxidation of olefins by peracids[17] (*cf.* Scheme XV-b) and also the mechanism proposed by Atkinson[18] and coworkers in their aziridination reactions utilising hydrazine derivatives. Scheme XVI on the other hand shows the concerted attack of the oxaziridine anion on the electron deficient carbon-carbon π bond of the olefin.

Although a definite choice between the two mechanisms is difficult to make in the absence of kinetic data, an attempt nevertheless was made to clarify the situation by utilizing the benz-5-oxo-2,5-dihydro-1,2-oxazole (**42**) with the tacit assumption that geometric constraints would disfavour the formation of the strained tricyclic system **43** (*cf.* Scheme XVII). Reaction of the cyclic N-acyl compound **42** in the presence of NaH with methyl acrylate *did not yield the aziridine* **44**; instead the principal product, formed in 55% yield, was the Michael adduct **45** — a result that strongly suggests the involvement of the oxaziridine as the effective nitrogen transfer reagent.[19]

As can be easily seen, the above reaction of aziridination has obvious advantages over the common azide method in that it is simple to perform, occurs at or below room temperature, and does not require thermolysis of the potentially explosive azides used as starting materials. Furthermore the reaction (in the cases studied so far) occurs with complete stereospecificity.

Scheme XVII

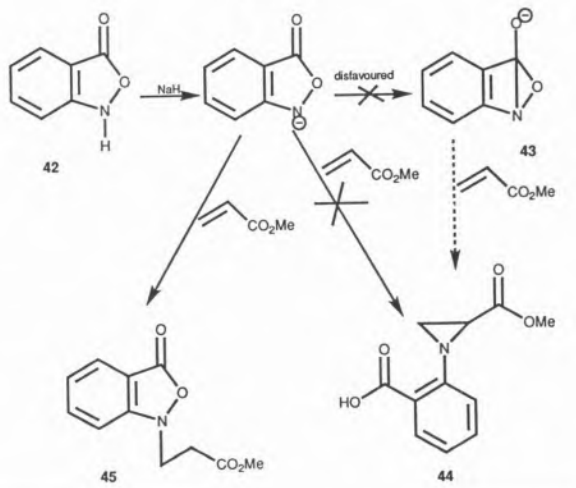

3. Aryl-Aryl Bond Formation via Radical Reactions

The use of radical reactions to effect carbon-carbon bond reactions of synthetic use is a relatively new field.[20] This stemmed from the lack of knowledge concerning the predictability and selectivity of free radical chemistry, for until the late sixties organic chemists tended to consider free radical reactions as erratic, capricious, and prone to give intractable mixtures of products. During the past decade this view has changed profoundly and it is now widely recognized that radical reactions, even with very complex and heavily substituted substrates, can be conducted in a highly selective and efficient manner, and often display advantages over alternative ionic processes.[21,22] A review [23] describes the uses of free radical methodology in the synthesis of natural products, and a recent book [24] offers a highly interesting account of the incidence of radical chemistry in a variety of topics such as the pyrolysis of chlorinated hydrocarbons, the synthesis of aldosterone and the generation of disciplined radicals.

3.1. A New Phenanthridine Synthesis

Most known addition reactions of radicals to aromatic rings involve net substitution for a hydrogen atom by the general mechanism outlined in (eq. 1).

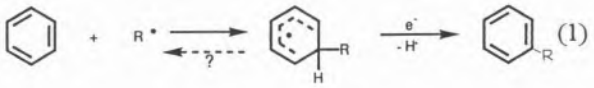

(1)

The addition reactions of alkyl and substituted alkyl radicals to simple aromatic rings are very slow.[25] The addition of aryl radicals to aromatic rings are considerably faster[26] but their preparative utility has been hampered by low regio- and chemoselectivity. However, the addition of an aryl radical to benzene, used as the solvent, can become a limiting side reaction when techniques like slow syringe pump addition of tin hydride are used and there is no good trap for the aryl radical[27] (*cf.*eq.2.)

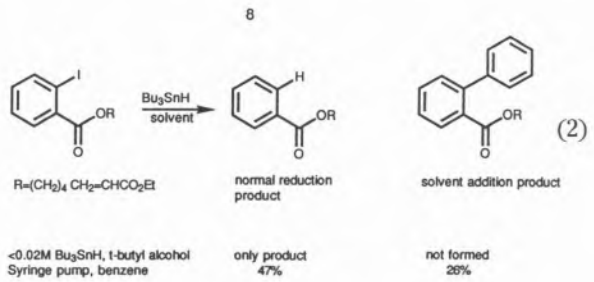

(2)

Applications of radical aryl-aryl coupling reactions in synthesis are scare. A literature survey showed that an aryl-aryl coupling reaction involving the use of stannyl compounds occurred when the aryl bromide **46** (Scheme XVIII) was treated with tributyltin hydride under standard conditions, to yield the phenanthrene **47**, presumably *via* radicals **48** and **49** and *not* the anticipated isomeric product **50**.[28]

Our interest in the synthesis of *Amaryllidaceae* alkaloids, such as lycoricidine **51**, from a fully aromatic precursor, led us to investigate the chemistry of aryl radicals formed by *n*-tributyl stannyl hydride (*n*-Bu_3SnH) and 1,1'-azobisisobutyronitrile (AIBN) treatment of

Scheme XVIII

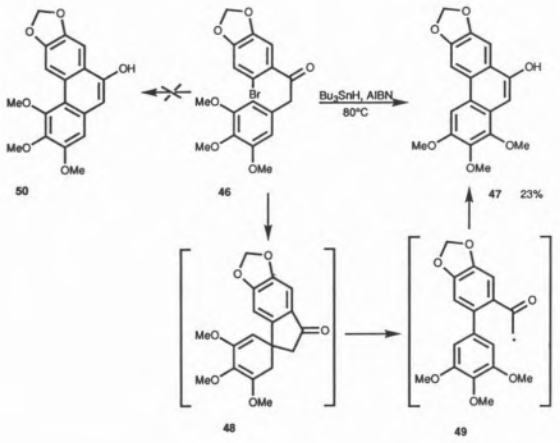

Scheme XIX

Radical Aryl - Aryl Coupling

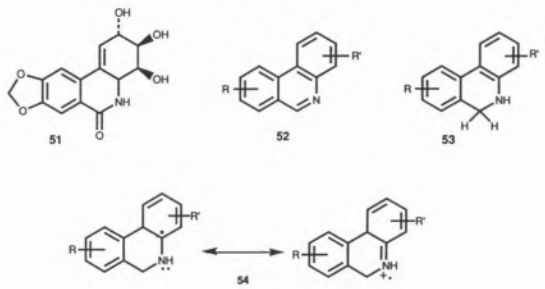

Table VI

Polyalkoxyphenanthridines by Radical Aryl-Aryl Coupling

Entry	$ArCH_2NHAr'$	Phenanthridine	Yield[a] (%)
1	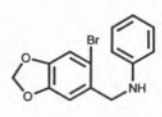	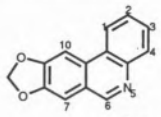	66
2	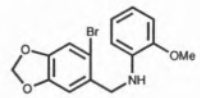	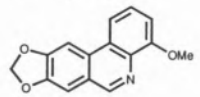	63
3	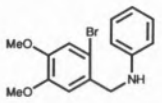	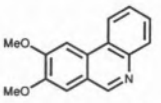	68
4	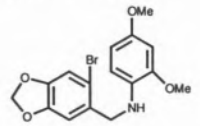	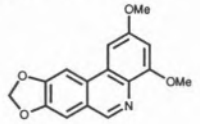	67
5	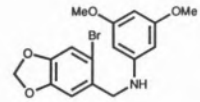	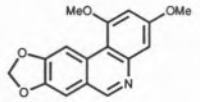	62
6	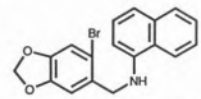	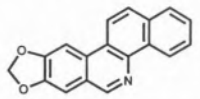	70

[a] Represents yields of products obtained after evaporation of the solvent, washing the residue with cold *n*-pentane, followed by chromatography on SiO_2 to separate small amounts of unreacted starting material and debrominated product (total 15%).

N-(*o*-bromobenzyl) anilines. The expectation that the cyclisation would be facilitated by the additional stabilization of the putative intermediate radical **54** was fully realized (*cf.* Scheme XIX).[29] A variety of polyalkoxyphenanthridines[30] **52**, by radical aryl-aryl coupling and subsequent aerial oxidation of the initially formed 5,6-dihydrophenantridines **53**, was obtained in synthetically useful yields (Table VI).

Taking the example (entry 4; Table VI) the addition of the *sigma* aryl radical formed **56** (Scheme XX) to the vicinal aromatic ring B, can, in principle, operate via a 6-*endo* cyclisation to yield the radical **57** or alternatively via a 5-*exo* mode to generate radical **58** (*ipso* substitution). The latter can suffer an aryl translocation to generate species **57** or rearrange, involving the nitrogen atom to produce a new cyclohexadienyl radical **59**. Both these radicals **57** and **59**, on loss of a hydrogen atom would lead to the dihydrophenanthridines **60** and/or **61** and thence, by aerial oxidation, to the heterocycles **62** and/or **63**. A careful analysis of the ^1H NMR spectra of the two isomeric phenantridines **62** and **63** (entries 4 and 5 respectively, in Table VI) provided a definitive answer to the question as to which of the two possible mechanisms was operating. It is well known that a methoxy substituent at C-1 in a phenantrene molecule[31] causes a pronounced diamagnetic deshielding of the proximate C-10 hydrogen. Whereas in the phenanthridine **63** (entry 5) the C-10 hydrogen resonates at Δ 8.81 as a sharp one proton singlet, in the isomeric phenanthridine **62** (entry 4) the same hydrogen possessed a normal chemical shift value (Δ 7.61, 1 H , singlet). Thus the absence, among the products isolated in the cyclisation of **55** (Scheme XX) of product **63**, strongly suggests that radical **57** is in the reaction pathway, and may originate directly from **56** or indirectly from **58**, via an aryl translocation. Similarly **55a** (Scheme XX, bottom) gave solely the phenanthridine **63**. This observation shows convincingly that the formation of phenanthridines is regiospecific and *does not involve a nitrogen to carbon migration in the initially formed spirocyclohexadienyl radicals,* if indeed they are formed.

Scheme XX

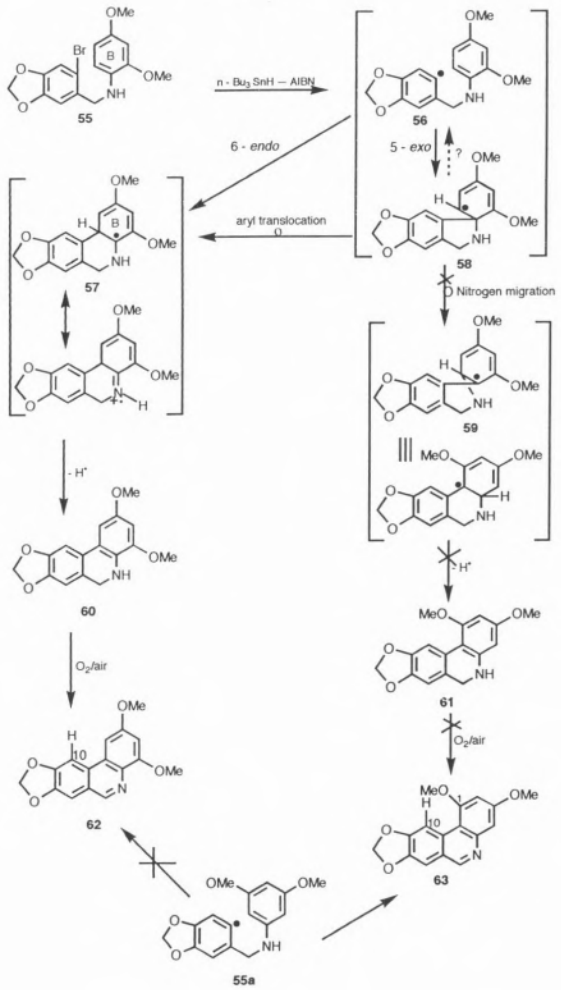

3.2. Applications in the Synthesis of Amaryllidaceae *Alkaloids*

Amaryllidaceae alkaloids represent a family of alkaloids of wide structural variety, and many of these have interesting biological properties.[32]

Application of the radical reaction previously described to **64** (R^1=CH_2CH_2OH) (*cf.* Scheme XXI) led to the synthesis of the functionalised phenanthridine **65**. With the use of appropriate reagents[33] , the intermediate **65** (R^1=CH_2CH_2OH) could be made to yield vasconine[34] (**66**), assoanine[35] (**67**), oxoassoanine[35] (**68**) and pratosine[36] (**69**). Extension of the method to the benzyl phenyl ether **70** (cf. Scheme XXII) yielded as the sole isolable product the benzopyran **71** (48%), probably arising from a *6-endo* ring closure. However, the aminobenzyl ether **72** (Scheme XXIII) easily prepared in excellent yield from simple starting materials, afforded in one step N-*nor*ismine **74** (26%), accompanied by the phenanthridine **75** (8%), the debromo compound **76** (10%) and the benzopyran **77** (10%).

The significant preponderance of products derived from the *5-exo* process (Scheme XXIII) at the expense of the *6-endo* mode in the cyclisation of **72** lends weight to our contention that a carbon centered radical adjacent to an amino group such as in **73** is indeed substantially stabilized.

Since we had earlier[37] devised an efficient method to convert N-*nor*ismine to the interesting alkaloid ismine **78** , this method provides an alternative and shorter synthesis of this natural product.

Scheme XXI

Synthesis of Amaryllidaceae Alkaloids

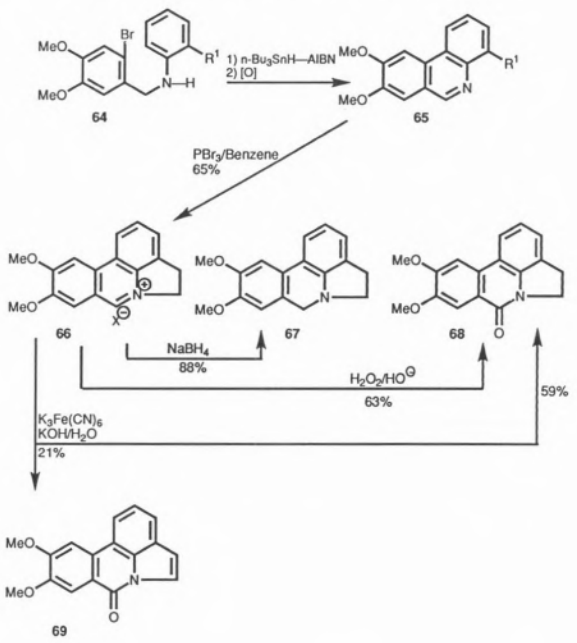

Scheme XXII

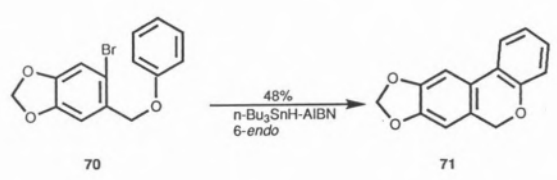

Scheme XXIII

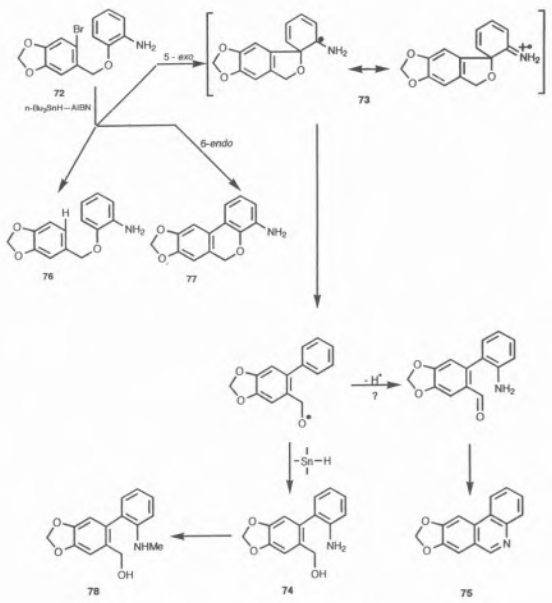

Conclusions and Prospects

The investigations detailed in this Account confirm that the area related to addition to and substitution at carbon-carbon π bonds is a fertile field for the development of reactions of value in organic synthesis. The mildness of the experimental conditions, high regiochemical selectivity observed and "low-tech" nature of this type of chemistry will certainly prove to be some of its greatest virtues. In spite of the spectacular success achieved by synthetic organic chemistry during the past three decades, nonetheless this branch of science appears as a remarkably immature one, when one is confronted with the formidable challenge of preparing, in an economic way, even relatively simple molecules. In this context reactions that are capable of forming molecular systems in a selective fashion using simple inexpensive reagents and "low-tech" conditions will assume an ever increasing industrial importance. No doubt this is a field where yet much new chemistry will be unraveled.

Acknowledgements

We wish to thank all our collaborators whose names appear in the references for their enthusiasm and dedication, without which this work would not have been possible.

References

1. J. B. Hendrickson, *Angew. Chem. Int. Ed. Engl.*, **13** (1974) 47.

2. R. M. Coates, W. F. Burgoyne, C. W. Hutchins, S. L. Bender, *in The Chemistry and Biology of Hydroxamic Acids*, Kehl, H., Ed., Karger, Basel 1982; p.15.

3. P. S. Almeida, A. M. Lobo, S. Prabhakar *Heterocycles*, **28** (1989) 653.

4. *Comprehensive Heterocyclic Chemistry*, A. R. Katritzky, C. W. Rees, Ed., Pergamon Press, Oxford, vol. 1, p. 202, 366 and vol. 6, p. 328.

5. P. S. Almeida, S. Prabhakar, A. M. Lobo, M. J. M. Curto, *Tetrahedron Lett.* **23** (1991) 2671.

6. For a recent review on the synthetic uses of hydroxylamines and their derivatives involving hetero-Cope rearrangements see: S. Blechert, *Synthesis* (1989) 71.

7. a) L. Horner, M. Steppan, *Justus Liebig Ann. Chem.*, **606** (1957) 24; b) T. Ohta, K. Shudo, T. Okamoto, *Tetrahedron Lett.* **23** (1978) 1983.

8. a) S. Prabhakar, A. M. Lobo, M. M. Marques, *Tetrahedron Lett.* **23** (1982) 1391;

b) A. M. Lobo, M. M. Marques, S. Prabhakar, H. S. Rzepa, *J. Org. Chem.*, **52** (1987) 2925.

9. P. S. Branco, S. Prabhakar, A. M. Lobo, D. J. Williams, *Tetrahedron* **48** (1992) 6335.

10. A. J. Carpenter, D. J. Chadwick, R. I. Ngochindo, (1983) *J. Chem. Res. (M)* 1913.

11. a) A. M. Lobo, M. M. Marques, S. Prabhakar, H. S. Rzepa, (1985) *J. Chem. Soc., Chem. Commun.* 1113;

b) L. M. Ferreira, A. M. Lobo, S. Prabhakar, M. J. M. Curto, H. S. Rzepa, M. Y. Yi, *J.* (1991) *Chem. Soc., Chem. Comm.* 1127;

c) P. P. O. Santos, C. L. Trindade, A. M. Lobo, S. Prabhakar, (1993) *Tetrahedron Lett.* 3793.

12. For the non-stereospecific N-unsubstituted aziridine formation by an AE pathway, see: N. Furukawa, T. Yoshimura, M. Ohtsu, T. Akasaka, S. Oae, *Tetrahedron* **36** (1980) 73.

13. M. M. Pereira, P. P. O. Santos, L. V. Reis, A. M. Lobo, S. Prabhakar, (1993) *J. Chem. Soc., Chem. Commun.* 38.

14. *1,3-Dipolar Cycloaddition Chemistry*, A. Padwa, Ed., Wiley - Interscience, New York; 1984.

15. *Azides and Nitrenes, Reactivity and Utility*, E. F. V. Scriven, Ed., Academic Press, London 1984; p. 116.

16. G. Boche, F. Bosold, S. Schroder, *Angew. Chem. Int. Ed. Engl.* **27** (1988) 973.

17. D. Swern, *Organic Peroxides*, Wiley - Interscience, New York, 1971, vol.II, p. 355; D. Swern, *Org. Reactions* **7** (1953) 378.

18. R. S. Atkinson, B. J. Kelly, J. Williams, *Tetrahedron* **36** (1992) 7713.

19. Unpublished observation: P. P. O. Santos, Ph.D. Thesis, New University of Lisbon.

20. a) B. Giese, *in Radicals in Organic Synthesis: Formation of Carbon-Carbon Bonds*, Pergamon, Oxford, 1986;

b) T. V. Rajanbabu, *Acc. Chem. Res.* **24** (1991) 139;

c) M. Ramadah, *Tetrahedron*, **43** (1987) 3541.

21. A. L. Beckwith, *Chem. Rev.* **22** (1993) 143.

22. For a comprehensive review of organic free radical chemistry see: A. Ghosez, B. Giese, W. Mehl, J. O. Metzger, H. Zipse, *in Methoden der organische Chemie*, (Houben-Weil), M. Regitz, B. Giese, Eds., Georg Thieme, Stuttgart (1989) Vol. E19a, Parts 1 and 2.

23. C. P. Jasperse, D. P. Curran, T. L. Feviz, *Chem. Rev.* **91** (1991) 1237.

24. *Half a Century of Free Radical Chemistry*, D. H. R. Barton, S.I. Parekh, Cambridge University Press, Cambridge, 1993.

25. D. P. Curran, *in Comprehensive Organic Synthesis*, B. M. Trost, I. Fleming, Eds., Pergamon, Oxford vol.4, p. 766; 1991.
26. J. K. Kochi, *in Free Radicals*, Wiley, New York, vol. 2, p. 231.
27. *Cf.* reference **25**, p.767.
28. N. S. Narasimhan, J. S. Aidhen, *Tetrahedron Lett.* **29** (1988) 2987.
29. A. M. Rosa, S. Prabhakar, A. M. Lobo, *Tetrahedron Lett* **31** (1990) 1881.
30. The photocyclisation method involving boron complexes of *C,N*-diaryl hydroxamic for the preparation of polyalkoxyphenanthridines was thwarted by the extreme instability of polyalkoxyphenylhydroxylamines [*cf.* S. Prabhakar, A. M. Lobo, M. R. Tavares, (1978) *J. Chem. Soc., Chem. Comm.* 884].
31. N. S. Bhacca, L. F. Johnson, J. N. Shoolery, *NMR Catalog No 349*, Varian Associates, Palo Alto; 1962.
32. a) G. A. Swan, *An Introduction to the Alkaloids*, Blackwell Scientific Pub., Oxford 1967; p.146;
b) W. S. Wildman, *in Chemistry of the Alkaloids*, S. W. Pelletier, Ed., Van Nostrand Reinhold, New York 1970; p.151.
33. A. M. Rosa, S. Prabhakar, A. M. Lobo, presented in part at the VII th FECHEM Conference on Heterocycles in Bio-organic Chemistry, Santiago de Compostela (Spain), Abstracts (1993).
34. J. Bastida, C. Codina, F. Viladomat, *J. Nat. Prod.* **55** (1992) 122.
35. J. M. Llabres, F. Viladomat, J. Bastida, C. Codina, M. Rubiralta, *Phytochemistry* **25** (1986) 2637.
36. S. Ghosal, K. S. Saini, A. W. Frahm, *Phytochemistry* **22** (1983) 2305.
37. S. Prabhakar, A. M. Lobo, M. M. Marques, M. R. Tavares, *J. Chem. Research* **5** (1985) 394.

The planets and Thermodynamics*

Os planetas e a Termodinâmica

JORGE CALADO

CENTRO DE QUÍMICA ESTRUTURAL, COMPLEXO I, INSTITUTO SUPERIOR TÉCNICO, 1096 LISBOA CODEX, PORTUGAL

The birth of modern science is linked to the first systematic observations of the solar system by Galileo in the 17th century. His first important publication, *Sidereus Nuncius* (1610), had a tremendous impact on fellow scientists as well as on painters and writers. This lecture attempts to draw a parallel between those pioneering observations and the current spate of space missions to explore the solar system. Although most of the direct measurements are carried out through spectroscopic techniques, the modelling of the structure of the planets (including, when relevant, their atmospheres) is based on kinetics and thermodynamics. In the 1960's, Venus provided the first example of a thermodynamic model applied to a planet. Among the most interesting bodies in the solar system are Titan (a satellite of Saturn) and Triton (a satellite of Neptune). Both have nitrogen atmospheres, but whereas Triton exhibits a frozen surface, with polar ice caps and geysers, the (invisible) surface of Titan should be extensively covered by an ocean of liquid ethane and methane. This is the realm of thermodynamics of simple molecules at cryogenic temperatures. Some recent phase equilibria and calorimetric measurements on the relevant systems are helping to form a coherent picture of the structure and atmosphere of these planets, in anticipation of the forthcoming (1996) Cassini mission.

O nascimento da ciência moderna coincide com as primeiras observações do sistema solar efectuadas por Galileu no século XVII. A primeira publicação importante de Galileu foi o *Sidereus Nuncius* (1610), que teve um grande impacto nos astrónomos da época, bem como em pintores e escritores. Esta lição procura estabelecer um paralelo entre essas observações pioneiras e a corrente série de missões interplanetárias. Embora a maior parte das medições directas seja feita através de técnicas espectroscópicas, a modelação da estrutura dos planetas (incluindo as respectivas atmosferas quando for o caso) assenta em bases cinéticas e termodinâmicas. Vénus forneceu, nos anos 60, a primeira aplicação da termodinâmica à modelação dum planeta. Entre os corpos mais interessantes do sistema solar encontram-se o Tritão (satélite de Neptuno) e o Titã (satélite de Saturno). Ambos possuem uma atmosfera de azoto, mas enquanto o Tritão exibe uma superfície gelada, com calotes polares e *geysers*, a superfície (invisível) de Titã deve estar extensivamente coberta por um oceano de etano e metano. Este é o domínio da termodinâmica das moléculas simples a temperaturas criogénicas. Estudos recentes de equilíbrio de fases e medidas calorimétricas efectuadas sobre os sistemas apropriados ajudam-nos a formar uma ideia mais exacta sobre a estrutura desses planetas, em antecipação da próxima (1996) Missão Cassini.

1. Historic Beginnings

In the beginning there was Galileo. It is usually impossible to determine the starting point of an important era, but for the birth of modern science this can actually be done. It occurred on the night of December 9, 1609 when Galileo looked at the sky through his makeshift telescope. He aimed it at the Moon and declared it to be "most beautiful and pleasing to the eye to look upon the lunar body", although what he saw was a stained ball, disfigured by mountains and craters, with the visible part separated from the invisible one by a crenelated line — Fig. 1.

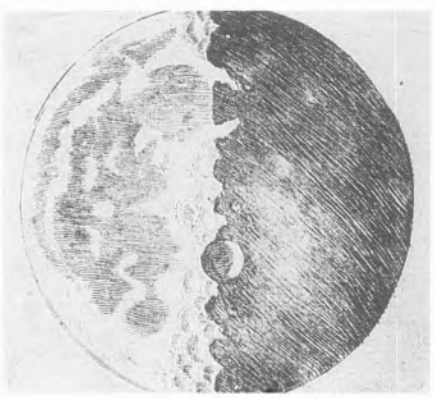

Figure 1. - Drawing of the Moon By Galileo

He also observed the phases of Venus, studied the constellations Pleiades and Orion, scrutinized the structure of the Milky Way and - on January 7, 1610 - discovered the first four Jovian satellites — Fig. 2.

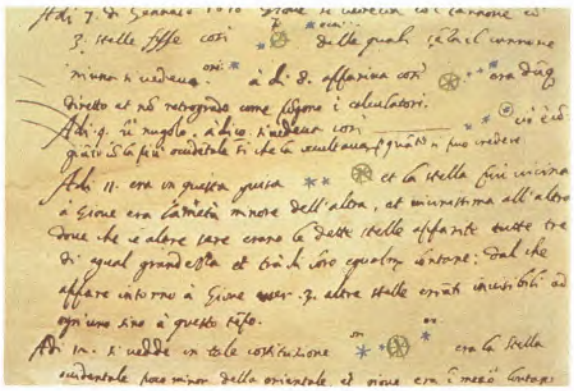

Figure 2. - Observation Notes by Galileo (in Italian!)

"On the seventh day of January in this present year 1610, at the first hour of night, when I was viewing the heavenly bodies with a spyglass, Jupiter presented itself to me; and because I had prepared a very excellent instrument for myself, I perceived (as I had not before, on account of the weakness of my previous instrument) that beside the planet there were three starlets, small indeed, but very bright". Galileo recognized that these starlets (a fourth one soon joined the first three) were satellites of Jupiter and promptly named them Medicean Stars, in honour of his future patron, Prince Cosimo II of Florence. Today they are, of course, known as the Galilean satellites and they have been named after four of Jupiter's mythological lovers - Io, Europa, Ganymede and Callisto.

Galileo published his findings a few months later (March 1610) in **Sidereus Nuncius** (The Starry Messenger) and this work created a sensation all over cultural Europe. It was praised by scientists and sung in verse by poets — Fig. 3.

A literal translation of the title page runs like this:

STARRY MESSENGER
unfolding great and very wonderful sights
and displaying to the gaze of everyone,
but specially philosophers and astronomers,
the things that were observed by
GALILEO GALILEI,
Florentine patrician
and public mathematician of the University of Padua,
with the help of a spyglass lately devised by him,
about the face of the Moon, countless fixed stars,
the Milky Way, nebulous stars,
but specially about
four planets
flying around the star of Jupiter at unequal intervals
and periods with wonderful swiftness;
which, unknown by anyone until this day,
the first author detected recently
and decided to name
MEDICEAN STARS

It should be noted that the word telescope was only coined in 1611; Galileo used the Latin word *perspicillum* or the Italian *occhiale* - here translated by spyglass.

The science of **Sidereus Nuncius** also created a new realism which was soon apparent in paintings like **The Assumption of the Virgin** (1612) by Lodovico Cigoli (a fresco in the chapel of Paul V in Santa Maria Maggiore, in Rome) or **The Flight into Egypt** (1609-10) by Adam Elsheimer (1578-1610), now in the Alte Pinakotheke in Munich[1] — Fig. 4.

SIDEREVS
NVNCIVS
MAGNA, LONGEQVE ADMIRABILIA
Spectacula pandens, suspiciendaque proponens
vnicuique, præsertim verò
PHILOSOPHIS, atq; ASTRONOMIS, quæ à
GALILEO GALILEO
PATRITIO FLORENTINO
Patauini Gymnasij Publico Mathematico
PERSPICILLI
Nuper à se reperti beneficio sunt obseruata in LVNÆ FACIE, FIXIS INNVMERIS, LACTEO CIRCVLO, STELLIS NEBVLOSIS,
Apprime verò in
QVATVOR PLANETIS
Circa IOVIS Stellam disparibus intervallis, atque periodis, celeritate mirabili circumvolutis; quos, nemini in hanc vsque diem cognitos, nouissimè Author deprehendit primus; atque
MEDICEA SIDERA
NVNCVPANDOS DECREVIT.
VENETIIS, Apud Thomam Baglionum. M DC X.
Superiorum Permissu, & Privilegio.

Figure 3. - Sidereus Nuncius (Frontispice)

Figure 4. - ADAM ELSHEIMER, The Flight into Egypt, 1610

Elsheimer was a German artist in Rome and probably got to know of Galileo's observations and detailed description of the sky through another fellow German and Roman émigré, Johannes Faber, physician and herbalist to the Pope. Faber was a man of many parts: a poet and patron of the arts who bought paintings from Elsheimer, but also an amateur astronomer and correspondent of Galileo. Indeed, Galileo used one of Faber's poems as a preface to his own **Il Saggiatore**, 1623 (The Assayer). Elsheimer's **The Flight,** although a small painting on copper, impressed for its faithful representation of the sky (which dominates the picture) and the double role played by the Moon, seen twice, up in the sky and also as a reflection on the lake. The work was popularized through an engraving (1612) by Hendrik Goudt and its fame reached Rembrandt whose **The Rest on the Flight into Egypt** (1647), at present in the National Gallery of Ireland in Dublin, bears a strong resemblance to it, in terms of composition and light values — Fig. 5.

Figure 5. - REMBRANDT, The Rest on the Flight into Egypt, 1647

The direct influence of **Sidereus Nuncius** on Elsheimer's painting is obvious. Not only the Moon appears stained according to Galileo's drawings in the book, but the whole sky is collaged from the astronomer's detailed descriptions: the Milky Way, carefully hazy and dotted with tiny stars, and a handful of recognizable constellations, like the Big Dipper and the Pleiades (the seven daughters of Atlas visible in Taurus). This is the same part of the sky evoked by Grimes's soliloquy in Britten's opera, **Peter Grimes** (1946)

Now the Great Bear and Pleiades
where earth moves,
are drawing up the clouds
of human grief
breathing solemnity in the deep night.

Who can decipher
in storm or starlight
the written character
of a friendly fate -
as the sky turns the world for us to change?

But if the horoscope's
bewildering
like a flashing turmoil
of a shoal of herring
who can turn skies back and begin again?

Galileo's work struck a chord in fellow astronomers. After reading **Nuncius** Kepler wrote to him in April 1610. *"there will certainly be no lack of human pioneers when we have mastered the art of flight... Let us create vessels and sails adjusted to the heavenly ether, and there will be plenty of people unafraid of the empty wastes. In the meantime, we shall prepare, for the brave sky-travellers, maps of the celestial bodies - I shall do it for the Moon, you Galileo, for Jupiter"* - a kind of new Tordesillas Treaty applied to the siderial space.

2. The Age of Space Discoveries

It was only in the 1970's, with the launch of the *Mariner, Viking 1, 2* and *3* and *Voyager 1* and 2 spacecrafts, that the age of space exploration truly began. The four Galilean satellites of Jupiter (there are now twelve more!) were observed and photographed by *Voyager 1* in March 1979 — Fig. 6.

Figure 6. - The Four Jovian Satellites: Io, Europa, Callisto and Ganymede

Three of them - Europa, Ganymede and Callisto - present similar patterns and are probably composed of up to 50% of water, mixed with rocky material. There is also evidence of water frost on the surface. Europa - the smallest of the Galileian satellites - shows an icy surface covered with huge fracture-like patterns; Ganymede has a cratered surface like the Moon, and Callisto displays the oldest surface, with a dense crater population. Io is the exception among the four, rich in sulphur and SO_2 and one of only three planets in the solar system exhibiting volcanic activity (the other two being the Earth and Triton) — Fig. 7.

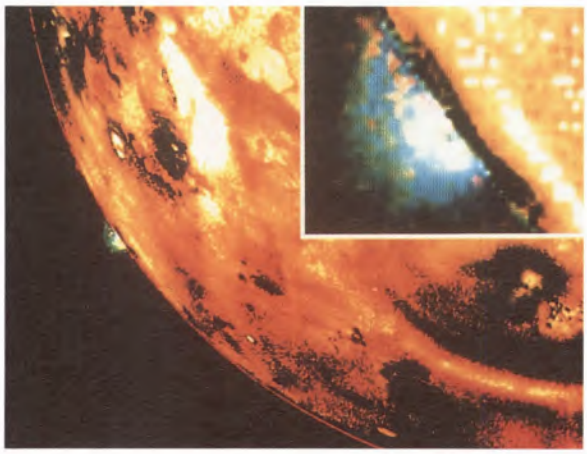

Figure 7. - Io, with a crater of 300 km and eruption height of 160 km

More recently, we have had the *Magellan, Galileo* and *Observer* Missions. The *Magellan* spacecraft, launched in 1989, was aimed at Venus, while the *Observer* started its voyage to Mars in September of 1992 and reached the planet in the Summer of 93. Unfortunately several faults in the system have stopped communication and turned it into a silent probe (it was supposed to observe Mars from a mapping orbit 390 km away, for a whole Martian year - 687 days). The appropriately named *Galileo* spacecraft was launched on October 18, 1989 and it will orbit Jupiter and penetrate its atmosphere in 1995, observing it for 2 years. It will carry out a detailed study of the more important Jovian satellites from distances as close as 200 km. En route to Jupiter, along its Venus-Earth-Earth gravity assist (VEEGA) trajectory, it observed both the Moon and Venus from unusual angles. In early November 1991 it made the first flyby of the asteroid Gaspra (16 km in diameter), and in late August of 1993 scrutinized another, Ida (32 km).

Even more exciting is the Cassini Mission, named after Jean Dominique Cassini, the Italian-born French astronomer who discovered four moons of Saturn (Tethys, Dione, Rhea and Iapetus, 1671-1684) and the 5000 km gap in the ring system, called the Cassini Division. Aimed at Saturn, Cassini is planned for launching in 1996, will reach its destination in 2002 and will orbit Saturn for 4 years, making extensive measurements. A separate probe called Huygens will descend onto Titan, Saturn's most important satellite, discovered by Christiaan Huygens (1629-1695) in 1655. It will also observe Jupiter and its satellites on the way to Saturn.

Finally, one should also mention CRAF (Comet Rendez-Vous Asteroid Flyby), scheduled for launching in 1995 for a meeting with Comet Kopff in August 2000. It will also observe Hamburga, one of the largest asteroids.

3. Experiment and Modelling

Since the direct observation, provided by these missions, is expensive, it cannot happen very often. There is thus the need to simulate, in the laboratory, the real conditions on the planets and this usually means working on multicomponent systems over wide ranges of temperature and pressure. At the same time thermodynamics and kinetics should be, and have been, used to model the chemistry of planetary atmospheres and atmosphere-surface interactions. It is the conjunction of these three approaches - direct observation, experimental and theoretical modelling - that makes possible the interpretation of Earth-orbital and spacecraft spectroscopic data which, in turn, lead to further experiments and assist on the planning and design of future spacecraft missions.

A first indication of the chemistry and thermodynamics involved is given by the compositions of the planets and their satellites, in particular the compositions of the atmospheres. This is summarized in Table I which shows the molecules in the solar system

TABLE 1. MOLECULES IN THE SOLAR SYSTEM

OBJECT	MAJOR SPECIES	MINOR SPECIES
Venus	CO_2	H_2O, CO, HCl, HF
Earth	N_2, O_2	H_2O, CO_2, CH_4, NO, O_3, N_2O, CO, NH_3, HF, HCl...
Mars	CO_2	N_2, O_2, CO, H_2O, H_2, O_3, NO
Jupiter	H_2	NH_3, PH_3, CH_4, CH_3D, C_2H_6, C_2H_4, C_2H_2, H_2O, GeH_4, CO, HCN, HD
Io		SO_2
Saturn	H_2	NH_3, PH_3, CH_4, CH_3D, C_2H_6, C_2H_2, CO
Titan	N_2	H_2, CH_4, CH_3D, C_2H_2, C_2H_4, C_2H_6, C_3H_4, C_3H_8, C_4H_2, HCN, HC_3N, C_2N_2, CO_2, CO
Uranus	H_2	CH_4
Neptune	H_2	CH_4, C_2H_6
Triton	CH_4 (or N_2)	
Pluto	CH_4	
Sun		CO, C_2, CH, CN, NH, OH, MgH, CaH, TiO, SiH, ZrO, CoH, NiH, H_2O, H_2, SiO
Comets		C_2, C_3, CH, CN, CO, CS, NH, NH_2, OH, H_2O, S_2, HCN, CH_3CN, CO^+, CO_2^+, CH^+, H_2O^+, OH^+, N_2^+, CN^+

Table I. - Molecules in the Solar System

A few features stand out. First, the overwhelming dominance of Hydrogen in the giant planets, which in a

way vindicates the idea, put forward by Prout (1785-1850) in 1815, that all substances are made of hydrogen. The giant planets (Jupiter, Saturn, Uranus, Neptune) have undergone little or no evolution since their formation. Secondly, the CO_2 atmospheres of Venus and Mars. Finally, a few special cases: Io, the Jupiter satellite, with SO_2; Titan, the Saturn satellite, with N_2, and Triton (a satellite of Neptune) and Pluto with CH_4. Titan also exhibits the largest variety of species.

The detection of molecules in small amounts provides clues to possible mechanisms involved in the formation and evolution of these celestial bodies. Interesting cases are, for instance, the detection of PH_3 or GeH_4 in Jupiter and Saturn, the presence of cyanoacetylene HC_3N in Titan or the (so far) exclusive presence of S_2 in comet IRAS-Araki-Akork. Comets provide good clues and at the same time pose interesting puzzles. H_2S, the most abundant sulphur-bearing molecule in the solar system ($H_2S/H_2O = 0.002$; $CS_2/H_2O = 0.001$) has been observed in comets, as well as the prebiotic molecules H_2CO (formaldehyde) and HCN - first stages in the origin of life.

Given the overwhelming presence of the Sun, it is rarely possible to develop a feasible model for the atmospheres of the various planets on the basis of classical thermodynamics alone. What happens is largely determined by a tug-of-war between photochemistry (driven by the Sun) and thermodynamics (driven by the interior heat of the planets). Several types of questions can then be considered:

(i) atmosphere-surface interaction for the terrestrial planets. These are planets like Venus or Mars which possess an atmosphere and whose lithospheres are well known.

(ii) deep atmosphere chemistry for the outer planets. These include the giant planets which are virtually all atmosphere. In the very deep atmospheres of their interior the temperatures are believed to reach 1000-2000 K and pressures range from hundreds to thousands of bar - the perfect environment for chemical reactions to come to equilibrium. Away from the upper layers of the atmosphere, photochemistry can probably be ignored. However, there are differences, even among these giant planets - three of them (Jupiter, Saturn and Neptune) emit more heat than they absorb from the Sun and thus have internal heat sources. On the other hand, no internal heat source has been observed on Uranus.

(iii) upper atmosphere chemistry and photochemistry.

(iv) atmospheres of the outer planet satellites Triton and Titan, which are quite unique, as will be explained later.

4. The Case of Venus

Venus is a terrestrial, not an outer planet, but is of interest here since it was the subject of the first comprehensive attempt to apply thermodynamics to the atmosphere of a planet. Starting with data provided by *Mariner 2*, and assuming chemical equilibrium between the surface rocks of Venus and the lower stratum of the atmosphere, Mueller developed a chemical model capable of explaining some of the observed atmospheric characteristics[2]. The assumption seemed justifiable on the basis of the high temperatures of the planet and the well-known catalytic properties of many metal oxides with respect to reactions involving such species as CO and CO_2. The global mean surface temperature of Venus is about 740 K (as opposed to 214 K for Mars) and the global mean surface pressure is about 92 bar (again to be compared with 6 mbar for Mars). This means that while the weathering processes on the surface of Venus are thermochemically dominated, on the surface of Mars they are photochemically dominated. Mars's atmosphere is so thin that UV light from the Sun reaches the surface of the planet causing photodissociation of CO_2.

Mueller divided the atmosphere of Venus into three layers: (i) a basal zone of chemical interaction with the lithosphere; (ii) an intermediate zone of frozen thermochemical equilibria and (iii) an outer zone ruled by photochemical reactions. Given the composition of the Venus atmosphere, the important parameter is the partial pressure ratio P_{CO}/P_{CO_2}. Following the pioneering work of Urey[3], Mueller and later Lewis[4] showed that the high CO_2 pressure of the Venus atmosphere results from the high temperatures occurring in that planet, which favour decarbonation reactions like the following

$$CaCO_3\ (\text{calcite}) + SiO_2\ (\text{quartz}) \rightarrow CaSiO_3\ (\text{wollastonite}) + CO_2$$

$$MgSiO_3\ (\text{enstatite}) + CaCO_3 + SiO_2 \rightarrow CaMgSi2O6\ (\text{diopside}) + CO2$$

whereas in the Earth the very different atmosphere was the result of much lower temperatures and the presence of life.

Still, some problems remain and it is generally accepted nowadays that a pure thermodynamic model cannot really explain the more complex features of the atmosphere of Venus. The atmosphere/lithosphere interface does not seem to have reached a state of chemical equilibrium, at least as far as the chemistry of sulphur is concerned. Existing models[5] predict that the reduced sulphur compounds H_2S and COS should be present in much larger concentrations than the oxidized sulphur gas SO_2, whereas the most recent data show that the opposite is true. And it is still not understood why Venus has 100,000 times less water than the Earth. (Hydrated silicates do not become thermodynamically stable until much further out in the cooler regions of the solar system). For one thing, Venus is too close to the Sun for a purely thermodynamic model to be viable.

5. The Outer Planets and the Need for New Data

The giant planets, from Jupiter onwards through Neptune, comprise about 99.5% of the planetary mass and are thus crucial to an understanding of the origin and

formation of the solar system. The main components are H_2 (89%) and He (11%), and typical internal pressures range from 300 GPa ($3x10^6$ bar) in Neptune to 2.5 TPa in Jupiter. In the deep interiors the temperature can reach thousands of Kelvin. These are drastic conditions, requiring very specialized technology, so it is no wonder that the relevant experimental data are not available. There have been some laboratory work on hydrogen-helium mixtures by Streett[6], among others, at the lower end of the high pressure range and some computer simulation (Monte-Carlo)[7] and perturbation theory[8] results in modest agreement with experiment. Helium has limited solubility in hydrogen at low temperatures, but the theoretical calculations indicate that it is completely soluble in molecular hydrogen at the pressures and temperatures encountered inside the giant planets.

A whole array of different phenomena happens in the satellites and make them at least as interesting to investigate as the major planets. Temperatures here are usually low (despite some occasional volcanic activity) but each one of them seems to be a unique case.

In the outer regions of the solar nebula, the first major condensate to form is water ice. As the temperature decreases CO and N_2 (which are the dominant gaseous forms of carbon and nitrogen), reach equilibrium with water ice and form clathrate compounds. In higher pressure environments the dominant carriers of carbon and nitrogen are CH_4 and NH_3, also capable of forming hydrates and clathrates with water. Eventually, as the temperature gets lower and lower, pure CO and N_2 freeze into their respective ices. It would be desirable to know the stability and thermodynamic properties of all these species, but unfortunately very few (or none at all) laboratory measurements exist for the majority of those clathrates, under the low temperature conditions of interest. Other important aspects requiring investigation are rate of formation and metastability. Another type of species requiring a more detailed study by spectroscopic and thermodynamic methods are van der Waals complexes like $(CO_2)_2$ and Ar-CO_2, important in Venus and Mars.

Even for some basic substances, like water, a lot of work still has to be done. For instance, Kouchi has reported that the vapour pressure of ice depends strongly on growth conditions[9]. Amorphous ice has a vapour pressure one or two orders of magnitude larger than that of crystalline (cubic) water ice — Fig. 8.

The vapour pressure depends greatly on the condensation temperature, T_c, and on the rate of condensation, R. Kouchi has also shown that a sample of ice grown by vapour deposition at low temperatures (< 100 K) and at a low growth rate (< 1000 nm/hr) seems to have up to two orders of magnitude higher vapour pressure at 140 K than another grown at higher temperatures and lower growth rates. These results are important for the interpretation of sublimation processes in space, like the emission of water vapour by comets.

In general, good low-temperature data are scarce, and often of poor quality, specially for solids. Masterson et

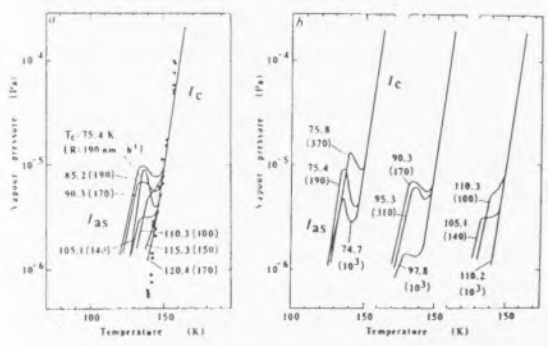

The temperature dependence of vapour pressure of H_2O ice produced at various condensation temperatures, T_c (*a*) and condensation rates, R (*b*). Values without parentheses are T_c in kelvin; values in parentheses are R in nanometres per hour. I_{am}, amorphous H_2O; I_c, cubic ice.

Figure 8. - Vapour Pressure of Water Ice and Its Dependence on Condensation Temperature and Condensation Rate

al. have recently measured the vapour pressure of acetylene in the range 80-90 K, using the thin-film infrared technique (TFIR)[10], and their results (10^{-6}/10^{-7} torr) appear to be lower by almost two orders of magnitude than the values extrapolated from higher temperature data — Fig. 9.

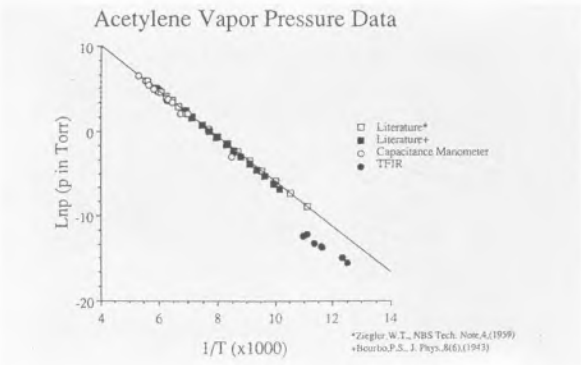

Figure 9. - Vapour Pressure of Acetylene

This has implications in haze production models for the atmospheres of Saturn, Uranus and Neptune. The same authors are now checking and measuring vapour pressure data for other organic substances, like diacetylene C_4H_2, HCN, cyanoacetylene H_3CN and dicyanoacetylene C_4N_2, all of which play an important role in planetary atmospheres.

Solid solutions and solid-solid-liquid equilibrium for systems involving N_2, CH_4, Ar, CO, etc at low temperatures, should also be more thoroughly investigated. They are fundamental to the understanding of the structure of Triton, Neptune's largest moon.

6. The Case of Triton

When *Voyager 2* finally encountered Neptune on August 24, 1989 the pictures were a source of wonder: here was one of the most beautiful planets of the solar system, with a Great Dark Spot almost the size of the Earth, a Little Dark Spot (both associated with picturesque white cirrus clouds, made of methane ice), striking cloud-spun contrasts, and faint, segmented rings — Fig. 10 . With a temperature of 59 K, Neptune is warmer than Uranus by a couple of Kelvin, due to intense internal heat.

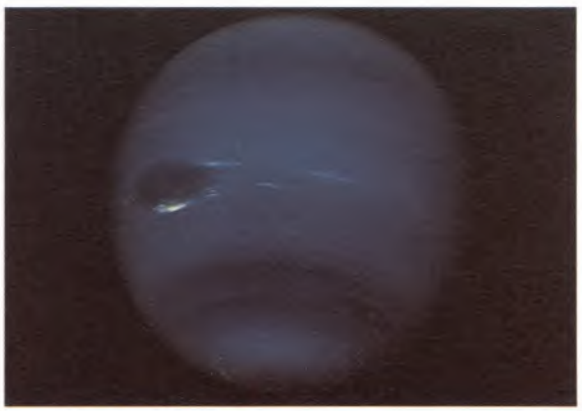

Figure 10. - Neptune (*Voyager 2*)

No less surprising appeared Triton, the first and largest of Neptune's satellites, which had been discovered by Lassell in 1846 — Fig. 11 . Part of its appeal lies in the fact that it may provide clues as to the nature of Pluto, the great forgotten body of the solar system (although NASA is now planning a "Pluto Fast Fly-by", to be launched possibly in 1999). Bright and clear (it is one of the most reflective objects in the solar system), Triton is also, consequently, one of the coldest - the surface temperature is 38K. It shares with Titan the distinction of being one of the only two moons with a permanent atmosphere. But Triton is three times further from the Sun than Titan.

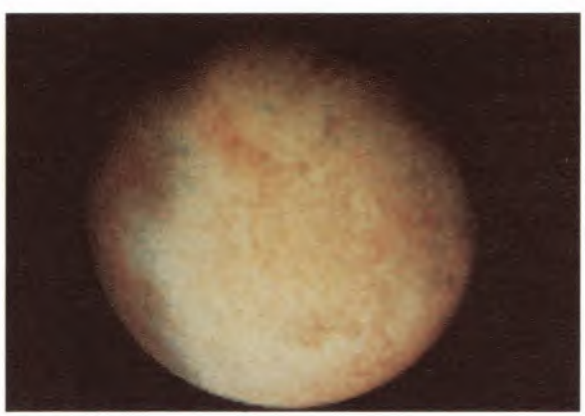

Figure 11. - Triton

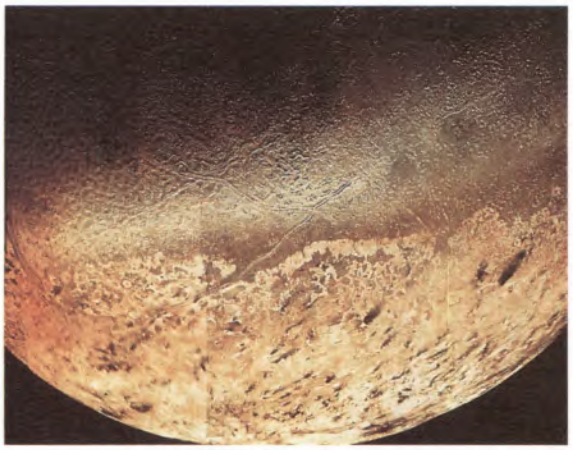

Figure 12. - Triton, with Southern Ice Cap and Geyser

Triton's southern ice cap of frozen nitrogen (N_2 freezes at 63 K) can be observed (*Voyager 2*; 25 August 1989) in Figure 12; the pinkish hue is caused by the presence of hydrocarbons. Concerted efforts to understand the main features of Triton's structure bore fruit in the first "Colloquium on Triton and Neptune" which took place in 1992 in Tucson, Arizona. As a result, a clearer picture of Triton's structure is beginning to emerge.

The atmosphere, resulting from the sublimation of the ice caps, is 99.9% N_2 with a trace of methane. At the 1992 Colloquium D. Cruikshank also reported the identification of CO and CO_2 ices on Triton's surface and Alan Stern mentioned a tentative identification of SO_2 frost. The very low surface pressure (16 microbar) and temperature preclude the existence of liquid phases, but the frosts show mobility over seasonal time scales. (On Triton, a seasonal year corresponds to 165 years on Earth). Above the ice cap, a fractured and warped terrain which resembles the rind of a "cantaloupe" suggests that internal pressures continue to remould Triton's surface.

A number of dark streaks on the surface, extending up to 150 km, probably arise from windblown debris, dust-devils of low hydrocarbon ices. Even more astonishing is the presence of active geysers, which go up 5 miles into the sky and then, caught by winds or reflected by the lower layers of the atmosphere, trail horizontally for another 90 miles. What are they? No-one really knows. Some investigators have suggested that they are cold jets of liquid nitrogen, arising from underground lakes. Others point to turbulent methane sublimation.

A more likely explanation lies in the internal structure of the planet. Triton has a density of 2.05, which is consistent with the existence of a small rock core (about 60 or 70%), then a mantle of (mostly) water ice, and finally a surface layer of solid N_2+CH_4 — Fig. 13 .

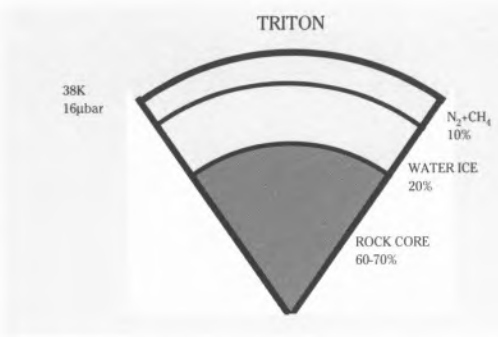

Figure 13. - Structure of Triton (not to scale)

It is the expansion, on freezing, of the water ice mantle that could have cracked the planet's surface, leaving ridges at the sides as oozing fluid froze. This explains why Triton presents a rather flat landscape, one of the very few moons which have entirely erased their densely cratered regions (the others are Io and Europa, but for very different reasons). As for the oozing fluid, it could well be a mixture of ammonia and water, plus some traces of hydrocarbons. Its melting point is about 175 K, a temperature believed to occur at a depth of roughly 200-300 km into the water mantle (these higher temperatures are caused by trapped radioactive material). This cold fluid forces its way to the surface and, on freezing, wipes away the craters.

The N_2+CH_4 surface layer covers probably only 1% of the planet's radius (Triton has a diameter of 2700 km) but, since it has been retained in its entirety, it could also be a few hundreds of kilometers deep. The dark material (mainly hydrocarbons) trapped in the water ice absorbs light, its temperature rises, the pressure builds up, some of overlying solid nitrogen sublimates and a geyser erupts. These are, of course, mere conjectures and lack of data, in particular thermodynamic data, prevents the testing of the model. There is a crying need for good measurements of solid-liquid and solid-vapour equilibrium for the N_2+CH_4 system at the low temperatures prevailing on Triton. Also of diffusion measurements in the solid phase, since there is migration of molecules through the various ices. In the case of Titan, where the current temperatures are a good 50 K higher than on Triton, experimental data are available and it has been possible to go further in the conjecture and interpretation of the planet's surface.

7. The Case of Titan

Titan is one of 17 known satellites of Saturn, and was the first to be discovered (by Huygens in 1655). It is, in many respects, unique and arises a great deal of interest in the planetary scientific community. *Voyager 1* had a close fly-by with Titan, and most of what we know about the planet comes from these observations. The essential features are summarized in Table II.

Titan

Physical or Chemical Data
At the Surface (altitude $z = 0$):
r_0 = distance to center = 2575 km
g_0 = gravity = 135 cm s^{-2}
P_0 = total pressure = 1.50 bar
T_0 = temperature = 94 K
n_0 = number density = 1.2×10^{20} cm^{-3}
Composition of the Troposphere (volume mixing ratio):
$N_2 > 0.97$
$CH_4 < 0.03$
$H_2 = 0.002$
At the Tropopause ($z = 45$ km):
$P = 130$ mbar
$T = 71.4$ K
$n = 1.1\times10^{19}$ cm^{-3}
Composition of the Stratosphere (volume mixing ratio):
$CH_4 = 1\text{-}3\times10^{-2}$
$H_2 = 2.0\times10^{-3}$
$C_2H_6 = 2\times10^{-5}$
$C_2H_2 = 2\times10^{-6}$
$C_2H_4 = 4\times10^{-7}$
$C_3H_8 = 2\text{-}4\times10^{-6}$
$CH_3C_2H = 3\times10^{-8}$
$C_4H_2 = 10^{-8}\text{-}10^{-7}$
$HCN = 2\times10^{-7}$
$HC_3N = 10^{-8}\text{-}10^{-7}$
$C_2N_2 = 10^{-8}\text{-}10^{-7}$
$CO = 6\times10^{-5}$
$CO_2 = 1.5\times10^{-9}$
$H_2O < 1\times10^{-9}$
CH_3D detected, abundance not available
Composition of Mesosphere and Thermosphere:
$N_2 = 2.7\times10^{8}$ cm^{-3} at $z = 1280$ km
$CH_4 = 1.2\times10^{8}$ cm^{-3} at $z = 1140$ km
(mixing ratio = 0.08)
C_2H_2 mixing ratio 1%-2% at $z = 840$ km
H atoms: disk-averaged Lyα airglow ~ 500 R^a
Haze Layers:
optical haze $z = 300$ km
UV haze $z = 400$ km

Table II. - Physical and Chemical Data for Titan

It is a billion miles away. Light takes over one hour to get there. Its atmosphere is intermediate between the highly oxidized atmospheres in the inner solar system and those of the Jovian planets which have massive amounts of H_2. The pressure at the surface is approximately 1.5 bar and the atmosphere is predominantly N_2, like that of the Earth, but there is a lot more N_2 than on Earth because the temperature is much lower, 93-95 K. The other significant component is CH_4 (< 3 mole per cent). Literally, dozens of other molecules have been identified in Titan's atmosphere, but it should be noted that all these molecular species can be derived, using known chemical kinetics, from the three parent molecules N_2, H_2O and CH_4, as is schematically shown[11] in Figure 14.

If massive, the atmosphere of a small planetary body (5150 km in diameter, compared with 3475 for the Moon) cannot be stable, either physically or chemically. UV sunlight and beams of electrons trapped in Saturn's magnetic field, impinge on the mesosphere (above the strastosphere), break C-H , O-H and N-N bonds, and

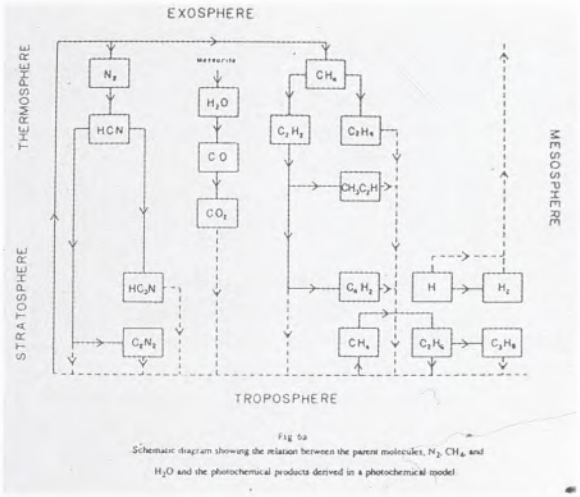

Figure 14. - Diagram of a Photochemical Model for Titan

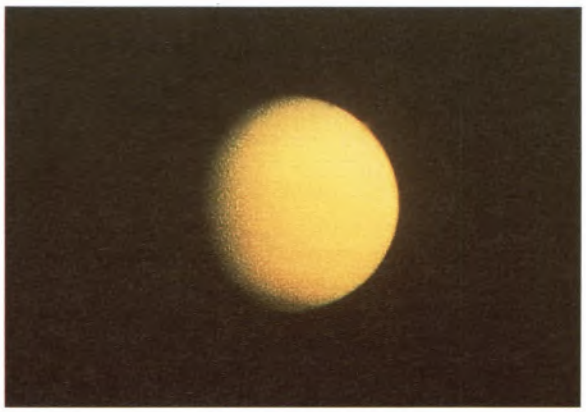

Figure 15. - Titan (Voyager 1, 9. November. 1980)

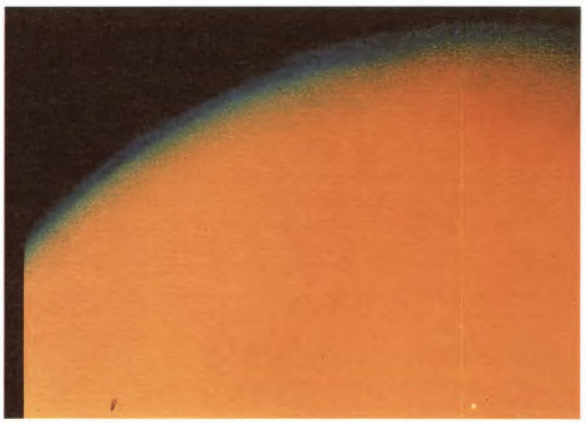

Figure 16. - Titan, with Polar Hood (Voyager 1, 12 November. 1980)

provide a source of radicals; the recombination of these organic radicals leads to the rapid formation of complex organic molecules. Some of this photochemistry is very well understood, although most of the rate constants have not been measured at the very low pressures - less than 1 torr - and low temperatures of interest. The photolysis of methane, for example, is an easy and accelerating process, since it is catalyzed by one of its own products, diacetylene[12], C_4H_2 (another is acetylene, C_2H_2). The lighter species, like H, produced in the photolytic chains, tend to escape into outer space, but the complex organic molecules, which build up in the stratosphere, condense at the tropopause, form polymers and aerosols, and ultimately rain down on the surface of the planet. This has been happening for the last 4 billion years and the continuing chemical evolution produces large amounts of photochemical aerosols which obscure the surface of the planet — Fig. 15, 16 . Titan is one of the darkest bodies in the solar system, opaque to the UV, with a geometric albedo of less than 5% (The albedo is a measure of brightness - the fraction of light that an object reflects, relative to a white disk of same diameter; for a white ping-pong ball it is 2/3). It is this thick photochemical haze enveloping the planet that has prevented the observation of its surface - hence the importance of the Huygens probe which in 2002 will descend into the atmosphere, eventually landing on Titan's surface.

Methane has thus been continuously depleted from Titan's atmosphere and despite its present abundance, it will be consumed in a time on the order of 10^7 years. It is a type of chemistry similar to that of coal formation and, likewise, not completely understood. Attempts have been made to reproduce in the laboratory the behaviour of such a complex 'soup' of organic chemicals and aerosols. Sagan and his collaborators irradiated with charged particles a mixture of N_2+CH_4 at low pressures and obtained a reddish-brown solid coating the cell. The analysis of this "tholin" revealed the presence of hydrocarbons and nitriles, including HCN, several of them implicated in paths that lead to life[13]. In other words, the same processes that led to life on Earth long ago, seem to be occurring in Titan now.

Recently Cabane *et al.*[14] proposed an Eulerian model to explain the formation and growth of these aerosols. They obtained a strong dependence of the 'monomer' (nearly spherical aggregates of smaller particles) radius on the pressure (i.e. the altitude) and concluded that the aerosols form at altitudes in the range of 350-400 km.

Under the cold temperatures existing in Titan, methane and even nitrogen can condense and thus the possibility of methane and nitrogen rain clouds and global methane oceans has been widely discussed. A fantastic picture emerged of a planet with clouds, rain, rivers, glaciers, polar ice caps. Titan would thus have a 'hydrological' cycle similar to that of the Earth, but

involving CH_4 instead of water. In this context Huygens's prediction, in **The Celestial Worlds Discover'd** (1698) is not all that far-fetched. He wrote: *"But since 'tis certain that the Earth and Jupiter have their Water and Clouds, there is no reason why the other Planets should be without them. I can't say that they are exactly of the same nature as our Water; but that they should be liquid their use requires, as their beauty does that they be clear. For this water of ours, in Jupiter or Saturn, would be frozen up instantly by reason of the vast distance of the Sun. Every Planet therefore must have its waters of such a temper, as to be proportion'd to its heat: Jupiter's and Saturn's must be of such a nature as not to be liable to Frost..."*. Substitute Titan for Jupiter or Saturn and Huygens's conjecture rings true.

Such a thick atmosphere, extending for over a thousand kilometers, exhibits complex composition, pressure and temperature profiles. The latter was first obtained from radio-occultation experiments[15] carried out by *Voyager 1*, assuming a pure N_2 atmosphere; the calculations have been refined by Lellouch *et al.*[16] using IRIS (infrared interferometer spectrometer and radiometer) spectroscopic data (also from *Voyager 1*) which unmistakeably revealed the presence of CH_4, and assuming again a uniformly mixed atmosphere. In Figure 17 the temperature of Titan's atmosphere is plotted as a function of height and pressure.

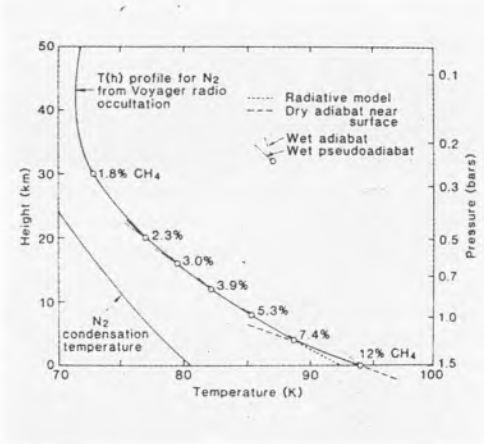

Figure 17. - Atmospheric Profile of Titan

The essential feature of this temperature profile is the thermal inversion which occurs at an altitude of approximately 40 km. Starting with a value of about 94 K at the surface of the planet (plus or minus a few Kelvin, according to latitude), the temperature decreases as the height increases, reaches a minimum value of about 72 K and increases steadily onwards. This thermal inversion is caused by an absorption of sunlight by the aerosols, with the corresponding greenhouse effect.

In the same figure the nitrogen condensation temperature is also plotted, proving that this gas does not liquefy under Titan's conditions. Methane is also not abundant enough to condense[17] (see dry adiabat near surface which matches the measured curve for the lowest 4 km). So if there are any oceans on Titan they cannot be made of either nitrogen or methane. However, an almost pure N_2 atmosphere is compatible with the presence of an ocean if the dominant oceanic constituent is less volatile than CH_4 and substantially lowers its vapor pressure. The photochemical model already discussed suggests a natural candidate and soon an ocean of ethane, several kilometers deep, was being proposed[18]. A C_2H_6-rich ocean with a CH_4 mole fraction of 0.10-0.20, plus an even smaller concentration of nitrogen is consistent with the radio-occultation data from the atmosphere and could function as a long-lived ($>10^9$ years) source for CH_4 photolysis. The atmosphere would still be composed mainly of N_2 (the more volatile of those components), plus some CH_4, maybe Ar. The overall picture that emerges[21] is shown in Figure 18.

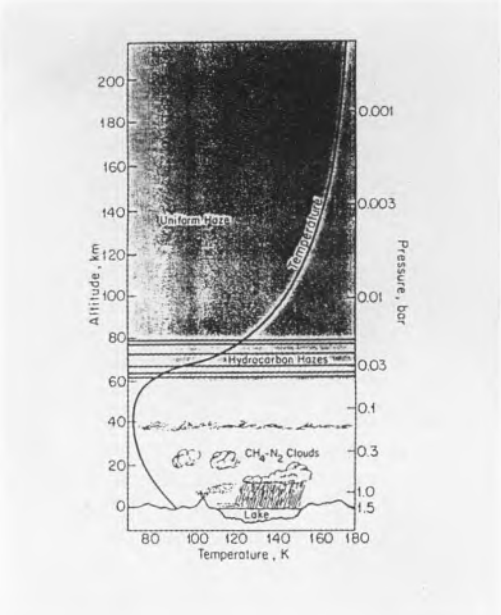

Figure 18. - Sketch of Titan's Atmosphere, Surface and Condensates

This is the accepted view today.

One problem remains - that posed by the tide, raised by Saturn, in the seas of Titan. Sagan and Dermott[19] have argued, on the basis of the high eccentricity of Titan's orbit around Saturn, that Titan must be either an all-ocean or an all-land world. In other words, oceans cannot coexist with continents, otherwise the *"the resulting tidal friction would have turned Titan's orbit into a circle in much less than the age of Titan"*. However, Duane O. Muhleman, from Cal Tech., was

able to show that radio waves could penetrate Titan's atmosphere, hit the surface, and be reflected back into space[13], something that would not occur if the planet was extensively covered by a liquid hydrocarbon ocean, several kilometers deep. Maybe something solid is floating out there, but it is difficult to see what. In the meantime, the project of the Cassini mission and the design of its Huygens entry probe (a NASA-ESA enterprise) require a more detailed knowledge of weather conditions on entry and of the nature of the planet's surface. Lorenz and Zarnecki have studied the CH_4 icing hazards to the probe and concluded that CH_4 hail and snow are not expected on the surface of Titan, and that the impact pressures of rain drops (which descend very slowly) are very small, one and a half orders of magnitude lower than on Earth[20]. Huygens will either float on the potential ocean or collapse against a bed of rockfrozen hydrocarbons. A first sketch of the probe is shown in Figure 19.

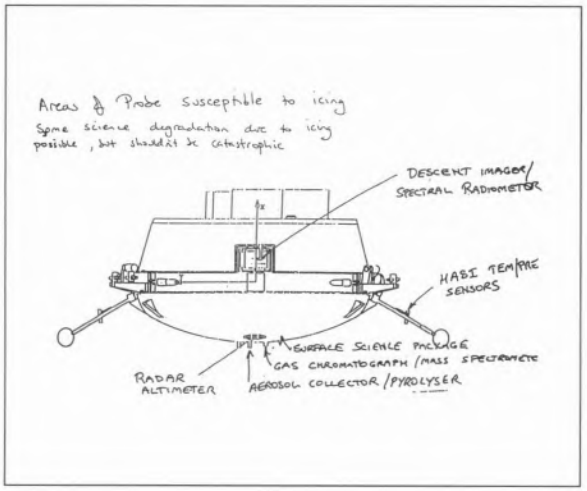

Figure 19. - Drawing of the Huygens Probe

It is, for this reason, that a thermodynamic model for the atmosphere and surface of Titan has to be built.

8. A Thermodynamic Model for Titan

To develop a realistic thermodynamic model for Titan we need some accurate thermodynamic data for the multicomponent system N_2-CH_4-C_2H_6-C_3H_8-Ar-...at the low temperatures prevalent on the planet, 90-100 K. Given their engineering importance, in relation to the natural gas industry, most of the components are well-characterized in the pure state. As for the mixtures, we have, at the most, some scattered data on a few ternary systems N_2-CH_4-C_2H_6, N_2-CH_4-C_3H_8, CH_4-C_2H_6-C_3H_8 and N_2-Ar-CH_4, and some good data for the various binaries, but with gaps at the lower end of the temperature range. The situation is summarized in Table III[21].

Availability of Experimental Data,
N_2-Ar-Hydrocarbon Systems

System	(p,T) Coverage	Assessment and Comments
N_2-CH_4	$T \geq 91°K$ $p \geq 0.2$ bar	Fair coverage of (p,T) relevant to surface-atmosphere equilibrium if several studies are combined (about 20 p,T,X measurements total). Data applicable to atmosphere-cloud equilibrium more limited, with only a few measurements down to 80°K (cf. review of Kidnay *et al.*[4]) *New modeling discussed here.*
Ar-CH_4	$T \geq 92°K$ $p \geq 0.16$ bar; $T \geq 105°K$ $p \geq 1.8$ bar	Six points below 92°K (ref. 5). Adequate coverage above 105°K (refs. 6, 7). Poor below 105°K and for low p relevant to small Ar abundances expected.
N_2-Ar-CH_4	$T = 112°K$ $p \geq 3.0$ bar	Limited to one temperature.[8] At T this high, low pressures correspond to Ar-dominated gas.
CH_4-C_2H_6	$T \geq 111°K$ $p \gtrsim 0.1$ bar	Good coverage above 111°K, cf. review by Hiza, Miller and Kidnay.[9] Needs extension down to 91°K or even lower (eutectic at 72.5°K). *New work and modeling discussed here.*
N_2-C_2H_6	$T = 110.9°K$ $p \gtrsim 0$ bar; $T \geq 101°K$ $p \geq 6.9$ bar	Useful data at 110.9°K (ref. 10); range of T only at high pressures.[11] Need coverage at lower (p,T). *New work and modeling discussed here.*
N_2-CH_4-C_2H_6	$T \geq 144°K$ $p \geq 68.9$ bar; $T \geq 171°K$ $p \geq 1.9$ bar	Available data[12,13] only at (T,p) much different than found on Titan. Three-phase $(\ell - \ell - v)$ data exists for $T \geq 117°K$, $p \geq 14$ bar (ref. 14). This most relevant ternary system needs study in the two-phase $(\ell - v)$ region to 90°K and lower.
CH_4-C_3H_8	$T \geq 90°K$ $p \gtrsim 0.01$ bar	Good coverage above 90°K, cf. review by Miller, Kidnay and Hiza.[15] Study could be extended to lower T, toward eutectic.
N_2-CH_4-C_3H_8	$T \geq 114°K$ $p \geq 2.9$ bar	Fair coverage above 114°K (ref. 16). Also three-phase $(\ell - \ell - v)$ data for $T \geq 117°K$, $p \geq 13.8$ bar (ref. 14).
Ar-CH_4-C_2H_6	$T = 116°K$ $p \geq 4.0$ bar	Limited to one temperature and relatively high pressures.[17]
CH_4-C_2H_6-C_3H_8	$T \geq 115°K$ $p = 1.0$ bar	Some useful data.[18] Needs study at lower (p,T).
N_2-Ar-C_2H_6, etc.	—	Other relevant systems not studied, or at much higher (p,T) than relevant for Titan.

Table III. - Availability of Experimental Data

First the quality and consistency of the available data have to be assessed. For instance, for the important CH_4-C_2H_6 system, the situation is the following - Figure 20 - in what concerns liquid-vapour equilibrium[22].

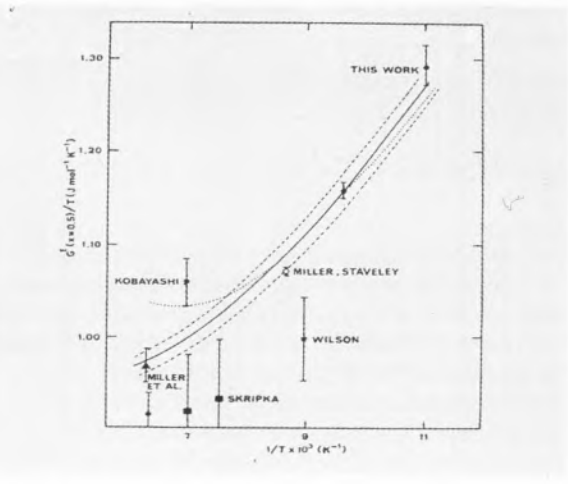

Figure 20. - Summary of VLE Data for CH_4-C_2H_6

Because the relevant temperatures are quite close to the triple-points of CH_4 and C_2H_6, extrapolations from higher temperature results can be misleading. The fundamental ternary system is N_2-CH_4-C_2H_6, which unfortunately had only been studied under conditions very different from those prevailing on Titan. We then embarked on an experimental program to fill the most crucial gaps for both VLE and LLVE. We also measured heats of mixing for the system N_2-C_2H_6. At the same time the results were being compared with theoretical calculations based on perturbation theory and with computer simulation. This work is the result of a research network, involving experimentalists and theoreticians in Portugal (Technical University of Lisbon), the U. S. A. (Cornell University) and Germany (Ruhr University, Bochum). What follows is a summary of the main conclusions relevant to Titan that can be derived from the study of individual systems.

Since Titan's atmosphere is basically made of N_2 (99%) and CH_4 (1%), it is this binary system which will essentially determine the properties and structure of the atmosphere. Starting with a CH_4 vapour mole fraction at the surface of $y(CH_4) = 0.14$, the following altitude-composition profiles can be derived for the atmosphere[21,23]— Fig. 21.

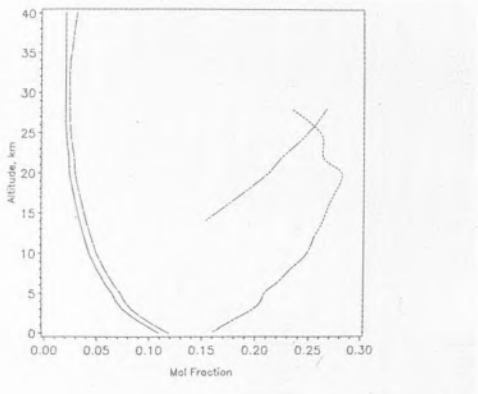

Figure 21. - Computed CH_4 and N_2 compositions in the Gas and in Liquid or Solid Condensate in Titan's Troposphere

The solid line on the left shows the saturation vapour mole fraction of CH_4, $y(CH_4)$; the lines on the right show the saturation liquid mole fraction of N_2, $x(N_2)$. Freezing of this CH_4-rich mixture occurs at 82 K (altitude of 12 km), and the corresponding mole fraction of N_2 in *solid* condensate is also shown (double — dashed line)[21]. Condensation does not occur above 28 km.

The C_2H_6+N_2 system exhibits liquid-liquid immiscibility. At the temperatures of interest, the solubility of N_2 in the C_2H_6-rich phase lies in the range $x(N_2) = 0.10$-0.20 and the solubility of C_2H_6 in the N_2-rich phase is about $x(C_2H_6) = 0.03$-0.06. The results in the literature exhibit some discrepancies and do not go below 111 K. Figure 22 shows the results obtained in Knapp's group in Berlin[24] as well as some earlier work of Lu *et al.* [25].

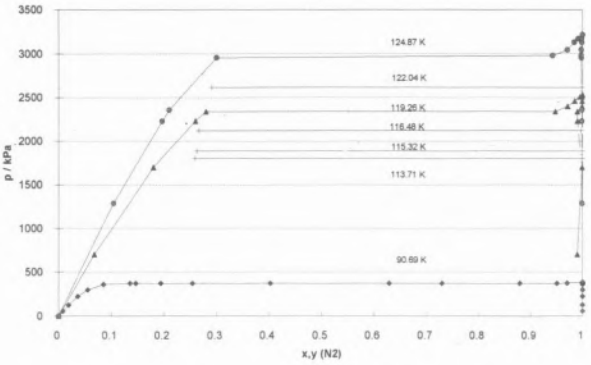

Figure 22. - Pressure-concentration diagram for N_2-C_2H_6

(There is also the ligh pressure liquid-liquid-solid equilibria obtained in Schneider's group in Bochum [26]).
We have extended this work down to about 90.7 K[27] (see Figure 22) and also measured the heats of mixing at 93 K[28] — Fig. 23

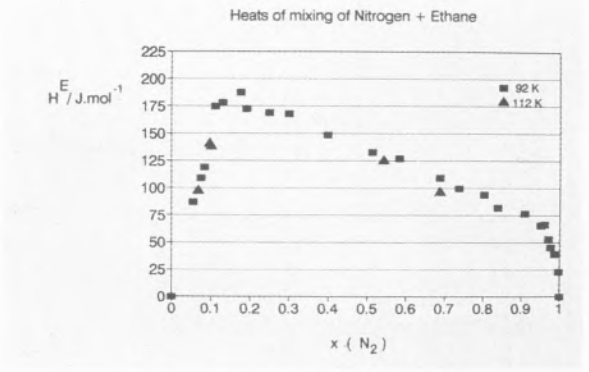

Figure 23. - Heats of Mixing of N_2+C_2H_6 at 93 K and $p = 9$ bar

We found the immiscibility gap to be wider than that predicted by extrapolation of the higher-temperature work.

This same system has also been studied by perturbation theory (using a WCA-type division of the potential) and computer simulation, and the results for the equimolar mixture are shown in Table IV

	G^E ($J.mol^{-1}$)	H^E ($J.mol^{-1}$)	V^E ($cm^3.mol^{-1}$)
Theory (93 K)	526	421	-1.74
Simulation (95 K)	394	250	-1.49
Experiment	550 (90.7K)	450 (92.3K)	-1.89 (105.0K)

Table IV. - Comparison of Experiment with Theory and Simulation for the N_2-C_2H_6 System

There is no adjustment, so this is pure prediction. Computer simulation for this system is difficult because the density is so high. Perturbation theory shows that, unlike V^E, both G^E and H^E do not appreciably vary with temperature.

In order to understand what happens on the surface of the planet we need data for the ternary system N_2-CH_4-C_2H_6. With this aim in mind a cryogenic, recirculating, direct sampling phase equilibrium vessel for the study of ternary systems was designed and built[29]. A simplified diagram of the apparatus is shown in Figure 24

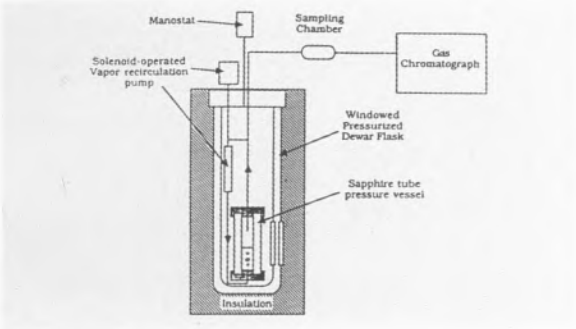

Figure 24. - Low-Temperature VLE Apparatus

It consists of a cylindrical sapphire tube pressure vessel, which has recirculating lines leaving the vapour phase and reentering the liquid at the bottom. Two sampling lines enter the top of the tube, and can be positioned to sample gas or liquid, and the analysis is carried out by gas chromatography.

Apart from three-body effects, all the information for the ternary system is contained in the three binary systems. In other words, the excess Gibbs energy, G^E, for the ternary system is given by the following expression

$$G^E = G^E_{12} + G^E_{13} + G^E_{23} + G^E_{123}$$

Putting $G^E_{123} = 0$ corresponds to assuming ternary ideality. For the general case G^E_{123} can be assumed to be of the form[30]

$$G^E_{123} = x_1\, x_2\, x_3\, (A + B\, x_1 + C\, x_2)$$

where x_1, x_2 and x_3 are the mole fractions of the three components. The activity coefficients can then be derived using standard thermodynamic relations.

In Figure 25 the ternary phase diagram for the N_2-CH_4-C_2H_6 is shown, including the major features of the Titan ocean-atmosphere equilibrium at 94 K, 1.5 bar[31]. For a given composition (in mole per cent) of CH_4 in the gas phase, the corresponding ocean composition is given by a point along the track at the upper left (the outer lines define the confidence interval)[31].

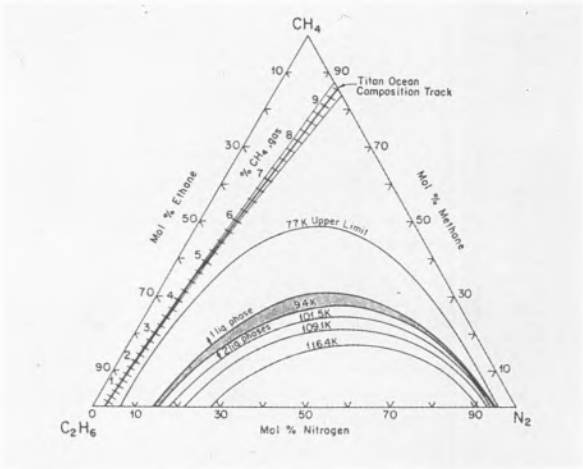

Figure 25. - Phase Diagram for the ternary System N_2-CH_4-C_2H_6

For instance, a CH_4 mole fraction in the vapour phase of 0.03 (3%) corresponds to a liquid (ocean?) composition (mole fraction) of approximately 0.20 in CH_4 and 0.75 in C_2H_6.

On the lower part of the Figure are shown the phase separation boundaries for this system for temperatures between 101 and 117 K. The expected conditions on Titan are such that no liquid-liquid immiscibility should occur (there is enough methane present to ensure a complete solubility of nitrogen in ethane). At about 111 K there is a density inversion: above this temperature the N_2-rich phase is less dense and floats on top of the denser phase, richer in C_2H_6, while at lower temperatures the N_2-rich phase sinks to the bottom.

An artist's impression of what Titan's surface should look like, based on the general ideas discussed in this paper, is shown in Figure 26.

Figure 26.- A Titan Landscape - Reality or Fiction?

This looks more like the realm of science fiction than that of true science, but we should remember that new science begins with a leap of the imagination which is, in itself, a form of fiction. The *"let us assume"* of science is nothing but a disguised way of the *"once upon a time"*...

References

1. Margaret M. Byard, *History Today*, February (1988) **30-38**.
2. R. F. Mueller, *Icarus* **3** (1964) 285-298.
3. H. C. Urey, *The Planets: Their Origin and Development*, Yale University Press, New Haven (1952)
4. J. S. Lewis, *J. Atmos. Sci.* **28** (1971) 1084.
5. J. S. Lewis, F. A. Kreimendahl, *Icarus* **42** (1980) 330.
6. W. B. Streett, *Astrophys. J.* **186** (1973) 1107.
7. W. L. Slattery, W. B. Hubbard, *Icarus* **29** (1976) 187.
8. D. J. Stevenson, E. E. Salpeter, *Astrophys. J. Suppl* **35** (1977) 221.
9. A. Kouchi, *Nature* **330** (1987) 550.
10. C. M. Masterson, J. E. Allen Jr., G. F. Kraus, R. K. Khanna, *Proc. 1st Int. Conf. Lab. Res. Planet. Atms.*, NASA Conf. Publ. **3077** (1990) 357.
11. Y. L. Yung, *Proc. 1st. Int. Conf. Lab. Res. Planet. Atms.*, NASA Conf. Publ. **3077** (1990) 181
12. T. K. Minton, A. E. Stiegman, T. A. Moore, M. Okumura, *3rd Int. Conf. Lab. Res. Planet. Atms*, Palo Alto (1991).
13. C. Sagan, *Parade Magazine*, December1 **6** (1991).
14. M. Cabane, E. Chassefière, G. Israel, *Icarus* **96** (1992) 176.
15. G. F. Lindal, G. E. Wood, H. B. Hotz, D. N. Sweetnam, V. R. Eshleman, G. L. Tyler, *Icarus* **53** (1983) 348.
16. E. Lellouch, A. Coustenis, D. Gautier, F. Raulin, N. Dubouloz, C. Frère, *Icarus* **79** (1989) 328.
17. V. R. Eshleman, G. F. Lindal, G. L. Tyler, *Science* **221** (1983) 53.
18. J. I. Lunine, D. J. Stevenson, Y. L Yung, *Science* **222** (1983) 1229.
19. C. Sagan, S. F. Dermott, *Nature* **300** (1982) 731.
20. R. D. Lorenz, J. C. Zarnecki, *European Geophysical Society Meeting*, Edinburgh, April 6-10 (1992).
21. W. R. Thompson, J. C. G. Calado, J. A. Zollweg, *Proc. 1st Int. Conf. Lab. Res. Planet. Atms.*, NASA Conf Publ. **3077** (1990) 303.
22. E. J. S. Gomes de Azevedo, J. C. G. Calado, *Fluid Phase Equil.* **49** (1989) 21.
23. L. C. Kouvaris, F. M. Flasar, *Icarus* **91**(1991) 112.
24. H. Kremer, Ph. D. Thesis, Technischen Universität Berlin, 1982, p. 174; G. Trappehl, H. Knapp, *Cryogenics* **27**(1987) 696.
25. P. Yu, I. M. Elshayal, B. C. -Y. Lu, .*Canad. J. Chem. Eng.* **47** (1969) 5.
26. K. D. Wisotzki, G. M. Schneider, *Ber. Bunsenges. Phys. Chem.* **89** (1985) 21.
27. E. M. Filipe, internal report
28. J. C. G. Calado, P. Gopal, J. A. Zollweg, W. R. Thompson, *Can. J. Chem.* **66** (1988)626.
29. D. H. Gabis, M. Sc. Thesis, Cornell University, 1991.
30. M. B. King, *Phase Equilibrium in Mixtures*, Pergamon, New York, 1969, p. 335.
31. W. R. Thompson, in *The Atmospheres of Saturn and Titan* (ESA SP-241, E. Rolfe and B. Battrick, Eds), p. 109. ESA Publ. Div., Noordwijk, Netherlands (1985).

* Adapted from a plenary lecture delivered at the *5th International Conference on Thermodynamics of Solutions of Non-Electrolytes*, Oporto, Portugal, 1992.